The role of a highly conserved eubacterial ribosomal protein in translation quality control

2015

Anusha Naganathan
University of Central Florida

THE ROLE OF A HIGHLY CONSERVED EUBACTERIAL RIBOSOMAL PROTEIN IN TRANSLATION QUALITY CONTROL

by

ANUSHA NAGANATHAN
M.S, University of Central Florida, 2010

A dissertation submitted in partial fulfillment of the requirements
for the degree of Doctor of Philosophy
in the Burnett School of Biomedical Sciences
in the College of Medicine
at the University of Central Florida
Orlando, Florida

Spring Term
2015

Major Professor: Sean D. Moore

ABSTRACT

The process of decoding is the most crucial determinant of the quality of protein synthesis. Ribosomal protein L9 was first implicated in decoding fidelity when a mutant version of L9 was found to increase the translation of a T4 phage gene. Later studies confirmed that the absence of L9 leads to increased translational bypassing, frameshifting, and stop codon readthrough. L9 is part of the large subunit of the prokaryotic ribosome and is located more than 90 Å from the site of decoding, making it difficult to envision how it might affect decoding and reading frame maintenance. Twenty years after the identification of L9's putative function, there is no mechanism for how a remotely located L9 improves translation fidelity. This mystery makes our picture of translation incomplete. Despite the high conservation of L9 in eubacteria, *E.coli* lacking L9 does not exhibit any obvious growth defects. Thus, the evolutionary advantage conferred by L9 in bacteria is masked under laboratory conditions. In order to uncover unique L9-dependent conditions, a library of *E. coli* mutants was screened to isolate those that rely on L9 for fitness. Interestingly, factors found to be synergistic with L9 had no known role in fidelity. Six independent mutants were isolated, each exhibiting a severe growth defect that is partially suppressed in the presence of L9. One class of L9-dependent mutations was present in an essential ribosome biogenesis factor, Der. Der's established function is in the maturation of the large ribosomal subunit. The identified mutations severely impaired the GTPase activity of Der. Interestingly, L9 did not directly compensate for the defective GTPase activity of mutant Der. The second class of L9-dependent mutations was present in EpmA and EpmB, factors required

to post-translationally modify elongation factor, EF-P. EF-P's established function is in the translation of poly-proline containing proteins. EF-P deficient cells were nearly inviable in the absence of L9; however, L9 did not directly influence poly-proline translation. Therefore, in each case, L9 improved cell health without altering the activity of either Der or EF-P. Remarkably, the *der* mutants required only the N domain of L9, whereas the absence of active EF-P required full-length, wild-type L9 for growth complementation. Thus, each mutant class needed a different aspect of L9's unique architecture. In cells lacking either active EF-P or Der, there was a severe deficiency of 70S ribosomes and the indication of small subunit maturation defects, both of which worsened upon L9 depletion. These results strongly suggest that L9 plays a role in improving ribosome quality and abundance under certain conditions.

Overall, the genetic screen lead to the discovery that bacteria need L9 when either of two important translation factors (Der or EF-P) is inactivated. This work has characterized the physiological requirement for L9 in each case and offers a new insight into L9's assigned role in translation fidelity.

Dedicated to my family

ACKNOWLEDGMENTS

My PhD experience has been truly meaningful under the mentorship of my advisor, Dr. Sean D. Moore. I am grateful for having worked with him as his first graduate student. He genuinely cared about my graduate training experience and provided an ideal learning environment. I cannot thank him enough for his constant encouragement at every step of my project, especially during times when my confidence was tested by failed experiments and by my own errors. He has been a patient teacher and a great role model during this entire journey. His philosophies and ideas as a scientist have tremendously influenced me and provided the perspective I need, as I enter the next phase of my career. I want to also thank all the members of the Moore Lab, past and present, for their support and their excellent company in lab.

I would like to thank all my committee members. They motivated me to do better at every stage and were always willing to provide guidance. I would like to specially thank them for always willing to schedule several committee meetings over the years to discuss my progress and offer advice. These committee meetings have helped me improve my presentation and communication skills.

I would like to thank my parents and my family for their love and support. Finally, I have shared every good and bad part of being a graduate student with my husband, Gowri and would like to thank him for being there through it all.

TABLE OF CONTENTS

LIST OF FIGURES

LIST OF TABLES

CHAPTER I: INTRODUCTION

History Of Studies On The Ribosome

In 1958, Francis Crick put forth the idea of the central dogma of molecular biology, which states that all genetic information flows from nucleic acid to nucleic acid or nucleic acid to protein. In his paper, he stated, "I shall also argue that the main function of the genetic material is to control the synthesis of proteins" [1]. Although the composition, structure, and the importance of proteins in biological systems were fairly well studied at the time, little was known about the machinery used to transfer information from nucleic acid to protein. Ribosomes serve as the fundamental machinery required to convert genetic information into proteins. The first evidence of the existence of ribosomes came from electron micrographs of disrupted animal and bacterial cells [2]. Micrographs of the endoplasmic reticulum showed the presence of "electron-dense particles" associated as clusters on either side of the membrane and were referred to as microsomal particles by Crick. These particles were merely speculated to be sites of protein synthesis. Soon after, it was shown that these particles are made up of RNA and protein, and were given the name ribonucleoprotein (RNP) particles [3, 4]. Analytical centrifugation allowed the separation of different kinds of ribonucleoprotein particles away from cell debris and their subsequent characterization. These particles could be separated on a linear sucrose gradient based on their sedimentation coefficient (or the Svedberg unit, S) [5-7]. Prokaryotic ribosomes are organized into two asymmetric subunits – the 50S large subunit and the 30S small subunit) and come together to form a 70S particle [5]. Up to eighty percent of the

ribosomes are involved in translation at any given time [8], meaning that most of ribosomes are present as polyribosomes (polysomes) (Figure 1).

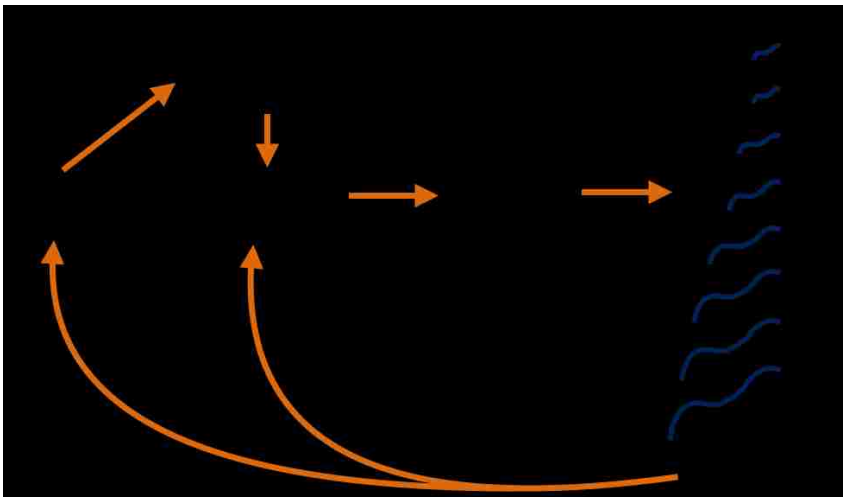

Figure 1. Organization of the ribonucleoprotein particles (RNPs)

The 30S subunit associates with mRNA, initiator tRNA, and initiatior factors to form the pre-initiation complex. The complex then finds a mature 50S subunit to form the 70S ribosome. 70S ribosomes that are actively translating a mRNA are called polysomes. The polysomes depicted here show an actively growing polypeptide chain. At the end of translation of a given mRNA, the nascent peptide is released and the ribosomal subunits are recycled to initiate a new round of translation.

The Decoding Property Of The Ribosome

Linus Pauling's work on haemoglobin protein chemistry provided clues that "errors" in the amino acid sequence of proteins can arise even in the absence of a genetic mutation [9]. The idea that ribosomes have an innate property of amino acid selection was considered and lead to the question - how do ribosomes discriminate between amino acids? Watson and Crick independently proposed an explanation - an adapter RNA molecule (now known as tRNA or transfer RNA) could base-pair with the correct triplet code (codon) to position the amino acid appropriately for polymerization. Studies by Offengand and Hoagland confirmed this so-called "adapter hypothesis" and showed that tRNAs can be fused covalently to each amino acid (a process now called aminoacylation) [10-12]. After the discovery of the messenger RNA [13], studies on tRNA-mRNA interaction showed that the thermodynamic base-pairing energy difference between a cognate and a non-cognate tRNA could drive selection of the correct amino acid by its corresponding tRNA. The ribosome was thought to only stabilize interactions between the tRNA and mRNA [14]. Although this explained amino acid selection to some extent, the selectivity of the ribosome *in vivo* was found to be much higher than that explained by *in vitro* base pairing alone [9, 12].

Studies using antibiotics such as streptomycin and paromomycin revealed that binding of antibiotics to the ribosome can introduce significant errors in translation [12, 15-18]. Moreover, resistance to antibiotics was mapped to many ribosomal genes, indicating that interactions within the ribosome do more than just facilitate a tRNA-mRNA interaction. The hypothesis of an "active site" for decoding on the ribosome was soon proposed. These

decoding interactions (unknown at the time) were said to determine the accuracy with which tRNAs were selected. It was not until the early 2000s that a clear picture of the interactions at the decoding site emerged. Today, we know that important conformational changes that occur after tRNA binding accelerate the selection of the correct tRNA [19]. These mechanistic studies were possible because of atomic-level resolution of crystal structures of the ribosome. The advent of X-ray crystallography to study ribosomal structure was an important milestone in our understanding of the extremely dynamic process of protein synthesis. Although ribosomes were crystallized as early as 1980 [20], structures were not available until the late 1990s. The crystal structure of the ribosome paved way for researchers to design more meaningful genetic and biochemical experiments to directly address key questions in translation [21-25].

The Composition Of The Ribosome

Bacterial ribosomes contain about 33% protein and 67% RNA [3]. Building the ribosome requires the efficient and proper maturation of long sequences of rRNA along with binding of ribosomal proteins and biogenesis factors. The 30S small subunit contains 21 r-proteins and one rRNA molecule (16S, 1542 nucleotides). The 50S ribosome contains 34 r-proteins and two rRNA molecules (23S, 2904 nucleotides) and (5S, 120 nucleotides) [26]. Ribosomal RNA is transcribed from seven rDNA operons (A, B, C, D, E, G, H), each with one copy of 16S and 23S and varying copies of 5S and tRNA genes [3, 17]. After transcription, the spacer and leader sequences flanking the mature rRNA sequence are processed and removed. The remarkable complexity and highly evolved architecture of the ribosome implies that a lot of cellular resources are

dedicated to ensure that ribosomes are built correctly. This is especially true for the formation of active sites of the ribosome: the 30S decoding center [25] and 50S peptidyl-transferase center (PTC) [27]. These two functional centers of the ribosome are located ~75 Å apart and communicate at each stage of elongation. The ribosome has three tRNA binding sites – A (aminoacyl), P(peptidyl), and E (exit) [28]; these sites span both the ribosomal subunits. The chemistry in the PTC is favorable for a nucleophillic attack of the alpha-amine of the A-site amino acid on the carbonyl carbon of the P-site amino acid. rRNA residues at the PTC (A2602 and U2585) are directly responsible for peptide bond formation [29, 30]. The decoding site hosts important conformational changes at each cycle of elongation starting from the binding of a cognate tRNA (along with EF-Tu-GTP) to tRNA accommodation [31].

The Process Of Translation

The goal of translation is to manufacture proteins that can fold and function properly. The earliest genetic studies on the ribosome [17] utilized mutants that conferred antibiotic resistance by altering translation fidelity. Two questions emerged from these studies – 1) what is the accuracy of protein synthesis? and 2) how does the ribosome distinguish between a cognate, a near-cognate, and a non-cognate tRNA [12, 32].

A “kinetic proofreading” model was suggested first by Hopfield in 1974 to explain the selectivity of the ribosome [33, 34]. Several kinetic and biochemical studies have confirmed this “kinetic proofreading” hypothesis [19, 35, 36]. According to this model, the ternary complex (consisting of elongation factor, EF-Tu, GTP and an aminoacylated tRNA) is presented at the A-

site of the ribosome (Initial binding). Only cognate tRNAs successfully bind, while non-cognate tRNAs dissociate readily (codon recognition). During a cognate interaction, the C75 of the aminoacyl tRNA basepairs with A-site rRNA residue G2553 and this anchors the tRNA to the A-site. If the correct tRNA is selected, GTP hydrolysis occurs, and EF-Tu is released from the ribosome (GTP hydrolysis). Near-cognate and non-cognate tRNAs have a higher probability of being rejected at this stage because their base-pairing interaction consumes a lot more energy for EF-Tu dissociation than cognate-tRNA (tRNA selection). Once tRNA is selected, the rest of the selected tRNA orients itself into the PTC (tRNA accommodation). The CCA end of the tRNA then interacts with 23S rRNA and is ready for peptide bond formation (Peptidyl transfer). Elongation is followed by the process of translocation, where the tRNAs move from A/P sites to the P/E sites, placing the subsequent codon on the A-site, ready for the next round of elongation. This process continues until a stop-codon is encountered at the A-site and is recognized by release factors for termination. Each cycle of elongation is driven by the GTPase activity of elongation factors EF-G and EF-Tu and involves movement of mRNA together with tRNA.

An alternative "allosteric model" was suggested by Nierhaus and his colleagues, which postulates that base-pairing interactions at the ribosomal E-site influences tRNA selection at the A-site [37]. However, the model has been debated in the field due to experimental evidence that argues against it [38, 39] . Nonetheless, there is strong evidence for the influence of alloteric interactions on translation fidelity in general and cannot be ruled out [37].

The Prokaryotic Ribosome As A Model For Macromolecular Assembly

It was demonstrated in the late 60s by Nomura and colleagues that all the information required to build a functional ribosome is present within the components of the ribosome itself [40, 41]. Nomura's group carried out elaborate reconsitution experiments and demonstrated that the ribosome is capable of self-assembly. If the ribosome can assemble itself, why do bacteria have "assembly" factors? [42].

Actively growing cells can synthesize upto 70,000 ribosomes during its lifetime and thereby constitute a large percentage of the bacterial biomass [5]. Kjeldgaard and colleagues showed that the number of ribosomes in a cell (of *Salmonella typhimurium*) is directly proportional to its growth rate, suggesting that the formation of ribosomes is the rate-limiting step to synthesis of proteins [4]. There are some important differences between *in vivo* and *in vitro* ribosome assembly which provide an explanation for the requirement of biogenesis factors. In an actively dividing cell, ribosomes assembly is exceptionally efficient (rRNA local structures are known to form in ~100 milliseconds and long range interactions in a few minutes), remains coupled to cell growth, and is completed in a matter of minutes. *In vitro*, formation of ribosomes takes about 20-30 minutes [43, 44] and requires conditions (of increased ionic strength and temperature) that deviate considerably from the cellular environment. *In vitro* assembly involves post-transcriptional binding of ribosomal proteins, whereas *in vivo* assmebly involves co-transcriptional binding of proteins [45]. *In vitro* studies have indicated a certain order of binding events and formation of specific intermediates. Recent studies using advanced techniques such as X-ray hydroxyl footprinting and quantitative

isotope labeling mass spectrometry that have shown multiple intermediates form at the early stages of assembly [44, 46]. The “concurrent nucleation” at multiple points strongly suggests there is more than one way to assemble the ribosome. In order to ensure that ribosomes are properly matured given the speed at which they are made, the cell utilizes “biogenesis” or “assembly” factors. Bacteria have about 40 biogenesis factors [26] and eukaryotes have over 200 [42] that aid in processes such as rRNA transcription, processing, and ribosomal protein binding. Moreover, intermediates formed *in vitro* may be very different from those formed invivo. The ribosome serves as a remarkable model for studying the assemblage of large, macromolecular complexes in the cell. The ribosome assembly process avoids thermodyanmic traps to successfully assemble its 54 proteins and large RNA molecules. Despite severel years of work in the field of ribosome assembly, the function of individual ribosomal or non-ribosomal proteins that facilitate this highly efficient process is poorly understood. Characterization of factors that regulate the quality of ribosomes is crucial to fully understand bacterial translation.

Why Do Ribosomes Have Proteins?

The interactions within the ribosome are governed by the critical architectures that are held together by its protein and RNA components. Many ribosomal proteins are present at the center of these crucial interactions. Despite our expanding knowledge of the molecular stages of translation, it remains unclear why the ribosome requires so many proteins, several of which are very highly conserved, yet non-essential [47]. Ribosomal proteins have long extended

structures which allow anchoring of rRNA in its place and these r-proteins are thought to serve as an “anchor” for maintaining the ribosomal architecture [48]. Is the sole function of ribosomal proteins to preserve and stabilize the important regions of the ribosome? There are conserved patches on ribosomal proteins that extend away from active sites or rRNA regions important for maintaining structural integrity. Thus, it appears that ribosomal proteins may be connecting the processes that occur in the ribosome to pathways outside the ribosome. The sheer number of proteins and the unique locations of their conserved regions on the ribosome suggests that they do not simply provide a scaffold for ribosomal RNA, but perform specific functions during translation [49].

Of the ~54 r-proteins on the prokaryotic ribosome, 34 are “core” proteins that are common to all three domains of life (bacteria, archaea, and eukarya) [50]. Ribosomal proteins unique to bacteria are an indication that important aspects of bacterial translation that have been preserved throughout evolution. Many of these ribosomal proteins are non-essential for growth, which hampers the interpretation of their function. To define the pathways that have preserved such proteins on the eubacterial ribosome, we need to identify interactions that connect these proteins to their function. This dissertation is an effort in that direction and is focussed on the interrogation the function of a highly conserved, non-essential, large subunit eubacterial protein, L9.

Background

Ribosomal Protein L9: Structure and conservation

The gene coding for L9 (*rplI*) is clustered with genes for PriB (*priB*) S6 (*rpsF*) and S18 (*rpsR*) on the *rpsF* operon [51]. L9 is highly conserved across all eubacteria, but absent in archaeal and cytoplasmic eukaryotic ribosomes [50]. Early structural data on L9 came from studies on *Bacillus stearothermophilus* and revealed the highly extended and unique architecture of L9 (Figure 2). The N domain of L9 primarily contacts the domain V of the 23S rRNA of the 50S [52] and its extended C terminus projects highly conserved amino acid residues away from the peptidyl transferase and the decoding centers [53]. The two highly conserved domains are connected via a nine-turn alpha helix that is invariant in length, creating a fixed distance between the domains [54, 55]. L9 improves reading frame maintenance by an unknown mechanism. The first evidence for this came from studies on an extreme form of programmed event of translational frameshifting (called translational bypass) of a T4 phage *gene60*. This programmed frameshifting event is required for the production of a DNA topoisomerase in T4 phage [56, 57]. A mutant form of L9 (*hop-1, Ser93Phe*) was isolated using a genetic screen as a suppressor of a defective version of *gene60* [58]. Later, mutational analysis revealed that the N domain of L9 has one highly conserved residue that influences bypass, while residues that increase bypass by more than ten-fold are present at the surface of the C-terminal domain of L9 [59]. These residues are located almost ~150 Å from the P-site of the ribosome. Because reading frame shifts are thought to occur at the P-site, it is mysterious why

the C domain of L9 would be positioned so remotely. We carried out a protein sequence allignment of L9 from several representative bacterial phyla and showed that the highly conserved residues of L9 are isolated to the N and C domains of L9 (Figure 2). This suggests that the orientation of the C domain with respect to the N domain is crucial L9's function. Although L9 has been linked to improving translation fidelity, cells lacking L9 do not exhibit any apparent growth defects [60-62] (Figure 3).

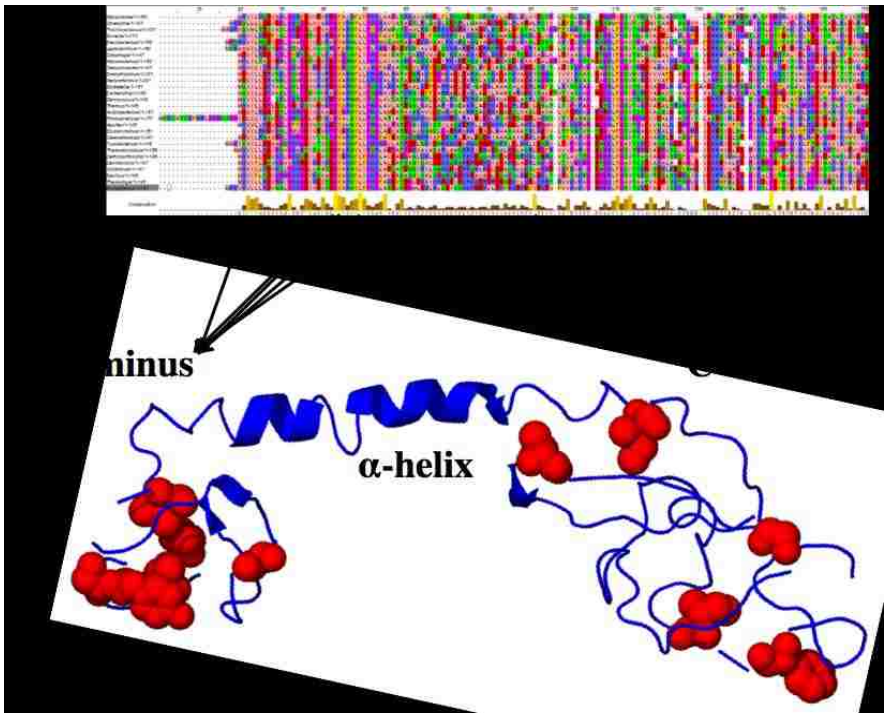

Figure 2. The conservation of the sequence and structure of protein L9

We carried out a multiple sequence allignment of L9 using ClustalW omega. The residues that are greater than 90% chemically conserved are highlighted (*in red*). The conserved residues are isolated to the two domains of L9 and the connecting helix is invariant in length. The structure of L9 has been modelled in Pymol using a crystal structure of the *E. coli* ribosome [53].

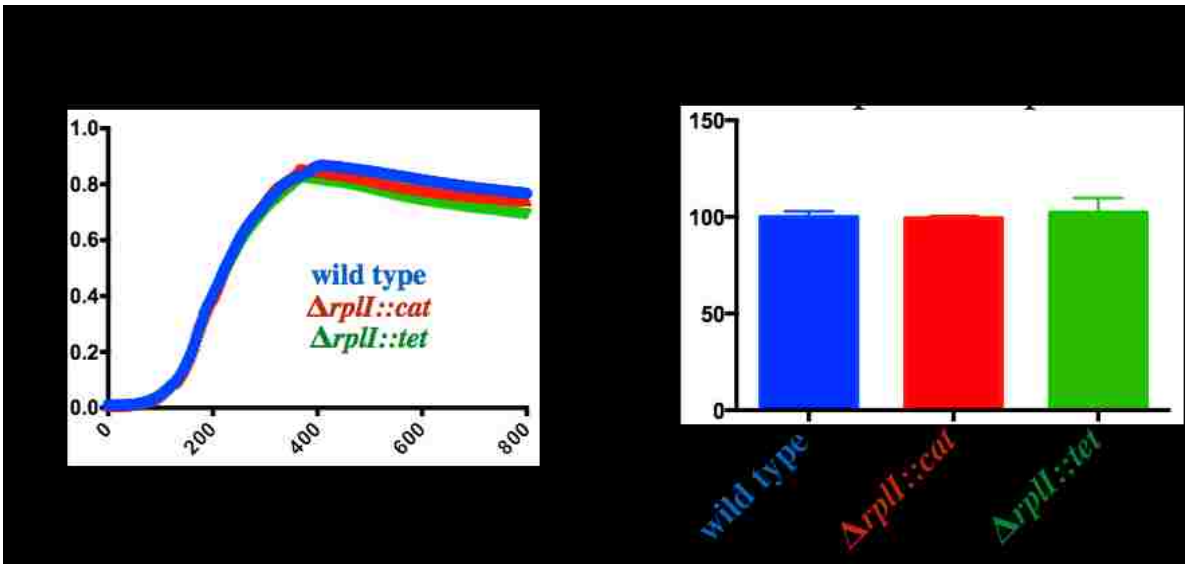

Figure 3. L9 deletion strains exhibit no significant growth pertubations.

A) We monitored the absorbance of cultures of wild-type vs two deletion strains of L9 (*ΔrplI::tet* and *ΔrplI::cat*) at 600nm. B) The data from the log phase of growth curves from (A) was fit to a linear equation to calculate growth rate. The growth rates of *rplI*- cells are represented as a percent of the wild-type growth rate. The error bars represent standard deviation from triplicate measurements. There is no difference in exponential growth between L9+ and L9- cells under laboratory conditions.

A Synthetic Lethal Approach Reveals the Reason for L9's Conservation

Because of non-essentiality of L9, we were able to take a novel genetic approach to investigate L9's function. We set out to identify conditions that make L9 essential for cell health. We modified an existing genetic screen for synthetic lethality (Figure 4) [63]. Using this genetic approach, we isolated six mutants each carrying a single point mutation that exhibited severe L9 dependence. Three of the six mutations were present in an essential GTPase Der while the other three mutations were in enzymes that post-translationally modify EF-P. An introduction to these two pathways and the existing literature is provided below. These *E. coli* mutants provided the first oppurtunity to understand why bacteria need L9 and establish situations where the demand for L9 is high.

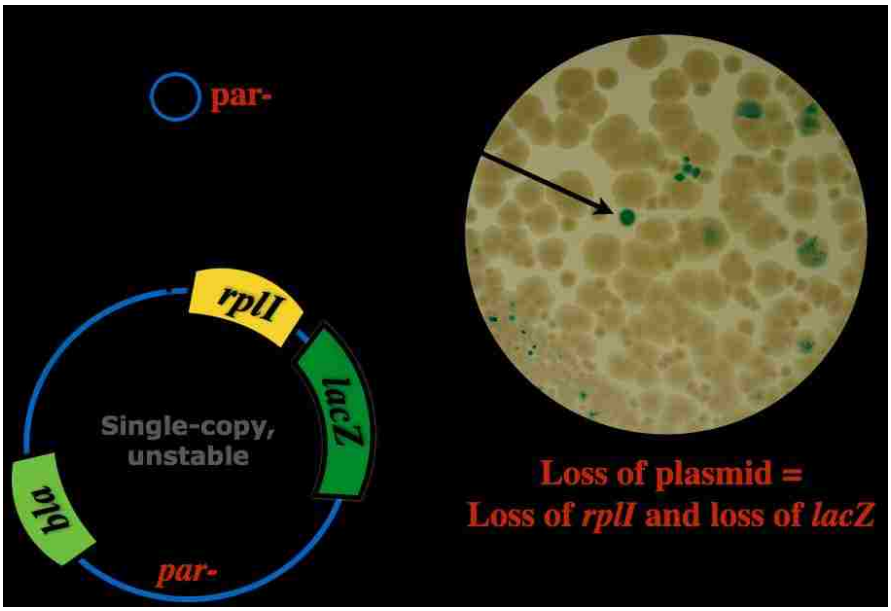

Figure 4. The modified synthetic lethal screen used to isolate L9-dependent mutants

Shown on the left is a schematic of the synthetic lethal tool (unstable plasmid) used for the screen. The plasmid has a defective *par* locus causing it to segregate randomly during cell division [63]. The gene coding for L9 (*rplI*) and LacZ (*lacZ*) were cloned under the control of a strong IPTG-inducible promoter (*trc*) [64]. Cells carrying the plasmid appear blue on an X-GAL indicator plate (shown on the right). The loss of plasmid indicates the absence of both L9 and LacZ. A library of random *E. coli* mutants was screened to isolate mutants that exhibit dependence on plasmid-borne L9 (a solid-blue phenotype).

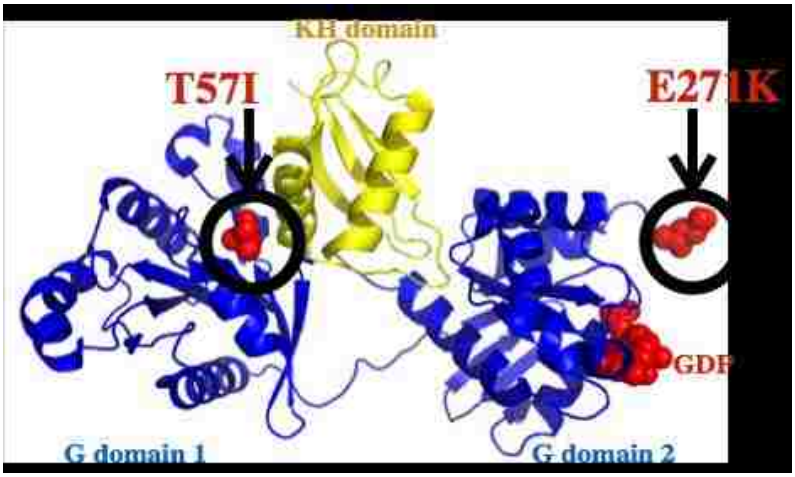

Figure 5. The crystal structure of Der from *Thermotoga maritima*

The enzyme Der contains two tandem GTP-binding domains connected to a RNA binding KH domain. The image was prepared in Pymol using the crystal structure of Der from Thermotoga maritima (Robinson 2002). Mutations in Der that causes L9 dependence were present in different GTPase domains (*highlighted in red*).

Essential Biogenesis factor, Der (EngA, YphC, or YfgK)

Bacterial GTPases are known to have critical roles in ribosome assembly and translation [65, 66]. Their function is generally coupled to their GTPase activity that drives key conformational changes during cellular processes such as translation. While in eukaryotes GTPases mostly participate in signal transduction, most bacterial GTPases have been implicated in ribosome biogenesis and translation. Ribosome assembly (RA) GTPases identified so far are not required for *in vitro* ribosome synthesis; however, most of them are indispensible for cell growth [66]. RA GTPases are known for their function in biogenesis because their absence results in the accumulation of ribosomal intermediates *in vivo*. Many GTPases serve as check points in ribosome assembly to prevent the accumulation of energetically unstable dead-end intermediates, which explains its importance in the cell. Of all the characterized bacterial GTPases, Der (double Era-like) is the only GTPase with two tandem GTP-binding and hydrolysis domains [67] (Figure 5). There are no homologs of Der in archaea or in eukaryotes, with the exception of some plants [68]. Der has been implicated in large subunit assembly in *E. coli* [69] and *Bacillus subtilis* [70] and found to be essential in several other bacteria [65]. The two domains of Der function in a co-operative manner and are both are required for GTPase activity [71]. We have identified a unique synergy between Der and L9. Two point mutations in Der (DerT57I and DerE271K) inactivate the enzyme activity of Der and cause severe growth dependence on protein L9. These mutants and their functional association with L9 have been characterized and the manuscript is presented here (in Chapter II). Der has been implicated in 50S biogenesis for two reasons - its association with the 50S subunit seems to be coupled to its

GTPase activity and the depletion of Der leads to severe 70S deficiency. Intermediates of 50S accumulate in Der-depleted cells (45S, 40S and 35S) in a Mg^{++}-dependent manner [69]. The Mg^{++} dependency and the accumulation of multiple intermediates suggests that the stabiliy of the 50S may be compromised at a late-stage of biogenesis in Der mutants [69].

Although some bacterial GTPases seem to be involved in cell division, whether this is simply a secondary effect of a ribosome maturation function is not known. The pleiotropic phenotypes of most of the ribosome-associated GTPases make it difficult to study their isolated function in biogenesis. The accumulation of improperly assembled ribosomes can pose a great threat to the cell. If misassembled ribosomes are allowed to initiate translation, the quality of proteins in the cell will be severely compromised. To fully understand quality control of translation it is important to identify what biogenesis factors do, when they act, and how they influence the quality of ribosomes entering translation. Performing directed functional studies aimed at understanding one biogenesis factor has been challenging because *in vivo,* biogenesis occurs very rapidly and is coupled to multiple events such as protein binding, RNA folding, and RNA modification. The synergy between a ribosome biogenesis factor like Der and a fidelity factor such as L9 provides the exciting oppurtunity to investigate the relationship between ribosome synthesis and ribosome function.

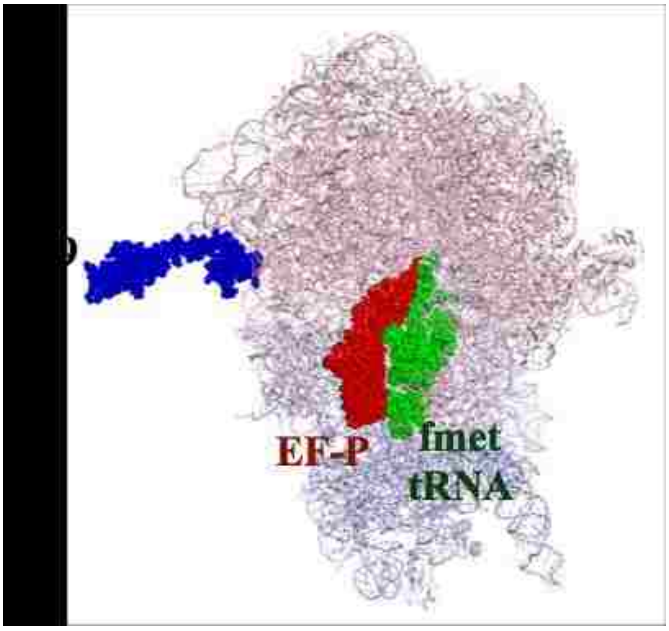

Figure 6. The crystal strucuture of the Thermus thermophilus ribosome bound to EF-P

EF-P (*in red*) binds between the E- and the P-sites of the ribosome and its modified lysine residue (K34) reaches into the peptidyl-transferase cavity of the ribosome. The L9-dependent mutants isolated in our screen were present in factors that modify the lysine (K34) of EF-P. L9 has been highlighted (*in blue*). The image was prepared in Pymol using the crystal structure from Thermus thermophilus [72].

Elongation factor, EF-P

Elongation factor P (EF-P) was first identified as a stimulator of peptidyl transferase activity *in vitro* [73, 74]. However, EF-P is not an essential component in *in vitro* translation assays and the gene coding for EF-P can be deleted in *E. coli*. Although the chemical reaction of peptide-bond formation occurs in the large subunit, EF-P was shown to require both ribosomal subunits for its stimulatory activity [75, 76]. The crystal structure of EF-P bound to the bacterial ribosome indicates that EF-P spans both subunits of the ribosome (Figure 6) and binds between the E- and the P- sites of the ribosome, with its C terminus binding near the anticodon stem-loop of the P-site tRNA (at the 30S) and the N terminus positioned near the CCA end of the P-site tRNA (at the 50S). A highly conserved patch on the N terminus of EF-P makes extensive contacts with the 23S rRNA near the PTC. This patch contains a lysine residue that is post-translationally modified by the addition of a β-lysine. Genes *poxA* (*yjeA* or *epmA*), yjeK (*epmB*), and *yfcM* (*epmC*) encoding enzymes 2,3-Aminomutase, Lysyl tRNA synthetase, and Lysine hydroxylase respectively are responsible for the modification of the lysine residue. The function of EF-P has come to light only recently. EF-P promotes translation elongation of certain poly-proline containing polypetides [77, 78] and thereby relives ribosome stalling of at these transcripts. The modification of Lys34 of EF-P by *epmA* and *epmB* is essential for EF-P's function in translation [79, 80]. Although EF-P is not essential for cell growth, *E. coli* cells lacking EF-P exhibit considerable growth defects and in *Salmonella*, EF-P's activity has been shown to increase virulence [81]. The eukaryotic EF-P ortholog, eIF5A is essential and has also been linked to polyproline translation [82].

The second class of L9-dependent mutations in our study was found in *epmA* (E116K and W117R) and *epmB* (W15amber). Unlike the *der* mutants, *efp* mutants require full-length L9 for complementation. The synergy between L9 and EF-P provides an explanantion for the highly elongated structure of L9. Considering EF-P's function in alleviating ribosome stalling, it is likely that the lack of EF-P activity results in increased accumulation of polysomes, causing a decline in the availability of 70S. Such situation puts a high demand on ribosome biogenesis. We observed that the presence of L9 alleviates ribosome biogenesis defects in EF-P-deficient cells, placing L9's importance in ribosome quality control rather than in the decoding process. Identifying the mechanism by which an *efp*- phenotype is suppressed by L9 will be important to fully understand the function of L9.

CHAPTER II: CRIPPLING THE ESSENTIAL GTPASE DER CAUSES A DEPENDENCE ON RIBOSOMAL PROTEIN L9

Introduction

Ribosomal proteins are a curious class of translation factors in that most of them do not appear to participate directly in protein synthesis [49]. Although the roles of some ribosomal proteins may be to maintain the architecture of the ribosome active centers, many typically possess regions of high conservation in areas that do not contact other ribosomal proteins or ribosomal RNA. There is mounting evidence that the conserved motifs in some ribosomal proteins are used to either regulate translation or to connect ribosomes to other important cellular processes [83-86] . Interestingly, some very highly conserved ribosomal proteins can be deleted from bacteria without inducing appreciable growth phenotypes, which obfuscates determination of their molecular functions [83, 87]. The bacterial-specific ribosomal protein L9 is an example of this non-essential class: it possesses a conserved secondary and tertiary architecture and contains several invariant amino acids, yet deletion strains grow well [61, 88, 89]. From the perspective that all highly conserved factors serve as windows to important cellular processes, we reasoned that a deeper understanding of L9 would help connect this enigmatic ribosomal protein to basic bacterial physiology.

Ribosomal protein L9 was initially characterized during the in vitro ribosome assembly studies in the early 1980s [52, 90]. From those studies, it was established that L9 is a primary ribosome binding protein in that it does not require other proteins to engage the 23S RNA. A

functional role for L9 in reading frame maintenance came from a genetic screen for E. coli mutants that increased translation through a partially defective phage bacteriophage T4 gene 60 bypass region [58]. The bypass event during gene 60 translation is remarkable in that the ribosome recognizes signals in the nascent peptide and mRNA that promote a 50 nucleotide "hop" before re-engaging the same mRNA to complete the synthesis of the encoded protein [56]. The hop-1 mutation was recovered and identified as Ser93Phe alteration in a highly conserved patch on the C terminus of L9. Subsequent studies demonstrated that L9 also influences frameshifting at codon repeats and stop codons [56] [91-93]. More recently, L9 deletion strains were shown to read through stop codons more frequently (out of frame) and encounter the 3' ends of their engaged mRNAs, which then invokes ribosome rescue systems [61]. Thus, at least one role for L9 is in maintaining translation fidelity, but nothing is known about the mechanism for this activity.

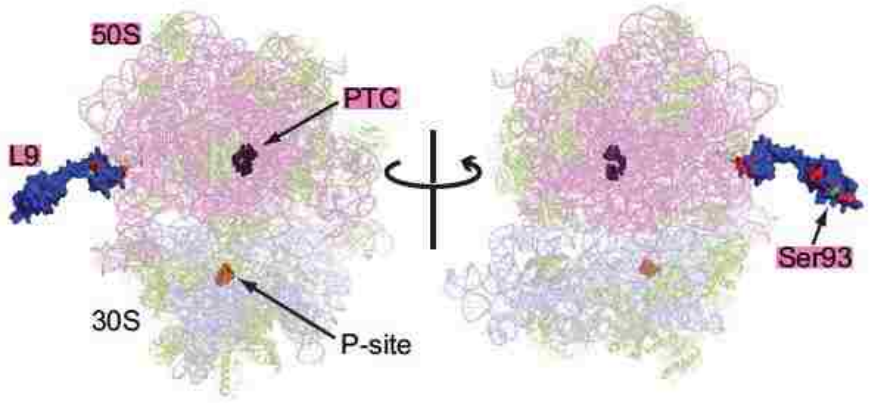

Figure 7: L9 on the ribosome.

A rendering of the crystal structure of the *E. coli* ribosome with L9 conservation is shown in two views (PDB files 2i2t and 2i2p). The 50S and 30S subunits are indicated with 23S rRNA in pink and 16S rRNA in slate. The locations of the peptidyl-transferase center (PTC) and the P-site are highlighted. L9 is surface rendered in blue with invariant amino acids in red. The *hop-1* residue that affects translation bypass, Ser93 is colored green.

Structurally, L9 is odd in that it projects from the surface of the large subunit near the base of the L1 stalk. L9's architecture is very highly conserved and is comprised of a globular N domain that docks with the 23S RNA, a long alpha helix of fixed length, and a globular C domain displayed away from the surface in crystal structures (Figure 7) [53, 94, 95]. Although the positioning of L9 in crystal structures implies a rigid conformation, chemical footprinting and crosslinking experiments suggest that L9 is dynamic and may engage portions of the L1 stalk RNA and also surrounding regions of the large subunit [59, 96]. In support of this idea, structural biologists recently demonstrated that L9 might be inadvertently stabilized in ribosome crystals through inter-ribosomal contacts. Indeed, ribosomes missing L9 can enter alternative crystal forms, a feature that allowed, for the first time, resolution of the GTPase-activating center [89, 95, 97].

Not only is the architecture of L9 conserved, but there are also collections of invariant amino acids in both the N and C domains. Considering the expansive evolutionary history of L9 in eubacteria (it is conserved in all bacterial phyla) it would seem that L9 plays a critical role in cell physiology that is frequently selected in nature. However, in tested cases, L9 deletion strains appear healthy. While it can be argued that a small fitness advantage is sufficient for evolutionary conservation, the other domains of life do not have L9 (aside from bacteria-like organelles).

The conservation of specific residues in L9 suggests that it interacts with other factors that are also very highly conserved. We are interested in identifying such factors, not only to develop a mechanistic understanding of L9's role in translation fidelity, but also to potentially

reveal new biochemistries. To move in this direction, we screened a chemically-mutated *E. coli* library for mutants that depend on L9 in the hopes we could recover mutations in essential factors that would point to the functions of L9. Here, we describe strains with mutations in the essential ribosome biogenesis GTPase Der (EngA/YphC) that grow better with L9 than without it [71, 98]. We show that the L9- dependent Der mutants are severely compromised for GTPase activity, which was previously shown to be critical for Der's essential function [69, 71, 99]. Purified L9 does not rescue the GTPase defects, nor does it alter the stimulatory activity of Der's GAP-like factor YihI, so the fitness afforded by L9 seems indirect. We put forward a preliminary hypothesis that the ribosome-binding domain of L9 may help stabilize structurally compromised large subunits synthesized when Der activity is limiting.

Materials and Methods

Strains and plasmids.

Strain TB28 (MG1655, *ΔlacIZYA*) was designated as wild-type E. coli for this study [63]. The gene encoding L9 (*rplI*) was deleted or modified by recombineering in strain SM1405 (X90, *ΔclpX ΔclpA* harboring plasmid pSIM5) using selection for either a promoter-less kanR ORF or promoter-containing tetR or catR genes [100]. Mutants of rplI were P1 transduced into TB28 and the modifications verified by diagnostic PCR and DNA sequencing [101, 102]. For complementation, Der variants, full length L9 (1-149), L9 $_{1\text{-}149}$-FLAG-His6, L9 $_{1\text{-}53}$-FLAG-His6, L9 $_{65\text{-}149}$-FLAG-His6, and YihI-FLAG-His6 were expressed from derivatives of the pTrc99a plasmid [64].

Der variants were overexpressed for purification from pET-3a (Novagen). The construction of the unstable reporter plasmid used for the screen is described in the Supplemental Material.

Chemical mutagenesis and library screening.

The screening strain AN226 (TB28, Δ*rplI::tet* harboring pRC-L9) was mutated using N-ethyl-N-nitrosourea (ENU, Sigma #N3385) using a published protocol as a guide [103]. An overnight culture of AN226 was diluted (1/50) in 1mL A-0 medium with 0.2 % glycerol, 0.5 mM IPTG, and 75 g/mL ampicillin. At early exponential phase, 26 mM of ENU (stock prepared in 0.1% acetic acid and 23% DMSO) was added to the culture. A parallel control culture received only the ENU diluent. After 20 minutes at room temperature, the cells were recovered in 1mL of LB medium containing 0.5 mM IPTG and 28 mM 2-mercaptoethanol (to inactivate the mutagen) for 2 hours at room temperature. The culture that received ENU exhibited ~95 % loss in viability compared to the mock. Dilutions of the library were plated on LB agar (with 40 μg/mL X-Gal, 0.2 % glycerol, and 0.5 mM IPTG) and screened at ~250 colonies per 90 mm plate. These mutants were cured of pRC-L9 and mutations causing the phenotype were mapped using transposon-based P1 transduction marker rescue (Supplemental Material). The mutations were then identified by sequencing the mapped locus. Three mutants had changes to *der*. All sequences were analyzed using *E. coli* K-12 MG1655 genome as wild-type (GenBank: U00096.2) [104].

Protein expression and purification.

L9-FLAG-His6 was purified under denaturing conditions, refolded on a Ni^{++} column by desalting, and then eluted under native conditions (Supplemental Material). YihI-FLAG-His6 was purified similarly, but under native conditions. L9 and YihI were further purified by hydroxyapatite chromatography. Purified proteins were exchanged into Buffer A (20 mM Tris-HCl, 25 mM NaCl, 0.05 % Tween-20, 5% glycerol, and 5 mM 2-mercaptoethanol, pH 8.0) prior to storage at -80 oC. The concentrations were determined by UV absorbance (L9 in GuHCl = 1,280 M^{-1} cm^{-1} and YihI in GuHCl = 6,890 M^{-1} cm^{-1}) [105]. We were unable to obtain ample soluble Der with either N- or C-terminal epitope tags and strains with C-terminally-tagged chromosomal der were very sick, suggesting a defective enzyme. Therefore, wild-type and mutant versions of untagged Der were overexpressed using a T7-expression system (pET-3a, Novagen) and purified conventionally (Supplemental Material). Briefly, overexpressed protein was purified from cleared lysates under native conditions using a combination of anion exchange, hydroxyapatite binding, and ammonium sulfate precipitations. Purified Der contained a contaminant that exhibited the absorbance profile of nucleic acid (likely GDP as has been reported) [67, 70, 106], which prevented quantification using UV absorbance. Therefore, the concentration of Der was measured using Bradford assays with BSA as a standard (Bio-Rad). GTPase assays. Der's GTPase activity was measured using a regenerative, coupled assay [107]. A 20X Assay Mix (20 mM NADH, 150 mM phosphoenolpyruvate and ~10 U/mL pyruvate kinase/lactate dehydrogenase mixture (Sigma #P0294) was prepared in Assay Buffer (20 mM Tris-HCl, 100 mM KCl, 0.05 % Tween-20, 5 % glycerol, and 5 mM 2-mercaptoethanol, pH 8.0) and frozen in aliquots at -80 C. It

is established that Der's GTPase rate is increased at high concentrations of potassium [98, 106]. In preliminary experiments, we determined that by increasing KCl or K-PO4, the rate of GTP hydrolysis could be accelerated to the point that stimulatory effects of YihI were no longer measureable (Supplemental Material). Therefore, our assay buffer was formulated to set the basal rate of wild-type Der at ~50% the YihI-stimulated rate so that stimulatory effects could be readily observed. Although the T57I and E271K mutants were also stimulated by potassium, the relative turnover differences were not affected. 2X assay mixes were prepared in Assay Buffer supplemented with GTP and a 2 mM $MgCl_2$ excess over the GTP concentration. 30 L of the 2X assay mixture was combined with 30 µL of 2X enzyme (diluted in Assay Buffer). 50 L of the mixed reaction was then transferred to a 96-well plate and the loss of absorbance of NADH was monitored at 340 nm at 1 min intervals. The slopes of straight lines fitted to the raw data were converted to GTPase rates using the NADH extinction coefficient and the background rates of controls lacking GTPase were subtracted [107]. Doping of GDP into pilot reactions established that the regeneration system was capable of converting >150 M GDP to GTP min^{-1}. Reaction rates were typically linear over several hours. The K_m and V_{max} values were determined at varying GTP concentrations by fitting to the Michaelis-Menten equation using Prism 6 (GraphPad software). The affinity of YihI for Der was determined by converting the stimulation data to fractional occupancy and fitting to the law of mass action to determine K_d (Supplemental Methods).

Conditional Degradation.

The conditional degradation system has been described elsewhere [101]. Briefly, the endogenous target gene was modified to encode a C-terminal peptide tag that is recognized by the processive unfoldase/protease ClpXP. The expression of ClpXP was then regulated from a plasmid. Strains were maintained in glucose to repress expression of ClpXP and then switched to medium containing arabinose to induce the protease and degrade the target. For this study, recombineering was used to replace wild type *rplI* with rplI-deg or rplI-cont using a downstream antibiotic marker for selection, (*rplI* is the last gene in the S6 operon) [100]. P1 transduction was used to move tagged versions of rplI into a Δ*clpX* strain with WT or mutant der. The strains were then transformed with a pBR-ClpXP plasmid library with randomized Shine-Dalgarno sequences to select candidate plasmids that allowed optimum expression of ClpXP for L9 degradation [101]. Transformants were tested for L9 degradation in the first ~30-40 minutes of induction using Westerns. For degradation experiments, a rich, defined MOPS-buffered medium was used to better control catabolite responses (Teknova) [108]. Mutant *derT57I* strains carrying tagged rplI and pBR-ClpXP were diluted from an overnight (1/100) into medium containing 100 g/mL ampicillin and 0.2 % glycerol and 100 L was grown with continuous shaking in a 96-well plate at 37 °C (Biotek Synergy MX). At early exponential phase, either 0.2 % arabinose or 0.2 % glucose was added. After ~40-50 minutes of induction, samples of the cultures were normalized for their absorbance at 600 nm for Western analysis, and a separate aliquot diluted (1/10) into a new well containing either glucose or arabinose medium. When the

cultures reached a density nearing the end of exponential phase, the sampling and dilution was repeated.

Microscopy.

Cells from control and L9-depleted cells were imaged using differential interference contrasting (DIC) from PBS-washed samples of liquid cultures. Cells were heat-fixed onto slides and covered with mounting medium (Prolong Gold, Invitrogen) prior to imaging (Zeiss Axiocam MRc5, DIC III). Cell lengths were measured using software from the microscope manufacturer (Axiovision).

Results

Mutations in der cause a dependence on L9.

To reveal pathways influenced by L9 in *E. coli*, we carried out a synthetic-lethal screen for mutations in other genes that compromise cell health in L9's absence [63]. We first deleted the chromosomal gene encoding L9 (*rplI*) by replacing it with a tetracycline resistance gene. Consistent with previous reports that L9 is non-essential, the Δ*rplI* strain formed colonies that were indistinguishable from *rplI+* cells and exhibited only a slight reduction in yield in liquid cultures [61, 88, 89]. We then placed a clone of the L9 open reading frame (ORF) on an unstable reporter plasmid under control of a controllable promoter (P_{trc}). The resulting strain was chemically mutated to generate a library and screened for colonies that retained the reporter

plasmid (synthetic lethality, indicating that L9 improved their fitness). Potential L9-dependent mutants (exhibiting a solid blue colony phenotype) were recovered at approximately 1 in 20,000 colonies. Three *rplI*-dependent mutants mapped to a common locus and DNA sequencing revealed that each had a point mutation in the ORF of the der gene (also called *engA* and *yphC*) [98]. The mutated der genes encode DerT57I and DerE271K (DerT57I was recovered and mapped twice independently). The T57I and E271K mutations alter very highly conserved residues in each of Der's two GTPase domains ("G domains") [67, 71]. T57 is within the G3 motif of G domain 1 and E271 is within the switch II motif of G domain 2. When cured of the support plasmid that supplies L9, the *derT57I* mutant was sicker than the derE271K mutant, but each still formed colonies (Figure 8, panel A). To verify that rplI indeed improved the fitness of the recovered der mutants, we used phage transductions to replace the rplI locus in the mutants to either another L9 null *(ΔrplI::cat*, as a control) or to wild-type (*rplI-cat*). Replacing the existing *ΔrplI::tet* with *ΔrplI::cat* did not rescue the growth defects. In contrast, restoring *rplI* in the chromosome improved growth to a level that was intermediate between the recovered rplI, *der* mutants and an *rplI+der+* strain (Figure 8, panel B). Thus, the fitness of these der mutants is increased when the cells have L9, but the mutant der genes cause growth reductions, suggesting they remain partially defective in the presence of L9.

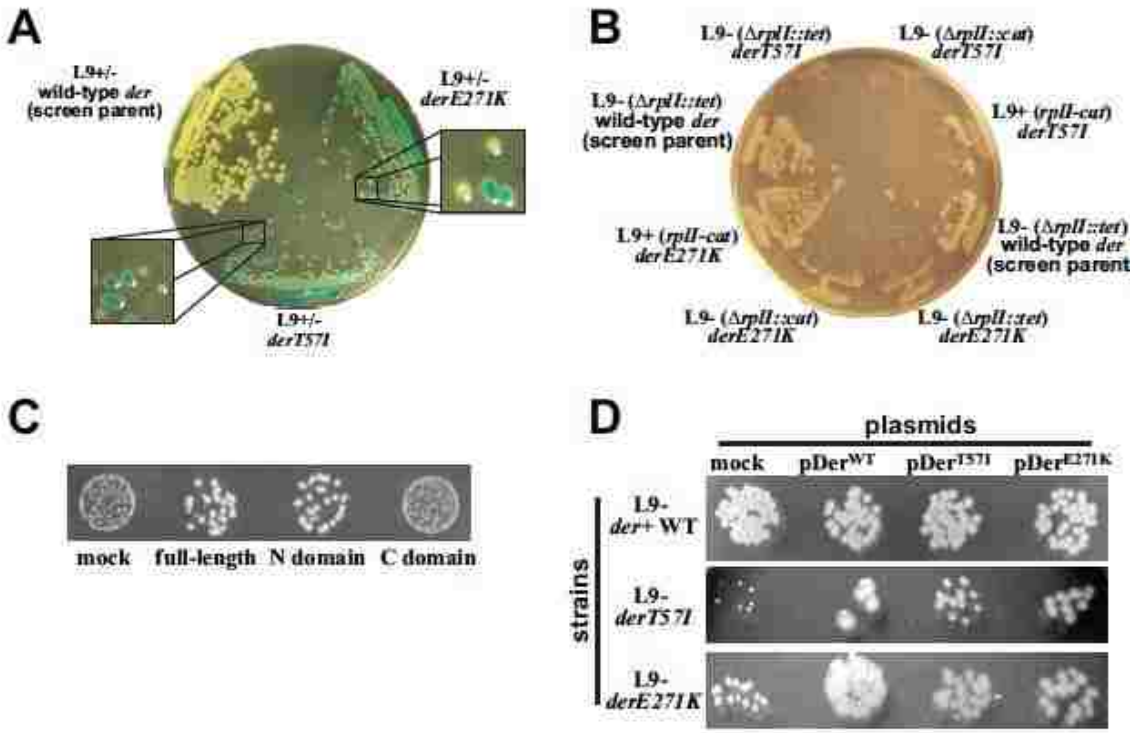

Figure 8: L9 improves the health of *der* mutants.

A synthetic lethal screen revealed mutants that grow better with an unstable reporter plasmid expressing L9. Panel A, a comparison of the parental screening strain to two recovered der mutants on an X-gal indicator plate. The parental cells did not require L9 and turned white during colony development from plasmid loss. Cells that grew better L9 maintained a blue color in the colony because plasmid-containing cells were more fit. The *derT57I* strain was sicker in the absence of L9 than was *derE271K*, evidenced by the relative colony sizes without the reporter plasmid. Panel B, strains cured of the reporter plasmid were transduced to replace the rplI locus in the chromosome. A control transduction replaced the original ΔrplI::tet and *ΔrplI::cat* and did not improve growth. Restoring rplI (rplI-cat) improved the health of both der mutants, but not to the level of the parental cells with wild-type der. Panel C, complementation of the *ΔrplI*, *derT57I* mutant with a mock plasmid, or plasmids encoding L9 1-149-FLAG-His6 (full-length), L91-53-FLAG-His6 (N domain), or L965-149-FLAG-His6 (C-domain). The N domain alone complemented the small colony phenotype as well trans-complementation of the chromosomal der alleles. Wild-type Der restored full health to each mutant (second column). Overexpression of either the T57I or E271K mutant improved the health of each mutant, but did not sicken cells with wild-type der in the chromosome. Therefore, each der mutant is partially functional and recessive.

The N-domain of L9 complements derT57I.

L9 contains highly conserved amino acids in both its N and C domains. To determine if either domain could suppress the small colony phenotype independently of the other, we expressed them from plasmids in the *derT57I* strain because of its easily scorable phenotype (L9 residues 1-53 and 65-149). Both full-length and N domain constructs improved the growth to comparable extents on plates and in liquid cultures (~60 % of *der+*). The C domain did not complement and grew similarly to the *derT57I* strain with a mock plasmid (~30 % of *der+*, Figure 8**,** *panel C* and not shown). We established that the C domain construct expressed protein of the predicted size from this construct in a separate experiment (not shown). Therefore, the N domain of L9 is necessary and sufficient for complementation of the *derT57I* allele.

The derT57I and derE271K mutants are partially functional and recessive.

We cloned the der_+, *derT57I*, and *derE271K* ORFs onto plasmids and introduced them into $\Delta rplI$, der_+ and der_{mut} strains. A mock plasmid lacking der was used as a control. Because homologous recombination was active in these strains and capable of replacing the mutant der loci, we plated dilutions of freshly-transformed cells to evaluate colony fitness without substantial outgrowth. This procedure also reduced the accumulation of second-site suppressors (described below). Introducing plasmid-borne, der_+ into the *derT57I* and *derE271K* strains fully restored colony and liquid culture growth (Figure 8, *panel D*, second column, and not shown). This finding indicates that the slow-growth phenotypes were caused solely by the

mutations in der. Plasmid-born versions of either *derT57I* or *derE271K* partially restored the growth of strains with the same alleles and also of the other mutant (Figure 8, *panel D* second and third columns). Moreover, these plasmids did not sicken cells with chromosomal der_+. Therefore, the recovered *der* mutants are recessive and they encode partially active Der variants that support growth better when more is expressed.

Suppressor mutations arise frequently in the derT57I background.

Our efforts to transduce the mutant genes to other strains were impeded by the weak screenable phenotype of *derE271K* and a rampant accumulation of escape mutants of *derT57I* that grew well and lost their dependence on L9. The observed frequency of escape in overnight cultures (10^{-2} to 10^{-5}) of *derT57I* was too high to be accounted for by same-site reversion (expected at ~10^{-9}). Therefore, to determine if the escape mutations were intra-or extragenic, we sequenced the der genes from four *derT57I* fast-growing escape mutants. Each retained the original T57I mutation, but contained an additional mutation in the same GTPase domain near the T57I position (Figure 9). This finding reinforces the conclusion that the T57I mutation in Der is solely responsible for the slow-growth phenotype and the dependence on L9. Also, unsuppressed *derT57I* strains are not able to be reliably cultured for biochemical studies.

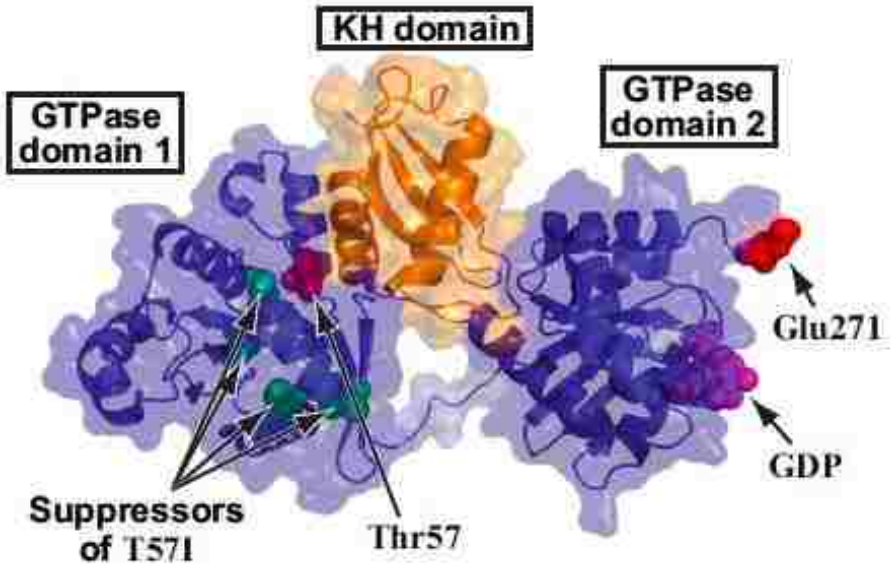

Figure 9: The locations of the L9-dependent Der mutants and T57I suppressors.

Shown is a rendering of Der from Thermotoga maritima (PDB IMKY) showing the locations of T57 and E271 and the relative positions of four E. coli T57I suppressors (A45V, R109G, T113A, V158G, in green). The GDP bound in G domain 2 is pink. In this conformation of Der, T57I lies at the interface between G domain 1 and the KH domain. E271K is in switch II of G domain 2.

The T57I and E271K mutations impair the GTPase activity of Der.

Prior studies indicated that GTP hydrolysis by each of the two GTPase domains is required for E. coli Der's essential function and that they act cooperatively [67, 98]. We discovered that der encoding a C-terminal FLAG-His_6 tag was unable to functionally replace wild-type *der* in the chromosome. Very sick strains with these tags spawned fast-growing escape mutants with frameshift mutations in the 5' end of *der* that prevented expression of the tagged enzyme. To avoid the possibility of aberrant behaviors stemming from tags on Der, the wild-type, T57I, and E271K versions were purified as untagged proteins for in vitro characterization. The reported apparent K_m of *E. coli* Der for GTP is ~140 μM (23). Therefore, we preliminarily measured the basal GTP hydrolysis rates for each enzyme at 1 mM substrate (near-saturating) using 0.125 to 2 μM enzyme. Under these conditions, we observed a dose-dependent increase in GTP hydrolysis rate for the wild-type enzyme and a turnover of ~1.5 min^{-1}, which is consistent with the reported basal GTPase activity of Der (Figure 10**,** *panel A*). Both mutants were severely compromised in their GTPase activities, with the E271K mutant possessing a higher turnover rate than T57I (~0.30 and ~0.02 min^{-1} respectively). Thus, the severity of the GTPase defects mirrored the severity of the growth phenotypes. Moreover, each mutation inhibited the GTPase activity of both GTPase domains, which supports a proposed highly-cooperative hydrolysis mechanism for Der [71]. To determine if the observed rate defects were from a loss in affinity for GTP or from a catalytic defect, we measured the

hydrolysis rates under varying GTP concentrations to obtain K_m and V_{max} values (Figure 10**,** *panel B*). In these conditions, wild-type Der exhibited an apparent K_m of ~0.22 mM and a V_{max} of 2.42 min^{-1}. We were unable to obtain these kinetic parameters for the T57I mutant because the hydrolysis rates were too low for fitting, but the E271K exhibited an apparent K_m of ~0.25 mM and a V_{max} of 0.2 min^{-1}. Thus, this mutant was not compromised in its ability to bind GTP and the observed slow rate may stem from a reduction in the mechanical cycling of the enzyme because the E271 residue is not in contact with the GTPase center.

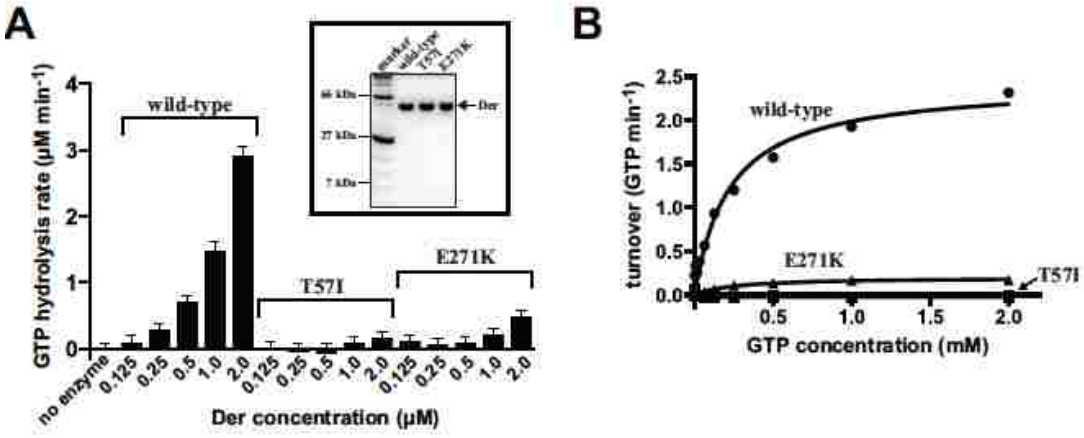

Figure 10: DerT57I and E271K are compromised in their GTPase activities.

Panel A, various concentration of wild-type, T57I, and E271K Der proteins were evaluated in a regenerative GTPase assay using a GTP concentration that nearby saturated wild-type (1 mM). *Inset*, Coomassie-stained SDS-PAGE of the purified Der proteins. Increasing the wild-type Der concentration increased the observed GTP hydrolysis at each concentration tested. The T57I and E271K mutants only displayed a measurable hydrolysis rate above background at high concentrations (~2 μM for T57I and ~1 μM for E271K). The error bars are the standard deviations from three measurements. *Panel B*, Michaelis-Menten kinetic analysis of each protein at varying GTP concentrations (0.008 to 2 mM). The wild-type was assayed at 0.5 μM and the T57I and E271K mutants were each assayed at 2 μM and then the rates were converted to turnover rate per enzyme. The K_m and V_{max} values for wild-type were 0.22 ± 0.04 mM and 2.42 ± 0.16 mM and these values for E271K were 0.25 ± 0.06 mM and 0.20 ± 0.01 respectively. The rate of GTP hydrolysis by T57I was too low for fitting.

Additional YihI partially complements the der mutants.

A recent study identified the highly conserved, non-essential protein YihI as factor that stimulates Der [109]. In particular, YihI was reported to increase Der's GTPase V_{max} by ~50 % and decrease its K_m by ~50 %. DNA sequencing revealed that *yihI* was wild-type in each of our *der* mutant strains. To determine if YihI influenced the fitness of the L9-dependent *der* mutants, we cloned its ORF onto a multi-copy plasmid under control of the P_{trc} promoter and introduced it into the *der* mutants. We and others observed that high levels of YihI severely inhibited growth (not shown) [109]; therefore, we tested for complementation under non-inducing conditions, wherein leaky expression from the plasmid would moderately overexpress YihI. Under these conditions, the additional YihI complemented both the colony and liquid culture growth of *derT57I* mutant as well as L9 did (~60 % recovery of growth rate), but neither protein complemented as well as wild-type Der (full restoration) (Figure 11**,** *panel A* and not shown). Providing additional YihI only subtly improved *derE271K* growth. These findings suggest YihI helps these mutants deal with their defective Der; however, we show below that this factor does not restore their GTPase activities.

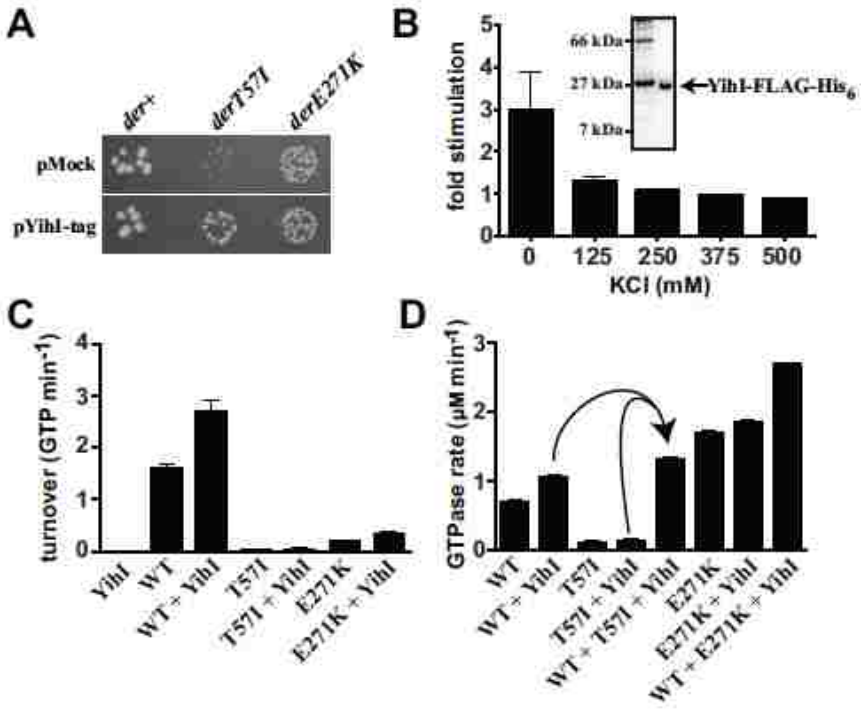

Figure 11: YihI complementation and stimulation of Der.

YihI with a FLAG-His6 tag on its C-terminus was expressed form a plasmid and used for complementation studies and to overexpress the protein for purification. Panel A, L9- strains with wild-type der, derT57I, or derE271K alleles. YihI complementation was evaluated under non-inducing conditions to reduce YihI toxicity. YihI expression partially complemented the derT57I and derE271K mutants, but did not restore wild-type growth. Panel B, the stimulation of wild-type Der (0.5 μM) with and without YihI-FLAG-His6 (5.0 μM) was measured with increasing KCl and presented as fold stimulation. At high concentrations of potassium, YihI did not stimulate Der. Panel C, under conditions that allowed approximately half-maximal YihI stimulation of 0.5 μM wild-type Der (YihI at 2.6 μM), GTPase activities were assayed in the presence of eitehr the T57I or E271K as competitors (each at 5 μM). The observed activity of wild-type mixed with T57I was the sum of the stimulated wild-type and the non-stimulated T57I, indicating that T57I did not appreciably compete for YihI (arrows). The E271K was partially stimulated by YihI and the mixture displayed the sum of both stimulated rates.

YihI stimulation is potassium sensitive.

To directly evaluate the influence of YihI on the Der mutants, we purified YihI so we could monitor its stimulatory effect in GTPase assays. Consistent with previous reports, Der's basal GTPase activity was stimulated by potassium [98, 106]. The rate also increased with added KPO_4 and did not increase with additional NaCl, so the stimulation was from the potassium ion as has been reported (not shown) [98, 106]. Surprisingly, we discovered that the stimulatory activity of YihI was inversely proportional to potassium stimulation. Without added KCl, YihI increased the weak GTPase rate of wild-type Der approximately three-fold. At concentrations of potassium greater than ~250 mM, the stimulation by YihI was lost. Curiously, YihI suppressed the additional stimulation observed at concentrations of potassium >250 mM (Figure 11**,** *panel B* and Supplemental Material). Therefore, YihI stimulation is sensitive to potassium concentration. Viewed another way, YihI helps Der function at lower potassium levels.

YihI fails to bind to or restore the GTPase activity of the Der mutants.

Using wild-type Der, we sought to establish an affinity between these factors under our standard assay conditions (100 mM KCl) by monitoring the increase in Der's GTPase activity as a function of YihI concentration. Consistent with the previous report of YihI activity under similar conditions [109], we observed ~50% increase in Der's GTPase when nearly saturated with YihI (Figure 11**,** *panel C*). We were able to derive a K_d between YihI and Der of 2.6 ± 0.6 μM

(Supplemental Material). Thus, the affinity between these factors is moderate and consistent with YihI serving a dynamic regulatory role [109]. Next, we evaluated the ability of YihI to stimulate the L9-dependent Der mutants. We did not detect activation of T57I at our highest tested concentrations (2 μM Der and 20 μM YihI). The E271K mutant could be stimulated, but only at very high protein concentrations (>2 μM E271K and 20 μM YihI, Figure 11**,** *panel C*). Moreover, although the E271K mutation did not reduce GTP binding, it responded similarly to YihI as mutants that have GTP binding site alterations (S16A and S216A) [71, 109]. Thus, YihI appears to aid in the turnover of the enzyme, but cannot restore the GTPase activities of the mutants despite the fact it partially complements the in vivo phenotypes. In previous work, it was shown that YihI does not require G domain 1 for binding [109]. We were interested in establishing whether YihI could bind to T57I because this protein has a wild-type G domain 2 and KH domain. Therefore, we performed an in solution competition experiment between wild-type and T57I for access to YihI. Using our Der-YihI affinity data as a guide (Supplemental Material), we established a condition where the wild-type enzyme was ~50% occupied by YihI (0.5 μM Der and 2.6 μM YihI). In doing so, small changes in the available YihI would manifest observable changes in overall GTPase hydrolysis rate. Because the T57I protein is nearly inactive, if this mutant is capable of binding to YihI to any appreciable extent, an excess of T57I over wild-type in the mixture should reduce the observed stimulation. We did not observe a reduction in the GTPase stimulation of 0.5 μM wild-type using 5 μM T57I as a competitor and the observed rate was the sum of the stimulated wild-type plus the basal T57I rates (Figure 11**,** *panel D*). Therefore, T57I had no detectable affinity for YihI. For comparison, adding excess

E271K to a reaction containing wild-type Der and YihI caused an increase in GTPase activity that was consistent with both enzymes being stimulated simultaneously. Because Der can function with T57 mutated (when second-site suppressed), these results emphasize a new importance of this highly conserved residue aside from routine GTP hydrolysis.

Purified L9 does not influence Der's GTPase activity.

When purified L9 was added to assays containing wild-type or mutant Der, there was no change in the GTPase rates. Moreover, L9 did not influence Der that was under YihI stimulation (Supplemental Material). This finding suggests that L9's complementation activity in the der mutants may be indirect. Alternatively, the purified L9 may not be active or appropriately presented to Der (technical limitations prevented us from testing ribosomes with and without L9 at sufficiently high concentrations for these assays).

L9 suppresses an elongated cell morphology caused by derT57I.

The synthetic lethal analyses revealed that the small colony phenotype arises when the L9 support plasmid is lost (Figure 8). On the surface, this observation could be interpreted in two ways: either L9 accelerated the growth rate of all *der* mutant cells in a colony (synthetic sickness), or there was a high mortality rate in the der mutants and L9 improves survivability (true synthetic lethality). L9 had the greatest influence on the phenotype of cells with the derT57I allele, so we focused on this mutant for viability and morphology studies. We were unable to grow homogeneous cultures of the highly compromised Δ*rplI*, *derT57I* mutant

because of the high frequency of second-site suppression (Figure 12**,** *panel A*, left plate). We devised a solution to this problem by employing a targeted protein degradation system to rapidly deplete L9 protein from *derT57I* cells at a convenient time [101]. By allowing L9 to suppress the *derT57I* allele during culturing, we were able to grow cultures of sufficient size for biochemical analyses. For this experiment, we modified the *derT57I* strain in three ways. First, we introduced a functional allele of *rplI* that encoded a degradation tag on the C terminus of L9 that is recognized by the processive ClpXP protease (*rplI-deg*); second, we deleted the chromosomal clpX; and third, we introduced a controllable ClpXP expression plasmid. A control strain had a tag on L9 that is not recognized by ClpX (*rplI-cont*). We prepared a dilution of an *rplI-deg*, *derT57I* culture grown with the proteolysis system off and plated it under conditions with the proteolysis system on. All of the colonies were small and reminiscent of freshly-isolated *derT57I* strains (Figure 12**,** *panel A*, right plate). Thus, the L9-deg protein was capable of suppressing the slow growth phenotype sufficiently to allow culturing without the accumulation of fast-growing suppressors. In an *rplI-deg*, *derT57I* culture, inducing expression of ClpXP caused a rapid depletion of L9-deg (Figure 12**,** *panel B***,** inset). Keeping in mind that L9 was still being expressed at high levels as a ribosomal protein, this result indicates that the degradation system was capable of overcoming the L9 synthesis rate and substantially reducing the half-life of the target protein. We noted that extended induction of ClpXP also caused a slight reduction in the L9-cont levels as well, indicating that the protease exhibited partial activity for this tag. This finding also suggests L9 protein levels may not be auto-regulated. The thorough depletion of L9 occurred by ~30 min, but we did not observe a pronounced reduction

in growth rate until ~4 subsequent mass doublings had occurred (Figure 12, *panel B*). This result is important because it demonstrates that ribosomes (or other important factors) synthesized in the presence of L9 and DerT57I are functional when L9 is removed. Thus, DerT57I likely functions in a difficult biogenesis step that, once overcome, no longer requires the support of L9. In addition, this experiment formally establishes that the protein product of *rplI* (and not its mRNA) is responsible for the suppression of this der allele. In a separate set of experiments, we determined that the degradation of L9 in *derT57I* caused a loss in plating efficiency to ~40% that of controls (Supplemental Material). We initially attributed this observation to a loss in cell viability. However, microscopic analyses revealed that culturing of the L9-depleted, *derT57I* cells invoked an aberrant, elongated cell morphology (Figure 12**,** *panel C*). The average cell length of L9+ *derT57I* was similar to L9+ *der+* cells (2.84 vs. 2.53 μm respectively). In contrast, when L9 was depleted from the *derT57I*, the average cell length increased to 4.65 μm with a high variance and the distribution of lengths formed clusters, with some cells being longer than 30 μm (Figure 12**,** *panel D*). Thus, the reduction in plating efficiency was likely caused by a reduction in cell division and not from growth inhibition per se. Overall, L9 appears to suppress a cell division defect caused by a crippled Der.

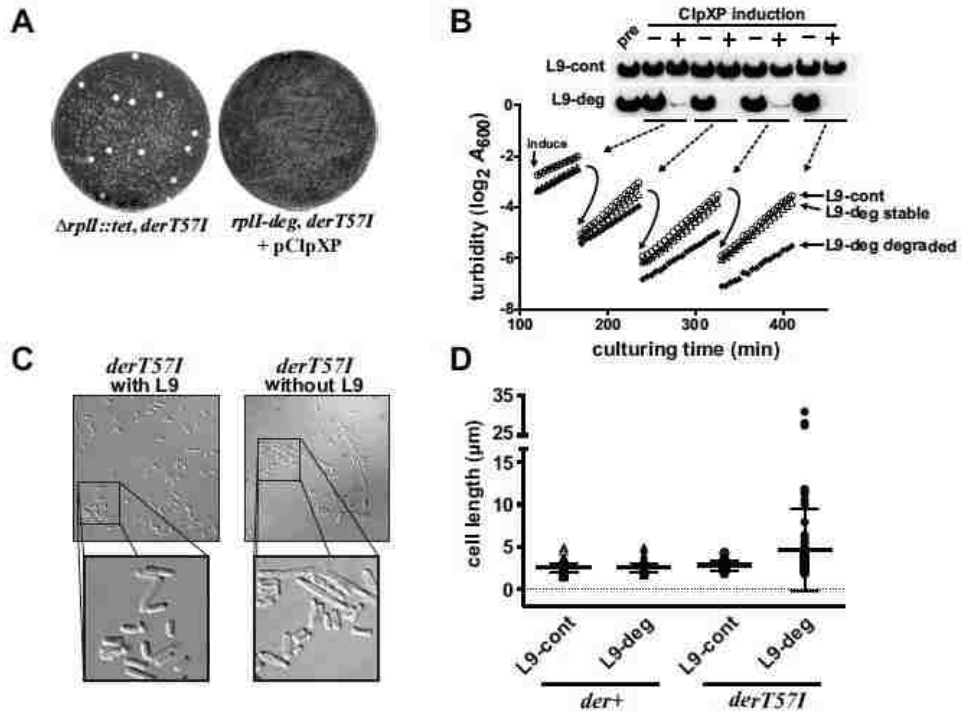

Figure 12: Conditional L9 degradation reveals an unsuppressed *derT57I* phenotype.

A *ΔclpX*, *derT57I* strain supported with either L9-cont or L9-deg was transformed with a controllable ClpXP expression plasmid and maintained under non-inducing conditions to reduce the accumulation of second-site suppressors. Panel A, providing L9-deg to the *derT57I* strain greatly reduced the accumulation of second-site suppressors. On the left is a representative plate showing the presence of suppressed mutant contaminants when *ΔrplI, derT57I* was grown as an overnight culture without L9 support. On the right is a plate of *rplI-deg*, ΔclpX cells containing pClpXP that were grown from an overnight culture to late exponential phase in glucose medium (ClpXP off) and then plated on arabinose to induce ClpXP and degrade L9-Deg. All colonies were small and reminiscent of freshly-isolated, unsuppressed *ΔrplI, derT57I* strains. Panel B, cultures of L9-cont and L9-deg were grown to exponential phase and then treated either with glucose (to repress ClpXP expression, circles and triangles) or induced with arabinose (to express ClpXP, crosses and diamonds). As each fast-growing culture neared the end of exponential phase, aliquots of each were diluted 10-fold into fresh medium to allow extended outgrowth. Separate aliquots were removed for Western analysis of the tagged L9 (above). L9-cont was stable and L9-deg was reduced to very low levels by the first sampling. The growth rate of the culture undergoing L9 degradation was reduced to 36% during the last outgrowth. Panel C, DIC micrographs of *derT57I* strains grown with L9 (L9-cont, pClpXP induced) or without L9 (L9-deg, pClpXP induced). Degradation of L9 caused the cells to become

elongated. Panel D, the lengths of 100 cells from each of the four different cultures grown with pClpXP induced for three outgrowths were measured from several micrographs and plotted along with their averages (long lines) and standard deviations. Average lengths (μm): L9-cont, der+ = 2.53; L9-deg, der+ = 2.53; L9-cont, derT57I =2.84; L9-deg, derT57I = 4.65.

Discussion

We identified mutations in the highly conserved and essential GTPase Der that cause a dependence on ribosomal protein L9 for improved fitness. The T57I mutant was independently recovered and mapped twice during our screen, probably as daughters of the original mutant that separated during recovery. This mutant displayed a pronounced phenotype and illustrates a balance between the inactivation of an essential enzyme and the ability to identify potential candidates during the visual screening of the library. In G domain 1, T57 is located within the G3 motif, which connects to the switch II region of this GTPase. Threonine is found at this position in nearly all Der orthologs and could play an important role in the function of the invariant flanking motif residues. G domain 1 is reported to be responsible for the majority of Der's GTPase activity [71, 106], so breaking the basic catalytic mechanism may explain the highly defective nature of this mutant. However, this GTPase domain is thought to undergo a dramatic reorganization during the GTP hydrolysis cycle. Structures of the Der ortholog from Bacillus subtilis show the G domain rotated such that the T57 location is positioned far away from the KH domain [106]. In contrast, in the Thermotoga maritima structure, T57 sits at a well-packed interface between G domain 1 and the RNA-binding KH domain [67]. Therefore, the T57I mutation may interfere with the ability of the domain to properly interact with the KH domain. The numerous second-site suppressors of T57I also support an architectural role for this residue because if it is required for GTP hydrolysis, only revertants should have functioned well. The E271K mutation sits in the switch II motif of G domain 2 [70]. Although there is generally a high variability in switch domains of GTPases [110-112], E271 appears invariant among all Der

proteins. Switch motifs in GTPases are thought to couple the energy of GTP hydrolysis to the movement of the switches and allow the enzymes to do mechanical work [112]. In the crystal structures of Der, E271 is not in direct contact with residues of the P-loop that gates the GTP hydrolysis site. Nonetheless, this residue is situated at a location that docks this switch against Der in the GTP-bound state. Envisioning a tensioned spring that gets released by GTP hydrolysis during the cycling of the enzyme, a mutation at this location could prevent the formation of a stable, high energy state of the switch. Our observation that the affinity for GTP of the E271K mutant was comparable to wild type also supports the idea that GTP binding was not inhibited, but that the cycling of the enzyme through high- and low-energy states was compromised. Perhaps even more compelling is the observation that the GTPase activity of G domain 1, which is reported to possess the majority of the observed GTPase activity [67], was also substantially inhibited by this mutation. We observed partial complementation of the phenotypes of each mutant by overexpressing YihI. This factor was identified as an interacting partner of Der that stimulated Der's GTPase rate by both lowering the K_m and increasing V_{max} [109]. Because YihI was not observed to stimulate GDP release, it was designated a GAP-like factor [109]. Unlike canonical GAPs, YihI is reported to stimulate Der only marginally and our stimulation data was consistent with this conclusion. One interpretation of these findings is that Der is not likely to be a signaling GTPase; so raising its basal GTPase rate several orders of magnitude, as traditional GAPs do, would not be warranted [113]. Alternatively, YihI may not serve a bona fide GAP function by contributing to catalysis and could be stimulating the GTPase activity by stabilizing a catalytically active conformation, an idea put forth by its discoverers [109]. We did

not observe *der*$_{mut}$ complementation by YihI that was better than that provided by L9, suggesting the growth defects caused by *der*$_{mut}$ persisted in the presence of excess YihI. Moreover, YihI is not universally conserved in bacteria and it is non-essential [109]; yet, overexpression is toxic (suggesting it can shield Der from important targets). Der has joined a growing list of GTPases that require high potassium levels for optimal activity [71, 106]. We discovered that YihI had no stimulatory activity when potassium was present at high levels. Interestingly, the potassium level in *E. coli* and *K. pneumoniae* (where YihI is present) is reported to fluctuate between ~100 and ~250 mM, whereas those of *B. subtilis* (where YihI is absent) are maintained at ~400 mM. [106, 114-116]. Perhaps YihI helps load Der with potassium or helps Der function when intracellular potassium levels are low. The goal of this project was to decipher why L9 is conserved in nature, so what is L9's role in Der physiology? Part of the conundrum stems from the fact that we do not know what Der specifically does. Der depletion for extended periods causes the accumulation of unstable and/or incomplete large subunits and defects in both 16S and 23S ribosomal RNA processing, which others have suggested points to a role in ribosome biogenesis [69, 71, 98, 99, 117]. Cells with deficient rRNA folding factors commonly display cold-sensitivities [66, 118]. We tested for cold-sensitivity in our *der* mutants and observed none (not shown). In addition, another group reported that overexpression of the stringent response factor RelA suppressed the growth defects caused by Der with mutations in either GTPase site, but not a der null [119]. A conclusion from that project was that the overexpressed RelA increased (p)ppGpp pools, restricted rRNA synthesis, and restored balance to the assembly process. We tested for the ability of overexpressed RelA

to suppress the L9-dependent Der mutants and, despite imparting a growth restriction in all strains, we observed no relative fitness increases in the mutants (not shown). Thus, the T57I and E271K mutants are distinct from Der variants with defective GTPase centers in this regard. An interesting feature of the large ribosomal subunits recovered from Der- depleted *E. coli* is that they are sensitive to reduced magnesium levels, suggesting they have not been assembled correctly [69, 99]. Curiously, when these destabilized subunits were evaluated for protein content, L9 was among the few proteins reported to fall off [69, 99]. This finding suggests that the binding site of L9 may be compromised when Der activity is reduced. In line with this notion, our studies indicate that the N-terminal domain alone is able to complement *derT57I* as well as the full-length protein. Additionally, the *hop-1* mutation in L9 is in a conserved patch on the C domain and this variant complements our Der mutants as well as wild-type (not shown). Considering there are extensive contacts between the N domain and the 23S RNA, it seems that this potion of L9 may be helping to stabilize the large subunit when Der activity is limiting. The physiological functions of Der and L9 remain a mystery. An additional approach we took to interrogate the role of L9 in the Der mutants was to evaluate translation bypassing in the mutants using established reporters. Aside from the complication of second-site suppression, we discovered a curious phenomenon that led us to abandon that approach (Supplemental Material). We used a targeted degradation system to get around a thorny genetic problem and to preliminarily interrogate the physiology of Der mutants as they lose the support of L9. We were pleased to find that the degradation system could deplete L9 so well considering it is a highly expressed protein that is tightly associated with the ribosome. We plan to use our

degradation system to evaluate the integrity of ribosomes built with a defective Der upon L9 depletion both in vivo and in vitro. In the preliminary investigation reported here, we revealed an elongation phenotype when the *derT57I* strain lost the support of L9. We also observed elongated cells in unsupported cultures of *derE271K* (not shown). We interpret these results as a problem with cell division caused by a defective Der and not necessarily a problem with biomass accumulation. Thus, *der* mutants were likely recovered in our screen because the loss of L9 promotes the retention of the reporter plasmid by reducing cell division. These findings raise interesting new questions about the roles of L9 and Der in ribosome assembly and in maintaining bacterial physiologies.

CHAPTER III: THE LARGE RIBOSOMAL SUBUNIT L9 ENHANCES SMALL SUBUNIT MATURATION AND ENABLES THE GROWTH OF EF-P DEFICIENT CELLS

Introduction

Translation fidelity is controlled on a number of levels; from tRNA aminoacylation, to mRNA decoding, to co- or post-translational surveillance [12, 19, 33, 120-122]. Numerous factors have been identified that influence the quality of protein synthesis, which is not surprising considering the complexity and the physiological commitment to this essential process. Among these, ribosomal protein, L9 reduces translational frameshifting, miscoding, and bypassing, but the mechanism for this activity remains a curiosity because L9's location precludes interactions with either the peptidyl transferase center or the decoding center [53, 88, 94]. Thus, L9's activity as a fidelity factor indicates that there is an important missing component in existing models of translation.

L9 has a highly conserved architecture consisting of two widely spaced globular domains connected by an elongated α-helix (Figure 13) [94, 123]. A mutation in the C-terminal domain (Ser93Phe) was isolated as a suppressor of a partially defective translational bypass reporter based on the bacteriophage T4 *gene60* mRNA [58]. It was subsequently determined that L9 is required to suppress bypassing, frameshifting, stop-codon "hopping", which suggests that there is a common mechanism behind each of these events [58, 61, 93, 124, 125]. In addition, it was demonstrated that conserved patches on the globular domains of L9 and the length of the connecting helix affect L9's activity, so the conserved architecture of L9 is also required for its

fidelity function [93, 124, 125]. Interestingly, despite a remarkable eubacterial conservation, L9 deletion mutants show little growth disadvantage under laboratory conditions [60, 61, 125-127].

Mechanistically, it is conceivable that L9 directly influences activities near the E-site, but a direct influence on the peptidyl transferase or the decoding centers is hard to reconcile (these are more than 70 Å and 90 Å away form L9 respectively). Recognizing that the ribosome is a champion of allosteric regulation over large distances, it is possible that L9 imparts a regulatory activity by influencing the decoding center under certain conditions; yet, no evidence for such distortions has been observed in ribosomes lacking L9 using chemical probing or X-ray crystallography [128, 129]. However, an absence of allosteric behavior is not evidence of its absence, as the structural analyses performed to date did not evaluate ribosomes in the process of frameshifting and bypassing.

As a requisite for establishing a molecular mechanism for L9's function, we implemented a genetic screen to identify physiological situations that are influenced by L9. This screen revealed that L9 suppresses growth defects caused by the inactivation of the essential ribosome biogenesis factor Der and we recently reported a biochemical characterization of this phenomenon [60]. Here, we report that our screen also revealed mutations in two of the three genes that post-translationally modify elongation factor P (EF-P). Deletion of these genes, or *efp* itself, renders cells highly dependent on L9. The post-translational modification of EF-P enhances its ability to stimulate the synthesis of certain polyproline motifs when EF-P engages ribosomes between the P and E sites [81, 130-134].

We discovered that both *der* and *efp* mutants exhibit a reduction in 70S pools and show defects in small subunit maturation; each potentially caused by an inability to meet the high ribosomal protein synthesis demand. L9 does not substitute for Der or EF-P activity; rather, L9 suppresses subunit maturation defects and partially restores pools of 70S particles. Taken together, L9's role in enhancing fidelity seems to most important when free ribosomes become limiting and the demand for high quality protein synthesis is elevated.

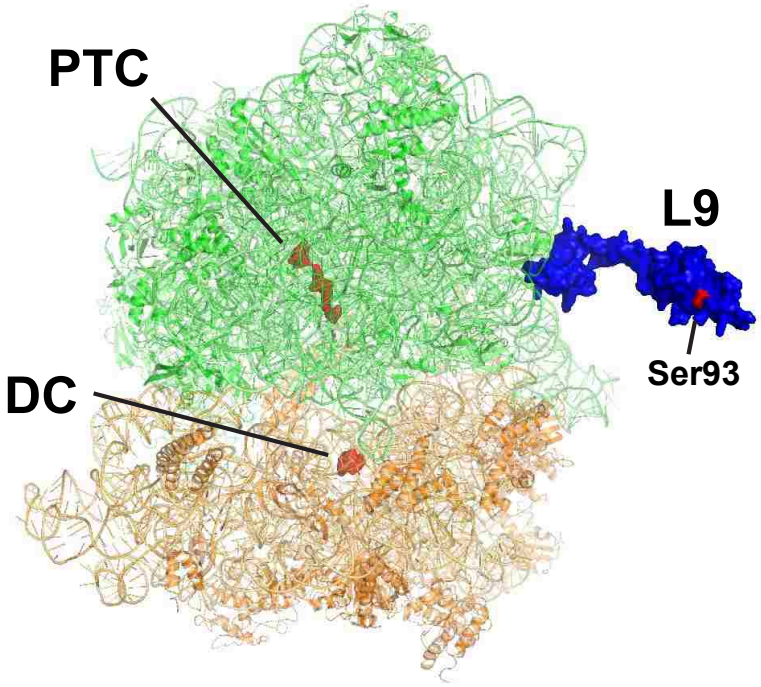

Figure 13: L9 on the ribosome

A crystal structure of the E. coli ribosome is shown with large subunit RNA and proteins in green, small subunit RNA and proteins in orange, and L9 in blue (PDB entries 3R8S and 4GD1). Residues of the peptidyltransferase center (PTC) and decoding center (DC) are shown in red along with the Ser93 residue in L9 that affects decoding fidelity.

Results

L9 increases translation fidelity independently of the miscoding surveillance system.

We evaluated L9's influence on growth in the presence of several well-characterized translation inhibitors and discovered that L9 provides a fitness advantage in the presence of antibiotics that promote miscoding (streptomycin, paromomycin, and neomycin), but not an antibiotic that blocks transpeptidation (chloramphenicol) (Figure 14). Therefore, consistent with reports of L9 increasing the decoding fidelity in a handful of engineered reporter systems, L9 likely acts to increase translation fidelity in general because these miscoding antibiotics indiscriminately act at multiple stages of decoding.

Recent reports describe a translation quality control system in bacteria that employs release factors 2 and 3 to prematurely terminate the synthesis of proteins in ribosomes with mispaired tRNAs in their P- and E-sites [120, 135]. Because mispairing is a requisite for many miscoding events, we considered the possibility that L9 may be involved in regulating this surveillance process, which could readily explain L9's influence on translation fidelity. However, L9 did not influence RF-3-mediated miscoding surveillance (Figure 28). Therefore, L9 increases translation fidelity via another mechanism.

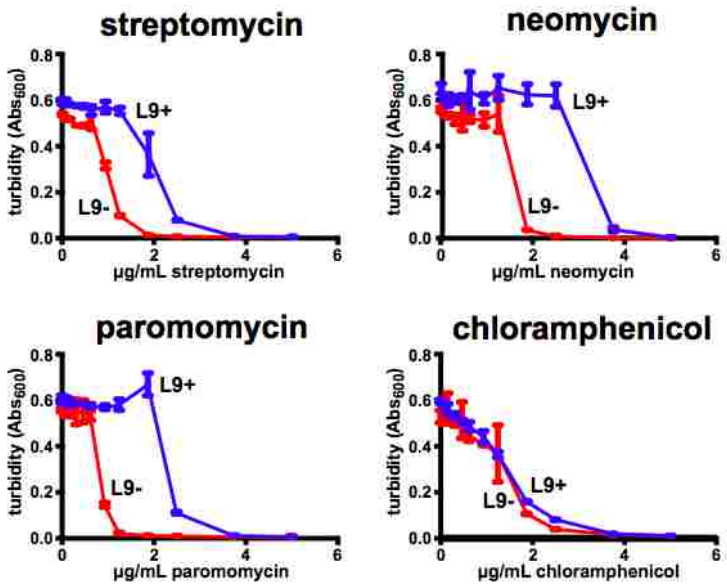

Figure 14: L9 improves resistance to aminoglycoside class of antibiotics.

A *ΔrplI* (L9-) was evaluated for its innate resistance to antibiotics and compared to the isogenic parent (L9+). Consistent with previous reports, the absence of L9 caused only a subtle reduction in growth yield in liquid cultures, but *ΔrplI* colonies are indistinguishable from wild-type. The turbidity of 100 µL cultures grown in a 96-well plate is shown for various concentrations of each drug. The bars are standard deviations from three experiments.

Mutations in EF-P modification genes cause L9 dependence.

Prelimnary attempts to integrate the drug resistance and frameshift reporter data into a mechanistic model for L9 function suggested that there may be unrecognized pathways that are influenced by L9 activity or that compensate for its absence. To identify such factors, we used a synthetic lethal screen to identify *E. coli* mutants that require L9 for fitness [60]. One class of mutants was found in enzymes responsible for post-translationally modifying EF-P [131, 136]. In many bacteria, EF-P is modified by the addition of hydroxyl-β-lysine to a conserved lysine residue and the modification required for enhancing EF-P's established functions [130, 132, 133]. One L9-dependent mutant contained an amber stop-codon in *epmB/yjeK* (*epmB-W15am*), whose product converts α-lysine to β-lysine [137]. In addition, two of the L9-dependent strains contained missense mutations in the predicted active site of EpmA (*epmA-E116K* and *epmA-W117R*, formerly *poxA* or *yjeA*) [81], the enzyme responsible for attaching the β-lysine residue to the highly conserved Lys34 of EF-P. When cured of the L9 support plasmid, each mutant exhibited poor growth, with the *epmA-W117R* mutant displaying the most pronounced phenotype (Figure 15).

We verified that the mutated EF-P-modification genes were responsible for the dependence on L9 by providing wild-type copies of each from a plasmid (Figure 15). We also established that restoring *rplI* in the chromosomal alleviated the sicknesses caused by the mutations in these genes (Figure 16). Finally, we generated new *ΔrplI* strains containing full deletions of *epmA*, *epmB*, and *efp* ORFs. These strains were extremely sick, only forming small

colonies after 24h of incubation, so null alleles were likely missed during our screen because of near-lethal phenotypes (Figure 17).

In some bacteria, β-lysyl-EF-P is additionally hydroxylated by EpmC (formerly, YfcM) [131]. However, we did not recover mutations in *epmC* and a *ΔrplI, ΔepmC* strain grew as well as *epmC+*, which is consistent with reports that this additional hydroxylation does not improve EF-P function [131, 133]. Taken together, these data indicate that complete inactivation EF-P causes a severe dependence on L9 and that our recovered mutants likely produce a low level of active EF-P because they grow better than *Δefp cells* [132].

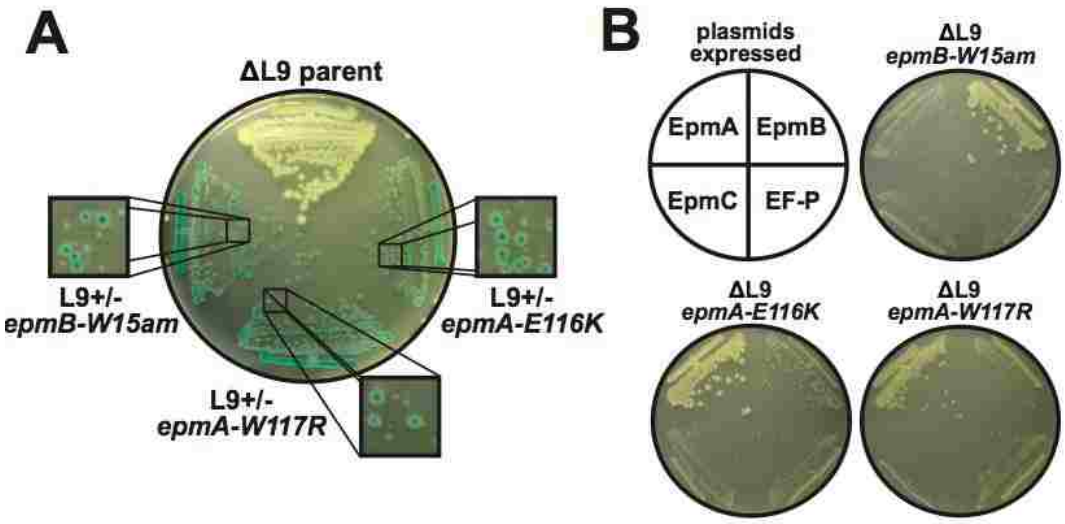

Figure 15: Inactivating EF-P causes L9 dependence

A genetic screen revealed mutants that depend on L9 for fitness. (A) An X-GAL indicator plate streaked with strains harboring a partitioning-defective plasmid that expressed both L9 and LacZ. The parent strain (*Δrpll::tet*) grew well without the L9 plasmid, which was readily lost upon outgrowth. Three recovered L9-dependent mutants contained defects in genes responsible for post-translationally modifying EF-P. The expanded views highlight the growth differences between colonies seeded from a cell containing the L9 plasmid (blue) and those that were seeded from cells without the plasmid (white). (B) The L9-dependent strains were transformed with plasmids that express wild-type versions of EpmA, EpmB, EpmC, or EF-P. Each mutant was only complemented by its respective wild-type allele. The *epmA-W117R* mutant was only partially complemented by excess wild-type, suggesting this mutant is dominant negative.

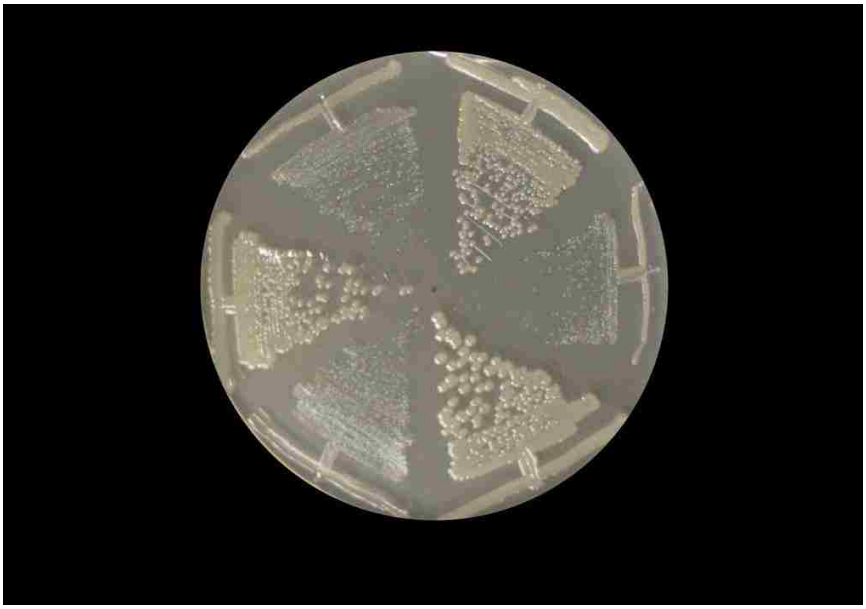

Figure 16: Partial restoration of growth sickness by chromosomal L9

In our intial screening of blue/white colonies in Figure 19, we observed that *epmA-W117R* was sicker compared to the other two mutants. This growth difference was easier to distinguish when the mutants were complemented by L9. The plate contains the three mutants (of *epmA* and *epmB*) that have been cured of plasmid-borne L9 and transduced to replace the chromosomal rplI locus using a cat-marker linked wild-type or ΔrplI. We also carried out liquid culture growth of the mutants, but this did not reflect the increased sickness of the *epmA-W117R* mutant. Moreover, the L9- mutants are easily suppressed in liquid culture and their growth rates are not reliable.

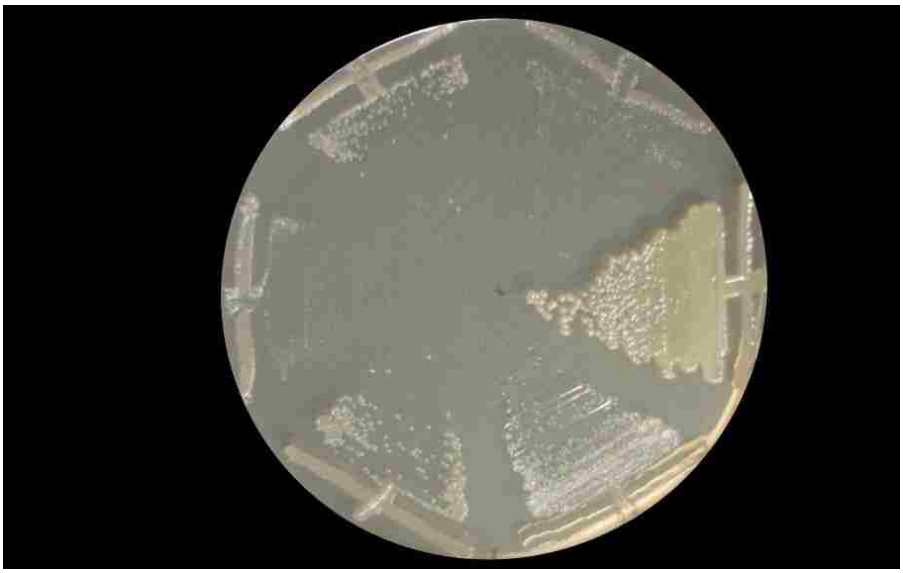

Figure 17: Near-lethal growth phenotypes of double deletion strains.

The growth defect caused by the complete inactivation of *efp* is more severe compared to that of the mutants recovered from the screen, suggesting that the mutants are not completely inactivated. We used recombineering to make strains with a deletion *(ΔrplI::cat*) or a wild-type *(rplI-cat*) L9 locus. P1 transduction was used to replace the existing chromosomal rplI locus in *ΔepmA*, *ΔepmB*, or Δefp.

The conserved architecture of L9 is required for suppression

The necessity of L9 in cells lacking EF-P activity provided a unique platform to interrogate the role of L9's preserved architecture. We engineered several variants of L9 expression plasmids and transformed the ΔrplI, epmA/epmB/efp double mutants to test for complementation. We made constructs that expressed each globular domain, that expressed the hop-1 bypass mutant, or variants with mutations in the connecting helix intended to distort the presentation of the C domain from the surface of the ribosome (a "flexible" linker and a more rigid, "bent" linker) [93, 125]. ΔrplI, epmA/epmB/efp double mutants were too sick for reproducible microbiological analyses, so we focused on characterizing the recovered point mutants.

Each mutant's slow colony growth was suppressed by the L9 variants in the same order: wild-type>flexible>bent>hop-1>C-domain=N-domain=mock (Figure 18). A similar suppression pattern was observed in liquid cultures during exponential growth, but there was more variability, which may have stemmed from the faster-growing escape mutants. In a separate experiment, we established that the *hop-1*, f*lexible* and *bent* L9 versions expressed well form these constructs (Figure 18). Overall, unlike the L9-dependent *der* mutants we previously described, the positioning and quality of L9's C domain clearly impacts its ability to suppress the growth defect caused by a reduction of EF-P activity. This finding reveals an unprecendented connection between the conserved architecture of L9 and translation elongation efficiency.

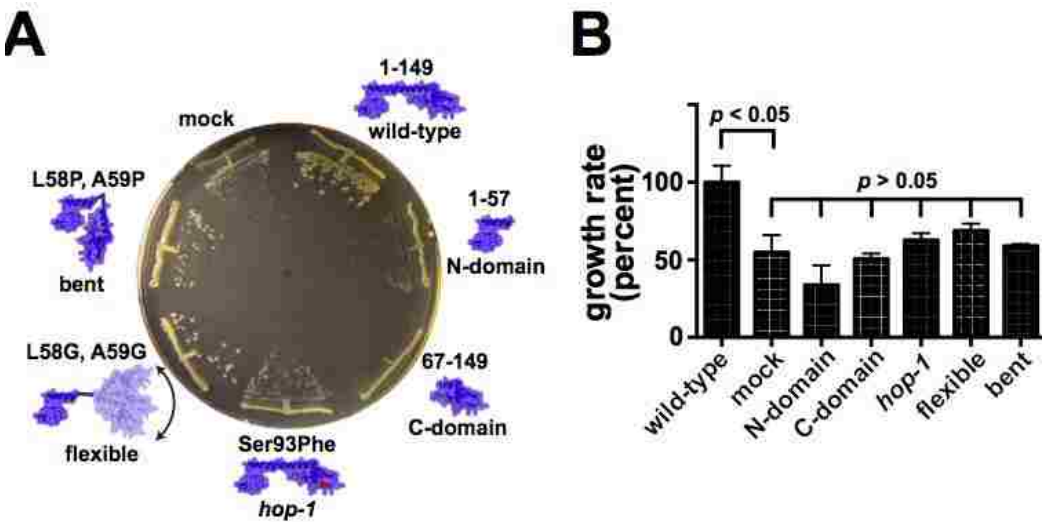

Figure 18: L9's conserved architecture is essential for complementation.

The L9-dependent mutant ΔrplI::tet, epmB-W15am was transformed with a battery of plasmids that express variants of L9. (A) A plate showing the relative colony size differences. (B) Liquid culture data of exponential-phase growth rates for the same strains in panel A. Providing wild-type L9 from a plasmid suppressed the growth defect caused by *epmB-W15am* the most and was indistinguishable from a strain that had the *rplI* gene restored in the chromosome (not shown). The N- and C-terminal domains failed to suppress the mutant and the hop-1, flexible, and bent versions only marginally suppressed it. Error bars indicate the standard deviations of three independent exponential phase growth rate measurements. Despite discernable colony size differences, the p values from Student's t-tests of the liquid culture growth rate data indicate that the growth rate advantage provided by the even most active the L9 variant (flexible) was not substantial.

Cells with inactive EF-P have reduced monosome levels.

Under our preparative conditions, sucrose gradients of *Δefp* lysates were deficient in monosomes relative to polysomes. The level of monosomes relative to the total in *Δefp* cells was reduced by ~50%, which is consistent with a prior study of ribosomes from *Δefp* cells [133] (Figure 19). When sedimented to better separate subunit peaks, the monosomes from *Δefp* cells unexpectedly resolved as two peaks (Figure 19). Using the relative spacing of the wild-type peaks as a metric, we calculated apparent s-values for these monosome peaks as ~67S and ~72S. Interestingly, we routinely observe shoulders on the monosome peaks derived from wild-type cell, which may be caused by the same monosome variants in different relative abundances. We also observed a comparable reduction of monosomes *ΔepmA* cells. Consistent with data in a prior report [138], our *ΔepmB::kan* allele exhibited a strong polar effect that concomitantly reduced EF-P levels (Figure 30), so we did not characterize this strain further. Gel electrophoresis of RNAs purified from the gradient fractions revealed that much of the RNA present in the 30S region of the *Δefp* gradient appeared to be either immature or fragmented (Figure 19) [139, 140] . In addition, in *Δefp* cells the level of 5S rRNA present in the 50S fractions was elevated relative to the level in the monosome peaks, suggesting that there was an accumulation of mature 50S subunits [123, 139]. We did not detect proteins missing form the 30S peak relative to wild-type by Coomassie staining, but small differences may have been masked by an abundance of mature forms. In conjunction with a recent report demonstrating that *Δefp* cells have reduced levels of several translation-related proteins (including KsgA/RsmA, which regulates 16S rRNA processing) [138, 141], these data are consistent with a

model wherein the loss of EF-P activity caused a deficiency of available ribosomes, possibly through a combination of slowed ribosome recycling, imbalanced protein production, and small subunit maturation defects.

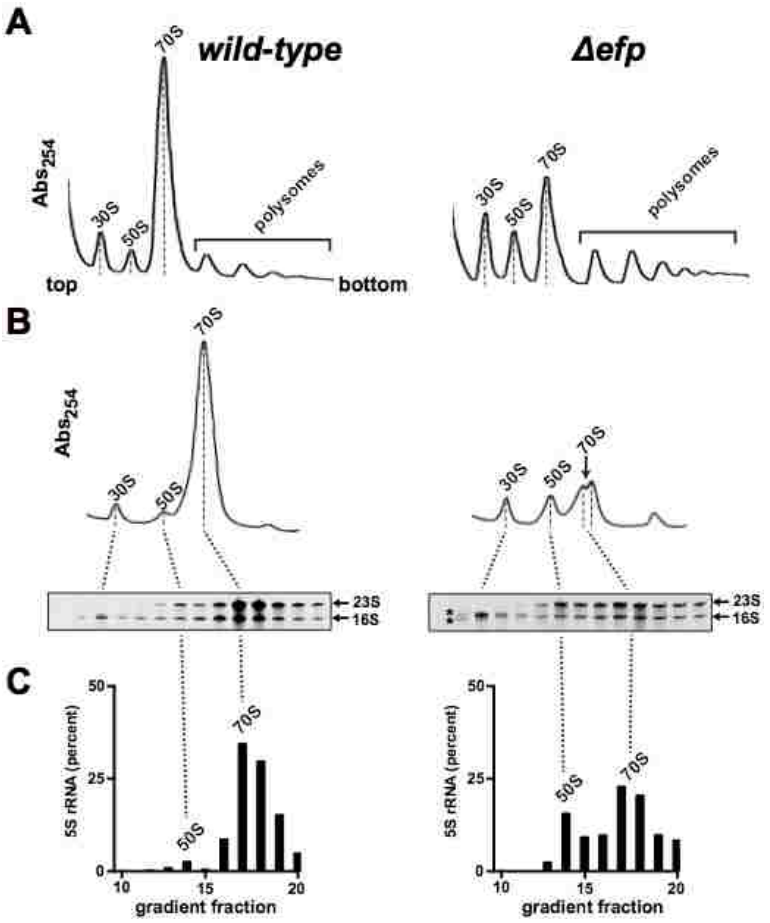

Figure 19: ΔEF-P strains have a severe ribosome deficiency

Lysates of wild-type and Δefp cultures were normalized by their 260 nm absorbance and resolved in linear sucrose gradients. (A) Profiles of each lysate were generated under conditions that resolved polysomes. (B) Gradients that resolved subunits from the same lysates in panel A. The dashed lines mark the peak centers that were used to calculate the s-values of particles and the dotted lines indicate the relative fraction locations. The calculated position of 70S in the Δefp gradient is indicated with an arrow. Under each gradient, denaturing gels stained with SYBR green II dye show RNAs purified from the indicated fractions. In the 30S region of the Δefp gradient, RNAs larger and smaller than mature 16S were abundant (asterisks). (C) In separate gels, the 5S RNA was resolved and quantified from the 50S and 70S peak fractions. The bar graphs show the relative amount of 5S across this region as a percent of the total in those fractions.

Depleting L9 from ΔepmA cells exacerbates the ribosome deficiency.

We sought to characterize L9's influence on ribosome quality in *Δefp* cells to gain insight into L9's mechanism of growth rate suppression. Unfortunately, our *ΔrplI*, *ΔepmA*/*ΔepmB*/*Δefp* double deletion strains were too sick to grow the larger cultures required for ribosome analyses. One strategy to overcome this limitation is to temporarily provide L9 to cells lacking EF-P activity to enhance growth, and then remove L9 at a convenient time for biochemical analyses. To achieve a conditional removal of L9, we employed a targeted protein degradation system to rapidly deplete L9 in *ΔepmA* cells [60, 101]. In this system, a functional variant bearing a C-terminal degradation tag is conditionally degraded by expressing a processive protease (ClpXP) that recognizes the degradation tag. This degradation system rapidly strips and degrades existing L9 from ribosomes and decreases steady-state levels substantially [60]. We established that the tagged L9 versions support the growth of EF-P related mutants as well as untagged L9 (not shown).

We elected to characterize the effects of L9 depletion in *ΔepmA* cells (as opposed to *ΔepmB* or *Δefp*) because they were the healthiest when suppressed by L9 and they did not display additional growth rate reductions when ClpX was absent. After allowing the L9-suppressed ΔepmA culture to enter exponential phase, the degradation system was activated and the cultures were grown for an additional 60 minutes prior to harvesting. Using western blots that monitored L9 levels, L9-deg declined over a period of ~15-30 minutes to a steady-state trace level (not shown). Therefore, this harvest time represents ~30 minutes of growth

with thorough L9 depletion. A parallel control culture contained an L9 variant with a stable tag (L9-cont).

The ribosome quality of the L9-suppressed (L9-cont) ΔepmA culture was reminiscent of a *Δefp* profile, with a heterogenous monosome peak (Figure 20). The depletion of L9 in this mutant caused an additional reduction in monosomes and further accumulation of 30S particles. Interestingly, the relative abundance of the two monosome peaks changed when L9 was depleted, suggesting that these forms are differentially affected by L9 activity. Peak areas from gradients of three independent experiments were quantified and we determined that the relative amount of 30S particles approximately doubled when L9 was depleted where as the level of 50S was essentially unchanged (Figure 31). As with the *Δefp* cells, the 30S peak had an abundance of particles containing immature 16S rRNAs (Figure 20). Upon L9 depletion, the abundance of this immature RNA increased and fragmentation became evident (Figure 20). We also evaluated ribosome quality from the same culture at later harvest time (additional 60 minutes) and the qualitative findings were the same (not shown). Thus, L9's ability to suppress the *ΔepmA* growth is correlated with increased maturation of small subunits and increased monosome abundance.

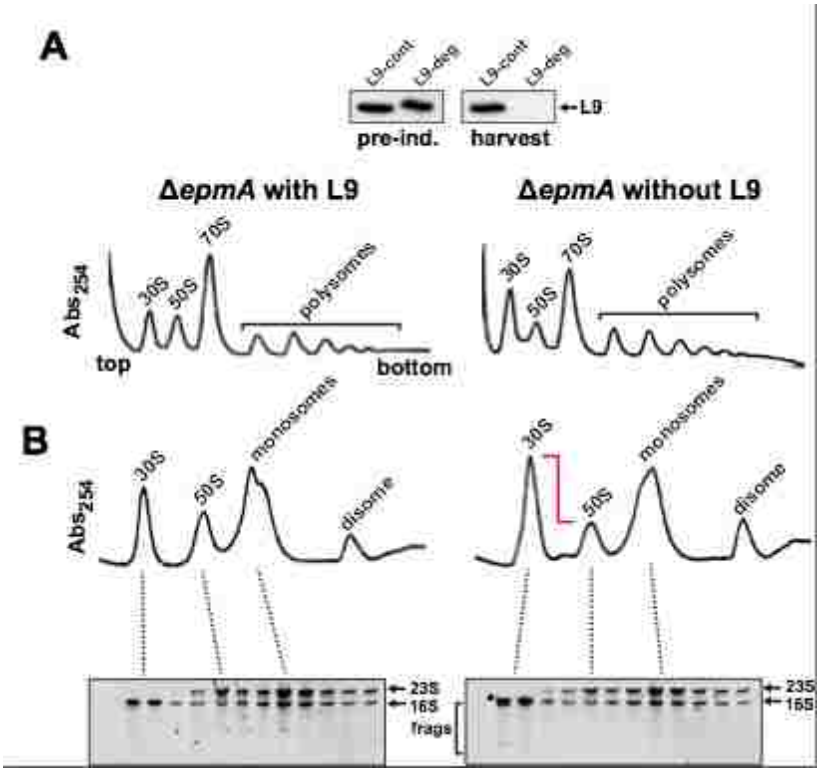

Figure 20: Depleting L9 from *ΔepmA* cells leads to small subunit defects

Cultures of *ΔepmA* cells expressing L9 with either a control or degradation tag were grown to early exponential phase prior to the expression of ClpXP protease to degrade L9-deg. Lysates were then prepared for cell fractionation studies. (A) A Western blot showing L9 levels before induction of the degradation system (pre ind.) and at the time of harvest. L9 was thoroughly depleted in the L9-deg culture, but not in the L9-cont culture (top panel). With L9 support (cells with the stable L9-cont), the ribosome profiles were reminiscent of those from rplI+ Δefp cells, displaying a reduction in monosomes (left panel). In the culture depleted of L9, the monosome pool was further reduced and 30S particles hyper-accumulated. (B) Sucrose gradients that resolved the subunit region for each lysate are shown with gels of purified RNAs. The monosomes resolved as two peaks and the depletion of L9 altered their relative abundances. In addition, 30S particles became more abundant, additional immature 16S rRNA accumulated (asterisk), and RNA fragmentation was evident (frags).

L9 also enhances small subunit quality in a Der mutant.

In a previous report, we showed that muations in Der also cause an L9-dependence that is satisfied solely by the N-terminal ribosome-binding domain [60]. In that study, we implemented the targeted degradation to deplete L9 in a *derT57I* mutant – the more severe of the two recovered der mutants, but we did not evaluate the quality of ribosomes under those conditions. Following our findings in EF-P related strains, we revisited this der mutant to determine if L9 also influences ribosome subunit quality in this background. In cells supported with L9, derT57I exhibited a start deficiency of monosomes and increased 30S and 50S particle abundances, consistent with reports of ribosome assembly defects upon long-term Der depletion (Figure 21) [69, 71, 99]. However, unlike EF-P deficient cells, the monosome peak was more homogenous.

Depleting L9 from the *derT57I* cells caused an additional reduction in monosomes and an accumulation of incompletely processed 30S, similar to the case of ΔepmA (Figure 21). However, unlike the L9 depletion study in ΔepmA cells, these changes in particle abundances were concomitant with a severe fragmentation of 23S RNA (Figure 21). This finding is consistent with a role for L9 in stabilizing the large subunit during late stage assembly when Der activity is limiting. Curiously, in conjunction with these changes, immature 16S RNA is also hyper-accumulated in *derT57I* 30S particles.

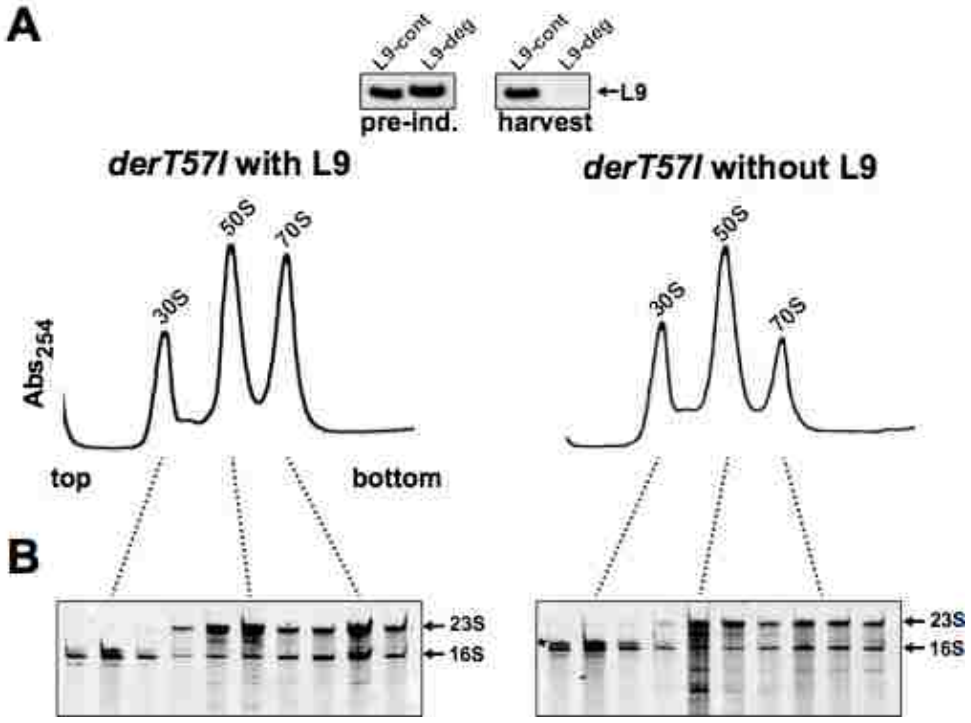

Figure 21: L9 also enhances small subunit quality in Der mutant

Cultures of *derT57I* cells with L9-cont or L9-deg were grown to exponential phase prior to depleting L9-deg. (A) A Western blot evaluated L9 depletion (top). With L9 support (L9-cont), the level of 70S particles was substantially reduced compared to *der+* cells and subunit material accumulated between the 30S and 50S peaks. L9 depletion further reduced the 70S peak. (B) RNA gels revealed that *derT57I* caused an increase in immature 16S rRNA (asterisk) and substantial 23S RNA fragmentation. Depleting L9 exacerbated both of these defects.

ΔrplI cells accumulate immature 16S rRNA in their 30S subunits, but not in their polysomes.

The preceding studies suggested that L9's activity influenced small subunit maturation in two cases in which the monosome pool was compromised for different reasons. Recent reports suggest that when small subunits with immature 16S rRNA enter the translation pool, decoding fidelity is reduced [142, 143]. These findings raised the exciting possibility that L9's established role as a fidelity factor may stem from this same mechanism. Therefore, we examined the quality and distributions of small subunit rRNAs in otherwise wild-type *ΔrplI* cells.

Although an absence of L9 did not affect the abundance of or distributions of ribosomal particles in sucrose gradients (Figure 31), we discovered that the 30S particles from ΔrplI cells contained approximately twice as much immature 16S rRNA when compared to wild-type). Immature 16S rRNA in 70S and polysomes was undetectable using stained gels, and it was previously established that the amount of 17S precursor in 70S particles is low [142]. We felt it was important to quantify 16S precursors in polysomes directly because 70S particles in sucrose gradients are typically a mixture of monosomes (engaged with tRNAs and mRNA) and contrived species formed by excessive magnesium driving idle subunits together, which do not necessarily reflect a competent translational pool. Therefore, we developed a highly sensitive RT-qPCR assay to detect established 16S precursors in polysomes.

In prelimnary experiments, we detected higher levels of immature 16S in polysomes from *ΔrplI* cells. However, because the qPCR method is very sensitive, we determined that this apparent elevation was due to small subunit contamination from top-down fractionations contaminating polysomes with 30S material form higher in the gradients (Figure 22). Therefore,

we fractionated gradients from the bottom-up for this experiment and prepared RNA for qPCR from those pooled polysome fractions.

Normalized RNA samples were subjected to RT-qPCR reactions that detected total 16S, or the “short precursor” (sp16S) or “long precursor” (lp16S) versions of the immature 5’ end [140]. In wild-type polysomes, we detected each immature form (Figure 22). Highly differential detection efficiencies for each species prevented us from establishing precursor to mature ratios using this technique. Surprisingly, the amount of immature 16S was lower in ΔrplI polysomes (~75% of wild-type). We also observed elevated immature 16S in 30S subunits, but not in polysomes, after the activation of the L9 degradation system in otherwise wild-type cells (Figure 22). While this perplexing finding suggests that L9 may be a part of a regulatory mechanism that controls the presence and distribution of immature subunits in the translation pool, an abundance of 16S RNA in polysomes is not likely to be the molecular cause of fidelity loss in *rplI* mutants.

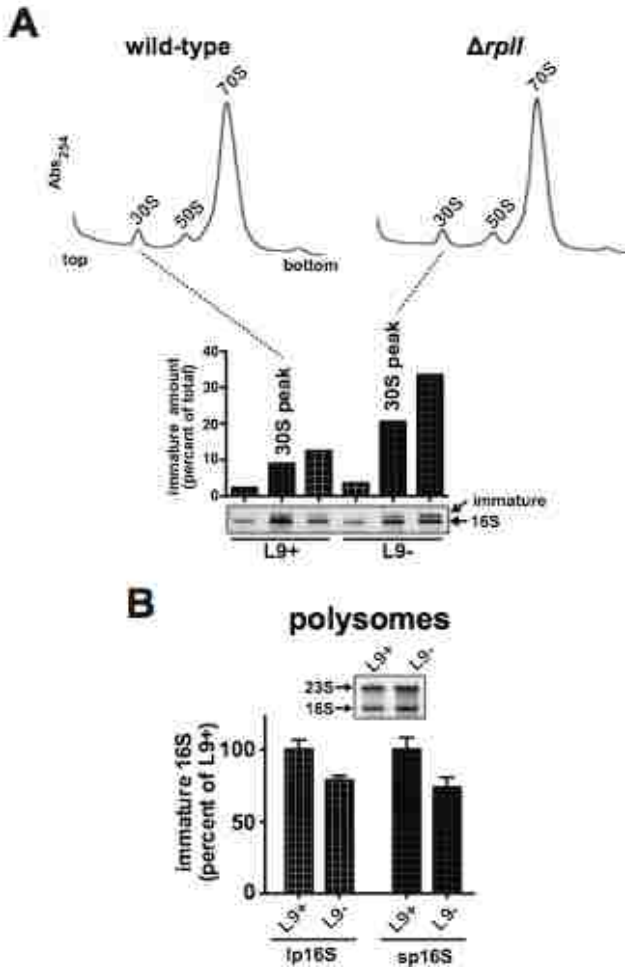

Figure 22: Immature 16S rRNA is found to be more abundant in Δrpll 30S particles but not in Δrpll polysomes

Lysates were prepared from wild-type and Δrpll cells and resolved using sucrose gradients. (A) 30S peak RNAs from each gradient were recovered by fractionating from the top-down, resolved in denaturing gels and stained with SYBR green II prior to densitometry. The quantified immature 16S from this gel is shown as a bar chart with the abundance reported for each of the three peak fractions. (B) Polysome RNA samples were collected using bottom-up fractionation. The inset shows RNA from the recovered polysomes, the immature precursor is not evident. The bar chart shows the abundance of immature lp16S (additional 115 5' nucleotides) and sp16S (additional 66 5' nucleotides) relative to total 16S determined by RT-qPCR. The amount of immature 16S is lower in the polysomes from Δrpll cells despite being overabundant in the 30S particles. Error bars are standard deviations from three measurements.

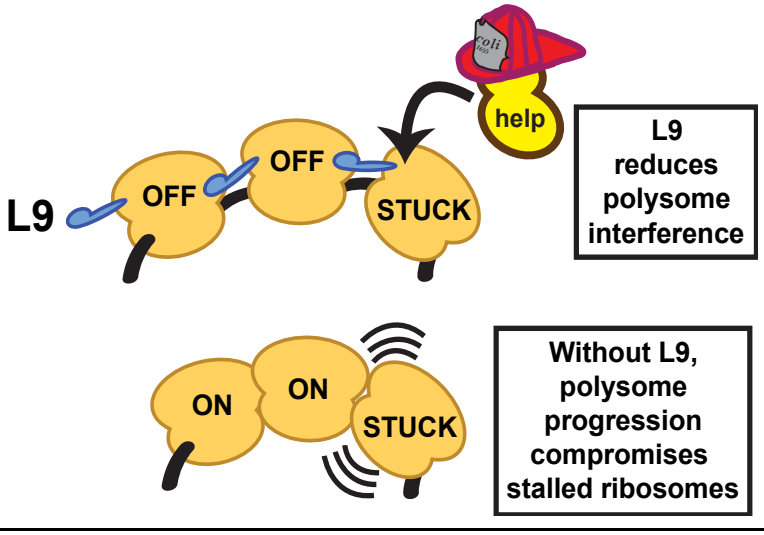

Figure 23: A model for L9's function in decoding

L9 may enhance fidelity of ribosomes in the context of polysomes. In this model, L9's C domain temporarily slows the forward thrust of ribosomes that trail trail ribosomes with unstable decoding center. Without L9, the forward push of trailing ribosomes compromises the stalled lead ribosome.

Discussion

We have uncovered a novel L9/EF-P synergy that stems from L9 partially restoring the pool of 70S particles and improving small subunit maturation when EF-P activity is compromised, which may be linked phenomena. It is important to emphasize that without a full-length, wild-type L9, Δefp cells are nearly inviable, which places special emphasis on the relationship between L9's conserved structure and this particular translation factor. Because L9 also restores the 70S pool in a der mutant, it appears that L9 becomes important when monosomes become limiting. Curiously, there are many plausible ways to disrupt ribosome biogenesis, but all six independently derived L9-dependent mutations were related to either Der or EF-P.

Although several general models related to translation fidelity could explain the observed L9-related physiological changes, an examination of the molecular contacts and the function of L9 during translation will be needed to tease apart a detailed mechanism. ΔrplI cells grow nearly as well as wild-type and we determined that L9 is not required for EF-P's function (Figure 33). Therefore, L9's activity is not likely to be specific to the expression of proteins containing EF-P dependent motifs. Nonetheless, we made an effort to determine if L9 affected the distribution of EF-P in sucrose gradients to see if there was a change in the abundance of EF-P engaged ribosomes. Unfortunately, we were only able to detect unassociated EF-P in the tops of sucrose gradients, not in polysomes (Figure 30). This observation is consistent with a report acts quickly to resolve translation problems [132]. When EF-P activity becomes limiting or absent, the life-time of stalled ribosomes is expected to increase and allow for other

molecular events to influence the translation of those messages (such as advancing mRNA degradation, crowding ribosomes, or activating toxin systems). As a corollary, the rRNA found in 30S particles from *Δefp* is reminiscent of the rRNAs generated by the action of the MazF toxin, so we are inspired to characterize the influence of this RNase on L9-related events in future work. Translation pauses also occur during miscoding events, programmed stalling, and at internal SD sequences [62]. A simple mechanism for an L9 activity affecting translation fidelity under a variety of circumstances would be for L9 to temporarily shut down trailing ribosomes to prevent their forward thrust from unseating or crowding stalled ribosomes (Figure 23). In support of this model, L9 forms a bridge between adjacent ribosomes in crystal structures and occludes the binding of factors at adjacent GTPase-activating centers [127, 128]. Likewise, the GTPase-activating center of a trailing ribosome would be occluded by L9 if stalled polysomes condense to a similar state.

In case of Der, there is evidence that the large subunits produced in Der's absence are structurally compromised (hypersensitive to Mg depletion) [69]. Although the same model for L9 function would allow enhanced protection of stalled ribosomes with unstable large subunits, only the ribosome-binding N domain of L9 is required to suppress the Der defect. In addition, L9 is reported to be one of the few proteins that dissociates from large subunits produced in Der's absence when Mg is depleted in vitro, so it seems that L9 aids in stabilizing a mature 50S conformation and partially compensates for a slow maturation step.

Immature small subunits over accumulate when L9 is absent and this increase is correlated with L9's suppression activity in both der and efp mutants. Others have reported

that small subunit maturation is also impaired by sub-lethal doses of aminoglycosides [144]. By rapidly depleting L9 in the *derT57I* mutant, we discovered that immature 16S accumulation is a downstream consequence of a large subunit defect. There are several possible explanations for a delay in SSU maturation, including a deficiency in the quality or production of small subunit proteins or processing RNases. However, genes associated with translation fidelity and stringent response were wild-type in fast-growing Δefp strains we analyzed (Table S1). Continuing this effort, we recently sequenced the genomes of several fast-growing Δefp and ΔrplI/Δefp escape mutants and tentatively identified the mutations responsible. The identified mutations are not in ribosomal genes or in any genes associated with ribosome production in the literature.

The RNA processing of the 16S 5' end is regulated by the methylation activity of KsgA, one of the several proteins found to be deficient in cells lacking EF-P activity [138, 141]. However, providing additional copies of ksgA and other biogenesis genes on plasmids did not enhance the growth of Δefp mutants (

Table 2. Cloned genes tested for multi-copy suppression of Δefp sickness.). Nonetheless, a late stage in small subunit production is a logical place for regulating the flow of small subunits into the translation pool, a model previously suggested by others [145-147]. Because we observed immature 16S hyper-accumulation in three different genetic backgrounds, we cautiously suggest that elevated 17S rRNA in small subunits is an effect rather than a cause, of some associated physiologies. Moreover, the amount of immature 16S we detected in polysomes is very low (and affected by trace contamination from preceding gradient fractions), so it is hard to justify major physiological influences of immature 16S in polysomes. L9 may influence 30S maturation by helping to orchestrate stoichiometric activation of subunits to reduce wasteful idling and subunit turnover in the absence of partners. Such a regulation would be optimal at late stages in assembly, after the established feedback checkpoints governing ribosomal RNA and protein production.

Materials and methods.

Strains and plasmids

Strain TB28 (MG1655, *lacZYIA::frt*) was designated as wild-type for this study. The generation of the rplI deletion strain and the unstable plasmid expressing L9 have been described previously [60]. EF-P, EpmA, and L9 expression plasmids were cloned into derivatives of pTrc-99a. Strain BW30270 (K12 MG1655 rph+; CGSC #7925) was used in addition to TB28 for the antibiotic sensitivity studies. A streptomycin-resistant strain, rpsL25 (CGSC #5522) was used

as a positive control to ensure that the streptomycin was responsible for the dose-dependent toxicity. *ΔrplI::tet* and *ΔprfC::kan* (KEIO #JW5873) were transduced into BW30270 for RF-3 studies and verified by PCR [60, 148]. RF-3 influenced frameshift reporter plasmids were previously described (a kind gift from Hani Zaher, Washington University, St. Louis) [120]. Ribosome biogenesis genes and initiation factor clones from the ASKA library were used for complementation tests (kindly provided by Gloria Culver, University of Rochester) [149].

Screening for L9-dependent mutants

The EF-P related L9-dependent mutants were recovered from a previous screen [60]. Briefly, an unstable plasmid harboring the only copies of *rplI* and *lacZ* were transformed into an *ΔrplI::tet* TB28 derivative. A chemically mutated library was then generated and screened for blue colonies (containing cells that needed the unstable plasmid to grow well). The locations of the *epmA* and *epmB* alleles were narrowed using co-transduction mapping using a random-insertion transposon donor library. The mapped regions were then sequenced. Each mapped region had only the reported mutation and *efp*, *epmC*, and *der* were wild-type. Also, *Δefp* and the previously identified L9-dependent *derT57I* allele were not synthetically lethal with each other [60].

Ribosome analyses

Cultures were mixed with an equal volume of crushed ice made with HT-10 buffer [20 mM HEPES-Tris, 100 mM K+-glutamate, and 10.5 mM magnesium acetate, 0.05 mM EDTA, pH

7.8] prior to harvest. 100X lysates were prepared in HT-10 suppremented with 0.05% Tween-20, 14 mM 2-mercaptoethanol, 20 U/mL RNase inhibitor (Roche), 20 U/mL DNase (NEB), 0.5 mM calcium chloride, and 0.1 mg/mL lysozyme and frozen at -80°C.

Lysates were cleared by centrifugation, normalized by 260 nm absorbance, and aliquots layered into either 10-40% (polysomes) or 10-30% (subunit) sucrose gradients prepared with supplemental HT-10 using a gradient master (Biocomp) and centrifuged in an SW-41 rotor (Beckman) at 35,000 (151,000 g)/ 40,000 (197,000 g) for 2.5/ 4 hours respectively. Profiles were recorded during fractionation with a gradient fractionator (Brandel) or by collecting samples from the bottom (Beckman). Fractions were stored at -80°C. RNA was extracted from the fractions by guandinium thiocyanate-acidic phenol chloroform extraction as previously described [150, 151]. Addition of chloramphenicol, a transpeptidation inhibitor to cultures has been used previously to stabilize polysomes during culture harvest [80]. We observed no substantial difference in gradients of lysates pre-treated with 100 μg/mL chloramphenicol. Primers that amplified the 5' ends of the target open reading frames or 16S rRNA species were used for real-time quantitative PCR [101].

Targeted L9 degradation

The L9 degradation system was previously described [60, 101]. Briefly, ΔepmA::kan, ΔclpX, rplI-tag strains carrying an inducible protease system (pClpXP) was cultured in exponential phase after induction by diluting cultures into fresh medium containing arabinose. The depletion of L9 was monitored as a function of induction time using Westerns. After

approximately 30 minutes of protease induction, L9 levels declined to trace levels. The depletion of L9 was also verified in the harvested samples.

CHAPTER IV: DISCUSSION

New details of bacterial protein synthesis and the molecular stages of the translation process have emerged in the last 10 years; however, the contribution of r-proteins like L9 in translation is yet to be fully recognized. The remote location of L9 on the large subunit of the ribosome complicates its assignment in translation fidelity. Moreover, L9 is non-essential for growth under laboratory conditions. In this study, we identified and characterized two cellular conditions that require L9 for fitness. One L9-dependent condition is caused by mutations in an essential GTPase called Der and the other L9-dependent condition is caused by the loss of function of elongation factor, P (EF-P).

Interestingly, we did not detect a synthetic lethal interaction between Der and EF-P. Thus, the physiological requirement for L9 in each case stems from a different underlying problem. We also established that each condition requires a different aspect of L9's unique architecture for growth complementation (Figure 8, Figure 18). We observed that L9 has no direct influence on either Der's GTPase activity (Figure 25) or EF-P's activity in translation (Figure 33). Instead, L9 influences the quality of ribosomes when either Der or EF-P is inactive (Figure 20, Figure 21). Our observations lay the foundation to develop and test different models to mechanistically determine whether L9 has a direct role in decoding fidelity or in ribosome biogenesis. L9 may improve ribosomal subunit maturation under certain conditions, influence the selection of mature subunits for translation intiation, or alter ribosome occupancy via inter-ribosomal communication during translation.

We observed that both classes of L9 dependent conditions exhibited increased accumulation of 16S precursor rRNA at the 30S fraction, a phenotype that worsened upon L9 depletion. The accumulation of precursor 16S rRNA is a commonly observed side-effect of both the 50S and 30S assembly defects [69, 110, 139, 142, 152]. Although Der is involved in 50S biogenesis, we and others have detected 16S rRNA precursors in Der-defective strains. If L9 actively participates in the maturation of either the 30S or the 50S subunit, L9- cells should have increased total precursor rRNA compared to wild-type. Furthermore, the presence of immature 16S rRNA has been associated with increased miscoding and the crystal structure of immature 30S particles exhibit distortions at the decoding center [140, 142, 143, 152, 153]. Considering L9's role in fidelity, we entertained the idea that delayed 30S maturation may be the reason for the decreased fidelity of L9- cells. Although we observed increased accumulation of 16S precursor in the 30S fraction of L9- cells (Figure 22), we showed using RT-qPCR that L9- polysomes had lower amounts of precursor than polysomes from wild-type. Polysomes represent bulk of the translating ribosomes in the cell. Therefore, actively translating ribosomes of L9- cells do not contain more total precursor rRNA than wild-type. Furthermore, there is no evidence of active site distortions (caused by precursors) in crystal structures of L9- ribosomes [126-128]. Taken together, L9 may influence the redistribution of the precursor rRNA-containing subunits during translation rather than its accumulation itself. This places L9 as part of a mechanism that inspects and differentiates mature from immature subunits before they enter the translation pool.

The initiation of translation begins with the formation of the preinitiation complex which consists of the 30S subunit, mRNA, initiator tRNA (fmet-tRNA), and initation factors [154]. The maturation of the 30S subunit is therefore the rate-limiting step for translation initiation. What prevents immature 30S subunits from forming preintiation complexes? Recent studies have discovered mechanisms that monitor the quality of subunits entering the translation pool [42, 147, 155-157]. Such systems either eliminate incompletely assembled subunits or place a short-term delay on small subunit maturation to prevent incorporation of immature subunits in translation. The complete maturation of rRNA involves multiple steps and this allows the cell multiple layers of regulation by which it can control the rate of rRNA processing, and thereby control ribosome assembly. The highly conserved nature of the leader and the spacer regions of the 16S rRNA and its importance in proper 30S maturation supports such a regulatory mechanism [158, 159].

Given our observations of ribosomal abnormalities, we considered how L9 might influence ribosome quality. We observed a 70S deficiency in both Der and EF-P mutants. The N-terminal, ribosome binding domain of L9 fully complements *der* mutants (Figure 8). Under conditions where 50S biogenesis is affected (as seen in *der* mutants), mature 50S subunits are scarce and the immature 50S particles are unstable [69]. The depletion of L9 exacerbates 70S deficiency, likely causing a delay in the maturation of the 30S (observed as increased precursor accumulation) and the degradation of inactive 50S subunits (observed as fragmented 23S rRNA) (Figure 21). L9 may improve 70S abundance by stabilizing the on-pathway 50S intermediates

and improving the efficiency with which it associates with the preinitiation complex. This explains the increased accumulation of inactive 50S subunits in the L9-depleted *der* mutant.

In the absence of *efp*, we observed severe small subunit defects and an indication of mature 50S accumulation (Figure 20). The depletion of L9 in the EpmA- strain also likely creates a delay in 30S maturation (causing increased accumulation of precursors). However, there was no indication of a 50S defect in the absence of EF-P activity, indicating that the cause of 70S deficiency in each class of L9-dependent mutants is different. Because the relative positions of the N and C domains are critical for growth suppression of *efp* mutants, it is possible that the C domain of L9 improves subunit association during translation initiation by increasing interaction between mature 50S and 30S preinitiation complexes. Although there is no evidence of L9 directly associating with preinitiation complexes, there is evidence of the C domain of L9 contacting the 30S subunit in crystal structures [126-128]. So far, our data support the conclusion that L9 does not directly participate in Der's or EF-P's activity; instead L9 somehow improves the quality of ribosomes entering translation. This model of L9's involvement in subunit selection or association during translation initiation provides an explanation for L9's location on the 50S subunit (required by Der mutants) and the highly extended structure of full-length L9 (required in EF-P deficient cells).

A recent cryo-EM structure of Der bound to the ribosome shows that it causes significant conformational changes to the 23S rRNA helices of the 50S subunit [160] . These conformations of the Der-bound 23S rRNA resembles those seen in a late-stage intermediate of the 50S [143]. Because Der has an established biogenesis function, it is conceivable that the

GTP hydrolysis of Der may allow the progression of a 50S intermediate into complete maturation and serve as a checkpoint during assembly. However, Der's GTPase hydrolysis rate is also significantly increased in the presence of 50S subunits [160]. Such an activation by mature 50S subunits argues against a direct role for Der in 50S maturation. Instead, Der could serve as a molecular switch on the ribosome that is required to regenerate 50S subunits after translation. The GTPase activity can provide the mechanical force required to recycle 50S subunits at the end of translation. Der mutants that are defective in GTP binding cannot bind to 50S, thus the lack of Der's GTPase activity may prevent the 50S subunits from either entering translation or being recycled efficiencty. There is precedent for such a checkpoint in eukaryotes [161, 162]. Whether Der participates directly in *de novo* 50S biogenesis or in 50S recycling, both cases explain why the GTPase-defective Der mutants in our study showed a severe 70S deficiency with a concomitant increase in absorbance at the 50S region. Intriguingly, YihI, a factor that stimulates GTPase activity of Der *in vitro* complements the growth of *der* mutants without directly stimulating mutant enzyme activity (Figure 11). It is possible that YihI may improve the ability of the 50S to increase GTPase activity of Der *in vivo*, supporting the idea that Der's interaction with 50S is required for its function.

It is important to note that the biogenesis defects seen in EF-P- cells can be a secondary effect caused by either increased buildup of ribosomes on poly-proline messages or decreased translation of a specific biogenesis or maturation factor. EF-P substrates are ribosomes that are stalled in during translation caused by a difficult PTC chemistry [72, 81, 130-132]. Therefore, it is important to consider a direct influence of L9 on translation. We established that L9 does not

directly participate in translation of EF-P-dependent transcripts (containing poly-proline) (Figure 33).

L9, along with the L1 stalk forms one of the most flexible regions of the ribosome. The role of the L1 stalk in translocation is well understood and its movement is known to be coupled to intersubunit rotation. In addition to interacting with the translocating tRNA, the L1 stalk also contacts parts of the 30S subunit [163-165]. The role of L1 in intersubunit movements and the presence of L9 at the base of the L1 stalk suggests that L9 may also influence large scale ribosomal movements. A cryoEM modelling of bacterial polysomes by Brandt et al., shows the the C-terminal domain L9 contacting the 30S subunit of a neighboring ribosome [166]. Recent crystal structures of elongation factors, EF-G and EF-Tu support the idea that L9 may contact a neighnoring ribosome during translation. L9 sterically interferes with the crystallization of the binding sites for these elongation factors [89, 167-169]. We observed an increase in the fraction of polysomes to free ribosomes in EF-P- cells (Figure 19), likely caused by increased stalling of actively translating ribosomes on polyproline messages. This accumulation of ribosomes on a single mRNA can put increased pressure on adjacent ribosomes to either fall off or shift the reading frame. Given the structural evidence of inter-ribosomal contact by L9, it is plausible that L9 of a stalled ribosome contacts the preceding ribosome. This physical contact by L9 can help temporarily relieve the forward thrust on the stalled ribosome, thus allowing time for the slow peptide bond formation to be resolved so that proteins can be synthesized properly. A role in inter-ribosomal contact places L9 as a regulator of reading frame maintenance, a role

previously discussed for L9 [88, 124]. This model also provides a simple explanation for L9's role in translation fidelity.

APPENDIX A: CHAPTER II SUPPLEMENTAL INFORMATION

Strains and plasmids

The unstable L9 expression / reporter plasmid (pRC-L9) was derived from pRC-7 (an ampicillin-resistant, mini-F plasmid with a defective partitioning locus, par-) [63]. To ensure high level expression of L9, the P_{trc} promoter from pTrc99a, which drove the expression of both L9 and LacZ, replaced the P_{lacZYA} promoter in pRC-7. LacZ expression was subsequently attenuated by randomizing two nucleotides in its ribosome-binding site and selecting for a clone that gave sufficient blue color on X-Gal / IPTG plates for screening without hindering cell growth. This plasmid also contains $lacI^Q$; however, expression from the P_{trc} promoter is not fully repressed on glucose medium, is moderate on glycerol medium, and strong when IPTG is present [64].

Mutation mapping.

Mutant strains exhibiting a dependence on plasmid-borne and chromosomal *rplI* for fast growth were selected for mapping. Each was cured of the pRCL9 plasmid (which rendered them slow growing) and then infected with a P1 phage lysate derived from a random-insertion, kanamycin-resistant transposon library formed in MG1655 (a gift from Thomas Bernhardt, Harvard University). Fast-growing kan_R tet_R transductants had the L9-dependence mutation replaced by a wild-type gene from the donor library and the mutation location was within a P1 genome length of the kan_R transposon [102]. A new P1 lysate was formed from fast-growing kan^R transductants and used to re-infect the original mutant strains. This analysis revealed that the recovered mutations fell into two complementation groups of three mutants each (a kan^R

marker near a given mutation was able to restore fast growth to separately-isolated mutants in the same group). Moreover, the ratio of fast- to slow-growing *kan*^{R} transductants reflected the distance of a given *kan*^{R} marker to each L9-dependent mutation [170]. The insertion locations of transposons near each mutant locus were identified using arbitrary PCR and DNA sequencing using a primer that annealed within the transposon (EZ-Tn5, Epicentre) [171]. These locations were plotted against the frequency that each marker that rescued the slow-growth phenotype to generate a plot that revealed the locations in the chromosome with the highest probabilities of containing the L9-dependent mutations. Sections of the genome in these regions (~5 kb each) were then amplified using PCR and sequenced. Only one mutation was found in each mapped region.

Protein expression and purification.

YihI-FLAG-His_6 and L9-FLAG-His_6 were purified using a C-terminal FLAG-His_6 tag after being overexpressed from clones in pTrc99a at 37°C in DH5-alpha. After induction with IPTG for 3 hours, cells expressing L9-FLAG-His_6 were harvested and washed in 1/10 the original volume with Cell Wash Buffer (25 mM K_+-HEPES, 100 mM K_+-Glutamate, pH 7.5). Overexpressed L9 is largely insoluble, but can be refolded from denaturing conditions. Therefore, expression cells were lysed in 1/200 the original volume with Denaturing Buffer (6 M guanidine hydrochloride, 25 mM K_+-HEPES, 0.05% Tween-20, 14 mM 2-mercaptoethanol, and 2 mM imidazole, pH 7.5). The lysate was centrifuged at 16,000 × g for 20 minutes to remove insoluble debris and the

supernatant was mixed with pre-rinsed Ni^{++}-NTA resin (Qiagen, 1 ml per harvested liter) and agitated at 4°C for 30 min. The resin was then collected by centrifugation, transferred to 0.45 µm pore centrifugal filter (Costar) and washed with four bed volumes of Denaturing Buffer containing 12 mM imidazole followed by six bed volumes of Desalting Buffer (10 mM Tris-Cl, pH 8.0) to refold the protein on the column. Soluble protein was then eluted in Native Buffer (25 mM K_+-HEPES, 100 mM K_+-glutamate, 0.05 % Tween-20, 5 % glycerol, pH 8.0) supplemented with 333 mM Imidazole. Refolded L9-FLAG-His_6 was further purified by binding to hydroxyapatite resin (Bio-Rad), washed with Native Buffer supplemented with 100 mM KH_2PO_4, and eluted with buffer containing 250 mM KH_2PO_4. The protein was finally exchanged into Buffer A (20 mM Tris-HCl, 25 mM NaCl, 0.05% Tween-20, 5% glycerol, and 5 mM 2-mercaptoethanol, pH 8.0) using pre-equilibrated size-exclusion spin columns (Bio-Rad, Biospin-6). For expression of untagged Der, the der gene (wild-type and mutant) was cloned into a T7-expression vector (pET-3a, Novagen). Strain SM1192 (a recA- ER2556 derivative, NEB) was transformed with untagged wild-type or mutant pET-Der. At mid-exponential phase, the cultures were induced with 0.5 mM IPTG for three hours. The cultures were then iced, harvested, and washed in 1/10 of the original volume (20 mM Tris-HCl, 100 mM NaCl, pH 8.0). Cells were lysed in 1/400 the original volume with Lysis Solution (1 X BPER (Pierce) supplemented with 0.25 mg/mL lysozyme, 14 mM 2- mercaptoethanol, 1 mM EDTA, and protease inhibitor cocktail (Roche)) at room temperature for 15 minutes. Following lysis, an equal volume of Nuclease Solution was added (20 mM Tris-HCl, 100 mM NaCl, 5 mM 2-Mercaptoethanol, 0.05 % Tween-20, 5% glycerol, 4 mM $MgCl_2$, and Benzonase (25 U/mL,

Sigma)). Once viscosity reduced, the lysate was cleared at 16,000 × g for 5 minutes and the soluble fraction was diluted, mixed with anion exchange resin (Hi-trap Q, Pierce), prewashed in Buffer A. The resin was washed with Buffer A containing 275 mM NaCl and the protein eluted in Buffer A containing 1M NaCl. The eluate was diluted with water, and pre-washed hydroxyapatite was added (Bio-Rad). After binding, the resin was transferred to a gravity column and washed with Buffer B (25 mM K_+-HEPES pH 7.4, 0.05% Tween-20, 5% glycerol, and 5 mM 2-mercaptoethanol). The resin was washed in Buffer B congaing 125 mM KH_2PO_4 and Der was eluted with 250 mM KH_2PO_4. The eluate was then chilled on ice and an equal volume of ice-cold 3 M ammonium sulfate was added to precipitate Der. The precipitated protein was re-suspended in Buffer A. After clearing insoluble material, the protein was again bound to anion exchange resin in Buffer C (25 mM K_+-MES, 25 mM NaCl, 0.05 % Tween-20, 5 mM mercaptoethanol, and 5 % Glycerol, pH 5.75), washed with 250 mM NaCl, and eluted with 500 mM NaCl. Most purification steps were carried out at 4 °C. Before storage and quantification, all proteins were buffer exchanged into Buffer A. Potassium activation of Der and YihI stimulation. Der GTPase activity was monitored with increasing concentrations of KCl with and without YihI. At 500 mM KCl, Der was stimulated ~15-fold (Figure 24**,** *panel A*, left side). Near-saturating YihI (5 µM) increased the rate without potassium ~3-fold, but did not stimulate at concentrations above ~250 mM (Figure 24**,** *panel B* right side). The ratio between these data sets was used to generate the fold-stimulation plot in Figure 11**,** *panel B*. Measuring an affinity between Der and YihI. The GTPase rate of 0.5 µM Der in 100 mM KCl was monitored as a function of added YihI. The GTPase rates were first plotted against total YihI for fitting to obtain

the maximal stimulation by YihI. This value represented fully-occupied Der at 0.5 µM, which is also the amount of YihI bound. The total YihI values in the data set were then adjusted by subtracting the amount bound to Der (using the observed GTPase rates) to obtain the unbound fractions of YihI. Re-plotting of the data allowed for a determination of K_d (Figure 24**,** *panel B*).

Evaluating L9's influence on Der activity. L9-FLAG-His_6 complemented the slow-growth phenotypes of the *der* mutants as well as untagged L9 (Figure 12 and not shown). L9-FLAG-His_6 was purified and added to GTPase assays in a 10-fold excess over the tested Der (0.5 µM wild-type, 2.0 µM mutant), with and without 5 µM YihI. Neither the basal nor the YihI-stimulated GTPase rates were affected by L9 (Figure 25).

Plating efficiency and morphology of L9-depleted derT57I cells.

Cultures of *rplI-cont/deg*, Δ*clpX*, *derT57I* harboring pClpXP were induced to promote L9 degradation as described in Figure 12. Samples of the cultures were plated to determine the colony forming units as a function of the turbidity at the time of sampling. The resulting data were fit to a first-order decay model with a plateau constant representing the limit at infinite time. The depletion of L9 in the *rplI-deg*, *derT57I* culture caused a reduction in plating efficiency by ~60 % (Figure 26). We considered the possibility that the Der defect may reduce expression of β-lactamase, which could also cause a reduction in viability under these conditions. We tested this idea by comparing the plating efficiencies of L9-, *derT57I* cells transformed with plasmids conferring ampicillin resistance (bla, periplasmic) to those that confer resistance to tetracycline (*tetR*, inner membrane) and chloramphenicol (*catR*, cytoplasmic). We observed no

differences in the plating efficiencies between these strains (not shown). Therefore, the observed reduction in plating efficiency when L9 was removed was not from a reduction in β-lactamase secretion.

Translation bypass assays.

We constructed a series of plasmids encoding translation bypass reporters based on those used to identify the original *hop-1* L9 mutant that first linked L9's function to translation fidelity (*rplIS93F*) [58]. In these reporters, sections of the phage T4 gene 60 were fused to lacZ. Gene60 translation invokes a remarkable 50-nucleotide bypass during translation to generate the encoded enzyme. This bypass requires several features in the nascent peptide and mRNA to drive the release of the ribosome and to repositioning it at the appropriate landing site [91, 172]. The quantitative assay then measures the amount of 60-LacZ fusion produced using Miller assays. We were struck by an obvious lack of reproducibility in our assays using wild-type cells with the reporter constructs. In our hands, typical variance in a Miller assay is ~5%, yet we were observing greater than 50% changes between experiments using the same reporter construct on different days (Figure 27**,** *panel A*). We traced the cause of this variance to an uncanny instability of the reporter plasmid. Although the cells were grown under antibiotic selection, many of them lost the plasmid as the cultures grew, as if partitioning had become defective. This was not observed in cultures harboring variants without the *gene 60* bypass segment. We went on to re-clone the reporter construct into a different plasmid backbone with a different origin and observed the same instability (not shown). Remarkably, we observed that L9 seems

to reduce the instability (Figure 27**,** *panel B*). In addition, we isolated the reporter plasmid from dark blue L9- colonies, re-sequenced, and re-transformed naïve strains and observed the same phenomenon. Aside from revealing that these constructs are inappropriate for evaluating L9 or Der's role in bypassing, these results suggest that the original screen for increased translation bypass that identified *hop-1* may have, in some fashion, selected for plasmid stability.

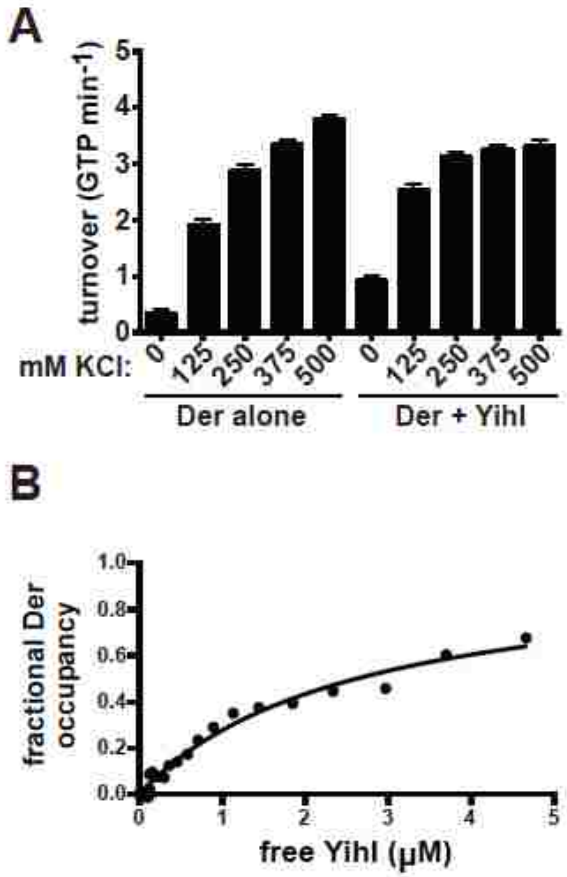

Figure 24: S1. Potassium and YihI stimulation.

Der GTPase activity (0.5 μM) with increasing KCl. On the right, Der in the presence of 5 μM YihI. At higher concentrations of KCl, YihI no longer stimulated Der and slightly inhibited it. Panel B, in our standard assay condition (100 mM KCl), the stimulation of wild-type Der (0.5 μM) with increasing YihI-FLAG-His6 concentrationswas used to determine an affinity constant between the two proteins. Three GTPase measurements at each YihI concentration were averaged and plotted against the fraction of Der occupied by YihI to obtain a Kd of 2.6 μM ± 0.6.

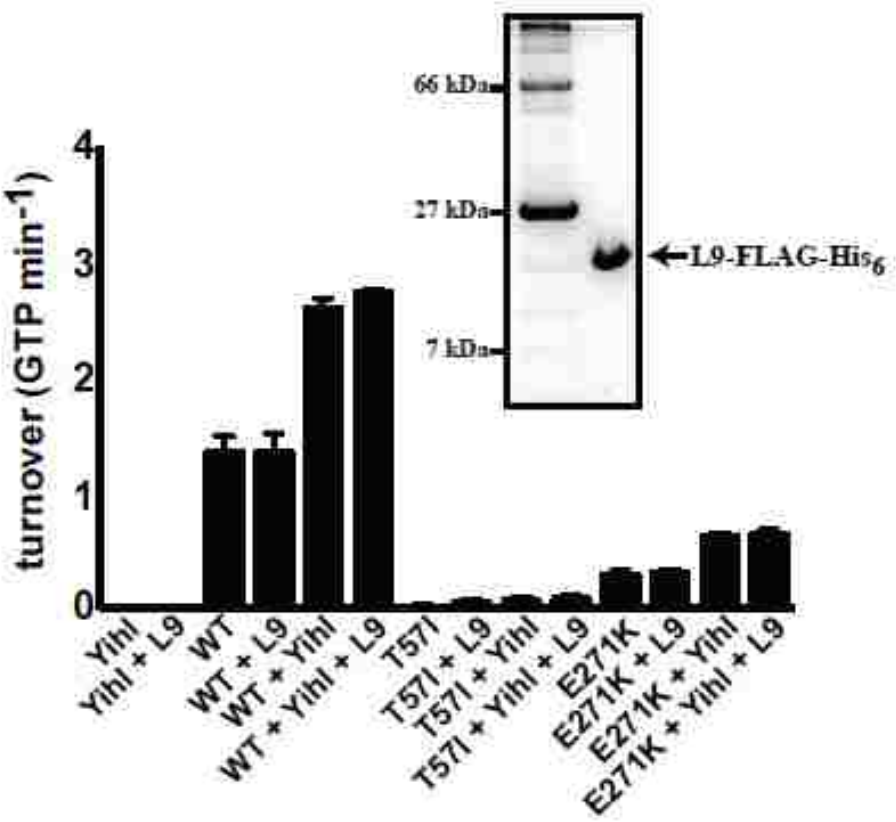

Figure 25: S2. L9 does not influence Der's GTPase activity or YihI stimulation.

The GTPase activities of wild-type and mutant Der were analyzed in the presence of purified L9-FLAG-His6. Pacel A, purified L9-FLAG-His6 was added to GTPase assays containing wild-type (0.5 μM Der, 5 μM L9) or mutant (2.0 μM Der, 20 μM L9) with or without YihI-FLAG-His6 (10-fold excess over Der). L9 did not influence the basal or YihI-stimulated GTPase activities of any Der variant. Inset, Coomassie-stained SDS-PAGE of the purified L9-FLAG-His6 protein.

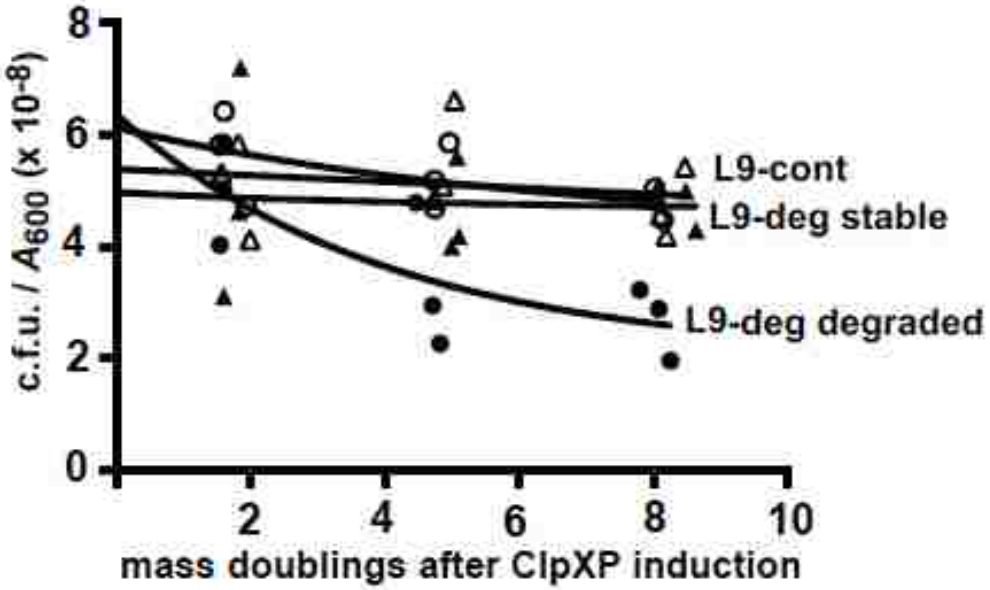

Figure 26: S3. Plating efficiency of derT57I when L9 is depleted.

Cultures of rplI-cont or rplI-deg, derT57I cells were cultured and uninduced (glucose) or induced (arabinose) for ClpXP expression. Samples of the cultures were plated to determine the colony forming units as a function of the turbidity in the plate well. The results of three experiments are shown for each condition: rplI-cont in glucose (open triangles); rplI-cont in arabinose (open circles). Each data set was fitted to a first-order decay model (solid lines) to estimate the plating efficiency at infinite culturing (which would otherwise spawn suppressors). The depletion of L9 in derT57I reduced the plating efficiency to ~40% that of the controls.

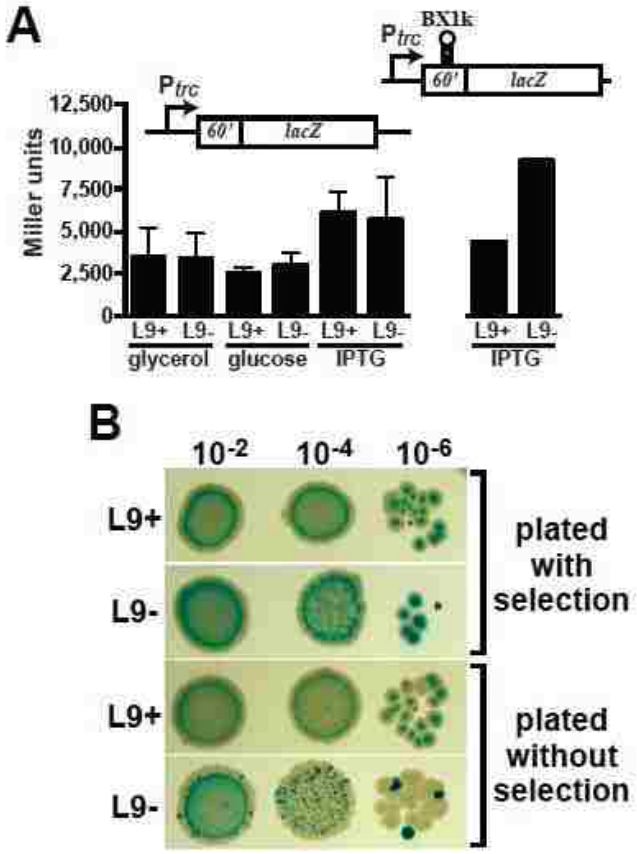

Figure 27: S4. L9 influences the stability of translation bypass reporters.

Translation bypass reporter plasmids were constructed that expressed the phage T4 gene 60 bypass region fused to lacZ. Pancel A, Miller units from cultures of L9+ and L9- cells harboring a reporter plasmid with a wild-type gene 60 segment under non-inducing and inducing conditions. Shown are the averages and standard deviations from five experiments. In the right section, Miller units are shown (average of two experiments) for the BX1k extended stem-loop construct used to screen for the original hop-1 mutation. Unlike the wild-type bypass region, this construct expresses more LacZ in L9- cultures. Panel B, L9+ and L9- cultures harboring the wild-type gene60 reporter plasmid were grown under antibiotic selection were sampled at the time of harvest for a miller assay, serially diluted, and plated with and without ampicillin selection on IPTG/X-gal plates. Note that the L9- culture was heterogenous, with some cells giving rise to colonies with high levels of LacZ and others with none. Also, the colony count under selective conditions was lower suggesting that a substantial population was losing the plasmid as the cultures grew.

APPENDIX B: CHAPTER III SUPPLEMENTAL INFORMATION

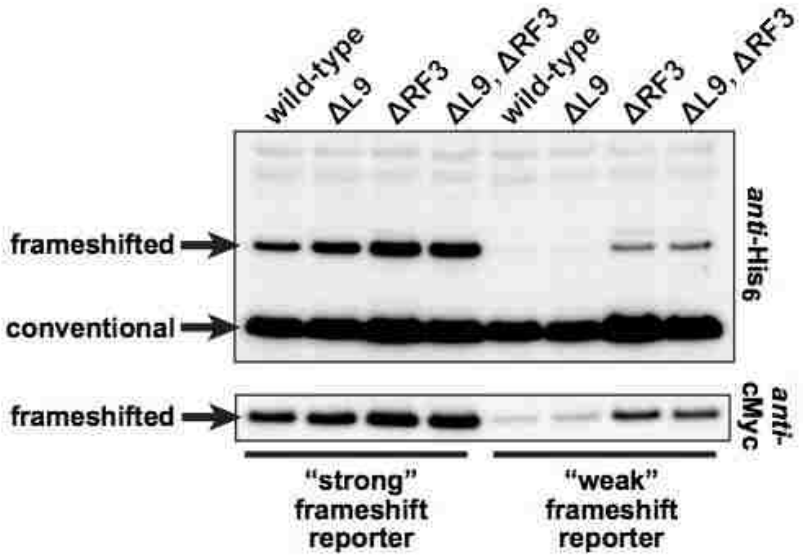

Figure 28: S1. L9 is not required for RF-3 mediated surveillance.

Test strains were transformed with plasmids that express reporters based on the well-characterized frameshift sequence found in prfB (kind gifts from Hani Zaher, Washington University in St. Louis). The constructs are described in reference [5]. In wild-type cells, frameshifting events are detected in the ribosome and the products are prematurely released through the activity of release factor 3 (RF3). Both non frameshifted and prematurely released products migrate at the conventional position in Western blots. Frameshifted products are longer because they read through an otherwise in-frame stop codon adjacent to the frameshift motif. The top panel is an anti-His_6 Western that detected all reporter products. The bottom panel is an anti-cMyc Western that only detected frameshifted material. The "strong" reporter contained a bona fide prfC sequence that promoted a high level of frameshifting. The "weak" reporter had alterations that reduced the level of frameshifting. The frameshifted material in ΔrplI cells was not statistically different than that observed in wild-type cells when separate Westerns were used to more accurately quantify the ratios of the two products using dilution series.

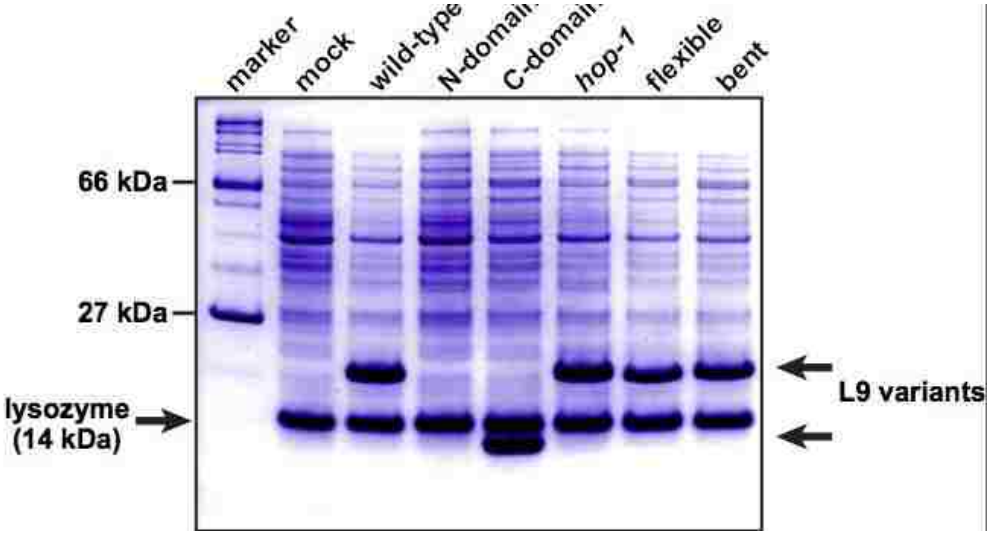

Figure 29: S2. Expression of L9 variants from plasmids.

Transformed strains were induced to express L9 variants and total protein was analyzed using SDS-PAGE. Each full-length version and the C domain expressed to high levels. The N domain construct did not accumulate to high levels, but was able to fully complement der mutants.

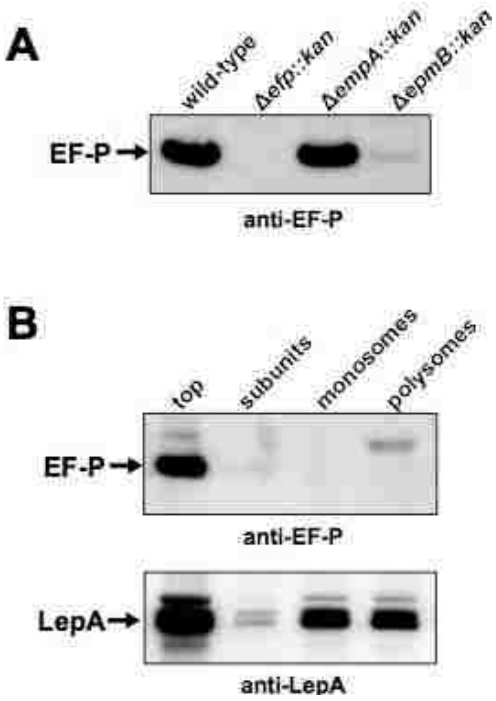

Figure 30: S3. EF-P abundance and distribution

EF-P was detected using Western blots with polyclonal antibodies. (A) EF-P levels were determined in normalized total protein samples from wild type, Δefp::kan, ΔepmA::kan, and ΔepmB::kan cells. (B) EF-P (top panel) and LepA (bottom panel) were detected in pooled sucrose gradient fractions from the top, 30S and 50S subunits region, monosome peak, and polysome region. Each pooled sample was precipitated with alcohol and resuspended in SDS-PAGE sample buffer for analysis. The band migrating above the EF-P band is not related to EF-P (detectable in knockout strains). The anti-LepA Western served as a control to evaluate protein content using a translation factor that also transiently associates with polysomes.

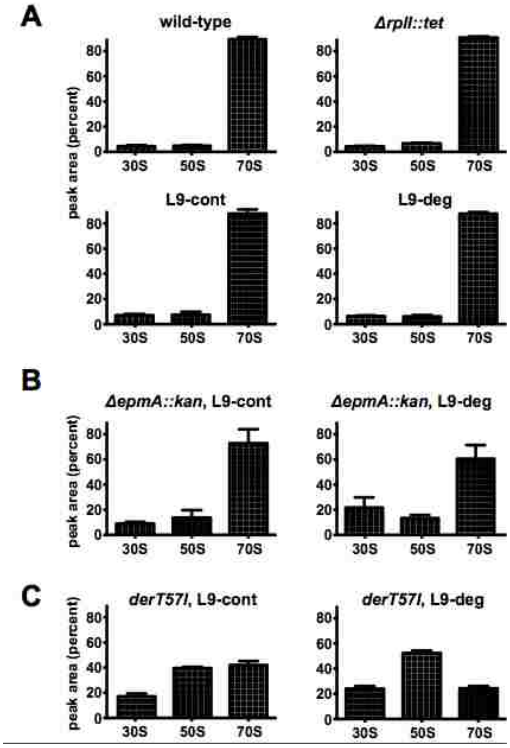

Figure 31: S4. Quantification of subunits and monosomes

Peaks were integrated from gradients derived from the indicated cultures and plotted along with the standard deviations from three independent experiments. (A) A comparison of 30S, 50S, and 70S peaks from wild-type and *ΔrplI::tet* cells (top) a well as cells that had the degradation system activated in cells with L9-cont and L9-deg. The degradation system did not reduce 70S material (~90% of total) and there was essentially no change in the relative particle abundances when L9 was absent or depleted. (B) Abundance of particles in ΔepmA cells with L9 support (L9-cont) or with L9 depleted (L9-deg). With L9 support, monosomes were reduced to ~70% accompanied by an increase in both 30S and 50S material. The abundance of 30S material nearly doubled when L9 was depleted, which was accompanied by a further reduction of monosomes to ~60%. Both monosome peaks were integrated together and considered as "70S" for this comparison. (C) Abundances in *derT57I* cells with and without L9 support. With L9, the 70S peak was ~45%. When L9 was depleted, the abundance of 30S and 50S particles increased and 70S decreased to ~25%.

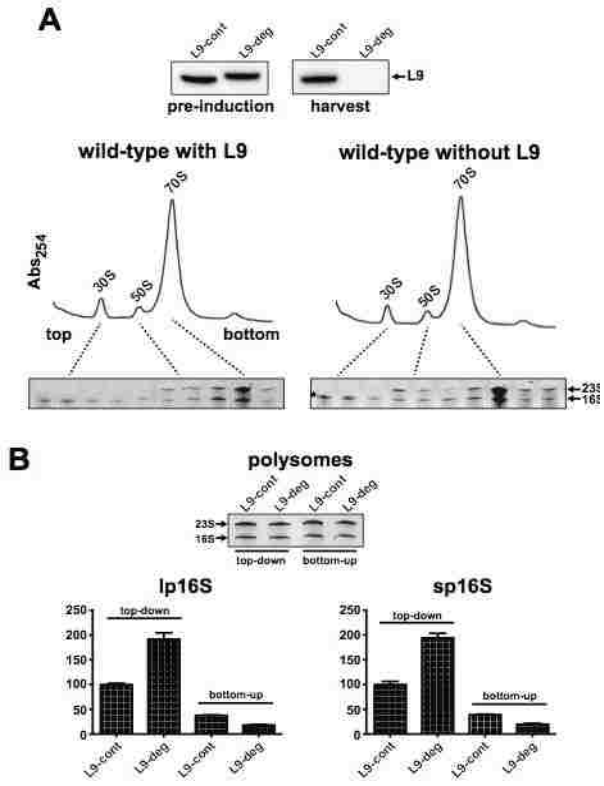

Figure 32: S5. Depleting L9 in wild-type cells recapitulates *rplI*- defects

The L9 degradation system was activated in otherwise wild-type cells. (A) Westerns show the abundance of L9-cont and L9-deg before activation of the protease system and at the time of harvest. Sucrose gradients of the two lysates have similar peak intensities, but there is more immature RNA in the 30S peak of the L9-deg sample (asterisk). (B) RNA samples were prepared from polysomes recovered from either top down or bottom-up fractionations of the same lysates. The inset shows RNAs from the recovered polysomes, immature 16S rRNA was not evident. RT-qPCR was used to quantify the lp16S (additional 115 5' nucleotides) and sp16S (additional 66 5' nucleotides) levels relative to total 16S. For comparison, the amount of immature 16S found in the top-down fractionated L9-cont gradient was set to 100%. Note that the fractionation method reversed the observed relative abundance. Error bars represent the standard deviation of four measurements.

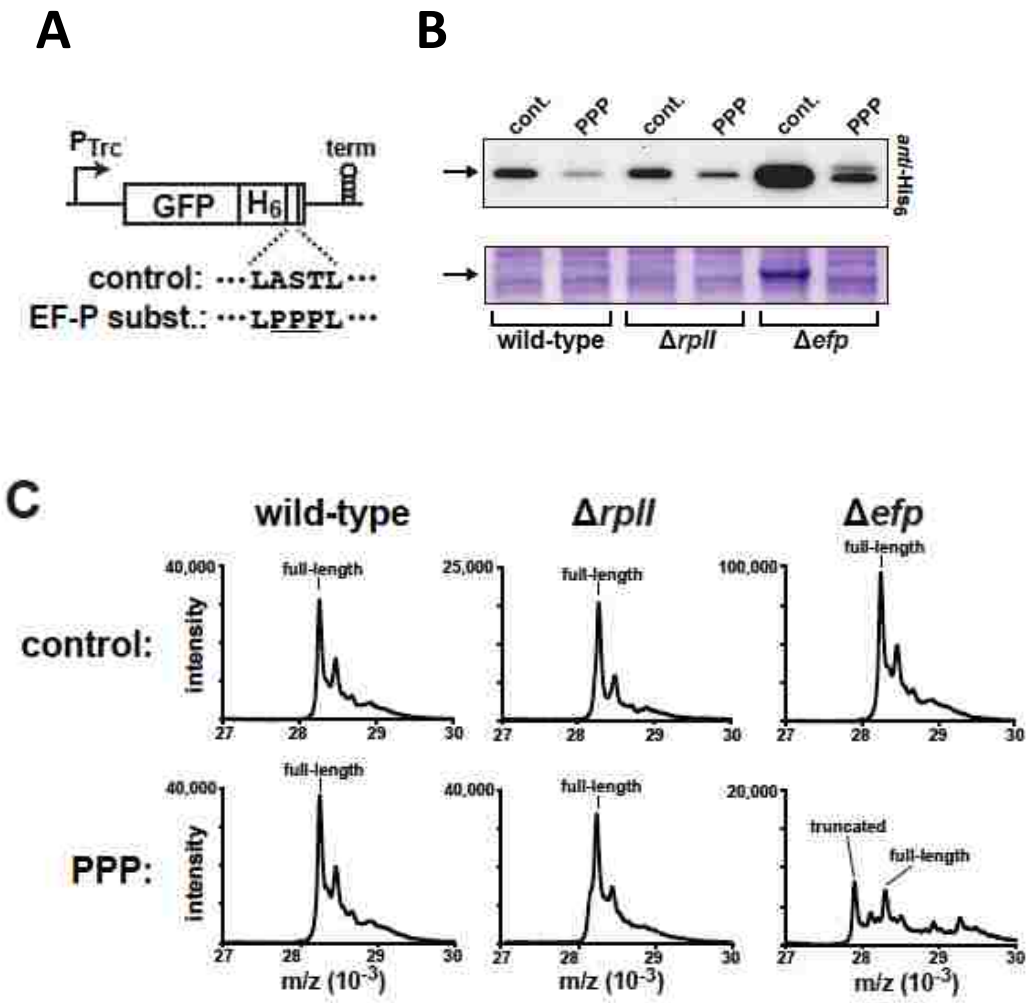

Figure 33: EF-P does not require L9 to function.

A. Plasmid based reporter constructs used to evaluate EF-P's activity in WT, ΔrplI, and Δefp strains. A control motif (AST) and a poly-proline containing motif (PPP) were fused to the C-terminus of GFP-His_6. B. Coomassie and Western blot of whole lysates were used to evaluate expression. The differences in expression levels correlated with difference in mRNA levels. C. The reporter proteins were purified using Ni^{++}-column chromatography and purified proteins were subjected to mass spectrometry. The translation of the poly-proline reporter was not reduced in L9- cells. However, the absence of EF-P leads to accumulation of a truncated form of the reporter protein.

Table 1. Genes sequenced in a fast-growing Δefp escape mutant

Each was wild-type. Functional annotations derived from www.ecogene.org

Gene	**Function/rationale**
der	ribosome biogenesis, mutation renders L9 dependence
eno	enolase, RNA degradosome component, in relA operon
mazE	antitoxin of MazF, in relA operon
mazF	RNase, toxin, in relA operon
mazG	NTPase, binds Era, in relA operon
relA	(p)ppGpp synthetase, stringent response regulator
rlmD	23S rRNA m(5)U1939 methyltransferase, in relA operon
rlmN	23S rRNA m(2)A2503, tRNA m(2)A37 methyltransferase, near der
priB	primosome component, in rplI operon
recG	DNA helicase, in spoT operon
rplI	L9, suppresses EF-P absence
rpoZ	RNAP omega subunit, in spoT operon
rpsD	S4, aminoglycoside resistance, miscoding (ram), or hyperaccuracy
rpsE	S5, aminoglycoside resistance or miscoding (ram)
rpsL	S12, aminoglycoside dependence (hyperaccuracy)
rpsR	S18, in rplI operon
SpoT	(p)ppGpp synthetase/hydrolase, stringent response regulator

Gene	Function/rationale
trmH	tRNA mG18 2'-O-methyltransfersase, in spoT operon

Table 2. Cloned genes tested for multi-copy suppression of Δefp sickness.

ASKA library clones were transformed into Δefp cells and evaluated for their ability to enhance the growth under different induction conditions (glucose = low, glycerol = moderate, IPTG = high). None improved the fitness. Annotations derived from www.ecogene.org.
Genes sequenced in a fast-growing Δefp escape mutant. Each was wild-type. Functional annotations derived from www.ecogene.org.

Gene	**Function/rationale**
deaD	50S subunit biogenesis
infA	translation initiation factor IF-1
infB	translation initiation factor IF-2
infC	translation initiation factor IF-3
ksgA	16S rRNA dimethyltransferase, mutation confers kasugamycin resistance
rhlE	RNA helicase in degradasome
rimJ	acetylates S5, 30S subunit biogenesis
rluB	23S rRNA pseudouridine synthase
rng	RNase G, 16S processing
rnpA	RNase P, tRNA and 4.5S RNA processing
rsgA	30S subunit biogenesis
rsmC	16S rRNA methylase
rsmE	16S rRNA methylase
rsuA	16S rRNA pseudouridine synthase
smpB	tmRNA binding and ribosome rescue

Gene	Function/rationale
yhbC	30S subunit biogenesis

REFERENCES

1. Crick, F.H.C., *On Protein Synthesis.* Symposia of the soceity for experimental biology, 1958. **12**: p. 138-163.
2. PALADE, G.E., *A small particulate component of the cytoplasm.*, in *J Biophys Biochem Cytol*1955. p. 59-68.
3. Richard L. Gourse, T.G., Michael S. Bartlett, J. Alex Appleman, and Wilma Ross, *rRNA transcription and growth rate-dependent regulation of ribosome synthesis in Escherichia coli.* Annu Rev Microbiol, 1996. **50**: p. 645-677.
4. Maaloe O, K.N., *Control of macromolecular synthesis: a study of DNA, RNA, and protein synthesis in bacteria.* New York; Benjamin, 1966: p. 1-284.
5. A. Tissieres, B.R.H., *Ribonucleoprotein particles from Escherichia coli.* J. Mol. Biol, 1959. **1**: p. 221-233.
6. Day, L.E., *Tetracycline Inhibition of Cell-free protein synthesis I. Binding of Tetracycline to components of the system.* Journal of Bacteriology, 1966. **91**(5): p. 1917-1923.
7. B.J. McCarthy, R.J.B., and R.B. Roberts, *The synthesis of ribosomes in E. coli* Biophysical Journal 1962. **2**: p. 57-82.
8. RY Young, H.B., *Polypeptide-Chain Elongation rate in E. coli B/r as a function of growth rate.* Biochem. J., 1976. **160**: p. 185-194.
9. Loftfield, R.B., *The Frequency of Errors in Protein Biosynthesis.* Biochem. J., 1963. **89**: p. 82-92.
10. Lipmann, D.N.a.F., *Amino acid transfer from Amino acyl-ribonucleic acids to proteins on ribosomes of E.coli.* Biochemistry, 1961. **47**: p. 497-504.

11. Offengand, P.B.a.E.J., *An enzymatic mechanism for linking amino acids to RNA.* Symposium, 1958. **44**: p. 77-86.

12. Ogle, J.M. and V. Ramakrishnan, *Structural insights into translational fidelity.*, in *Annu. Rev. Biochem.*2005. p. 129-177.

13. R. W. Risebrough, A.T., J. D. Watson, *Messenger-RNA attachment to the ribosome.* PNAS, 1962. **48**: p. 430-436.

14. Saunders, C.S.M.a.G., *Stability of the messenger RNA-transfer RNA-ribosome complex.* J. Mol. Biol, 1968. **32**: p. 521-542.

15. Davis, J.D.a.B.D., *Misreading of ribonucleic acid code words induced by aminoglycoside antibiotics.* The Journal of Biological Chemistry, 1968. **243**: p. 3312-3316.

16. Kataja, L.G.a.E., *Streptomycin-induced oversuppression in E. coli.* PNAS, 1964. **51**: p. 995-1001.

17. Morgan, M.N.a.E.A., *Genetics of Bacterial Ribosomes.* Annu Rev Genet, 1977. **11**: p. 297-347.

18. Noller, D.M.a.H.F., *Interaction of antibiotics with functional sites in 16S ribosomal RNA.* Nature, 1987. **327**: p. 389-395.

19. Wintermeyer, M.V.R.a.W., *Fidelity of aminoacyl-tRNA selection on the ribosome: Kinetic and structural mechanisms.* Annu Rev Biochem, 2001. **70**: p. 415-435.

20. Krzysztof Applet, A.Y., *The crystallization of ribosomal proteins from the 50S subunit of the E. coli and C. stearothermophilus ribosome.* Journal of Biological Chemistry, 1981. **256**(22): p. 11787-11790.

21. Yonath, F.S.a.A., *Structure of functionally activated small ribosomal subunit at 3.3 A resolution.* Cell, 2000. **102**: p. 615-623.

22. Nenad Ban, P.N., Thomas A. Steitz, *The Complete Atomic Structure of the Large Ribosomal Subunit at 2.4 A resolution.* Science, 2000. **289**: p. 905-919.

23. James M. Ogle, F.V.M.I., V. Ramakrishnan, *Selection of tRNA by the Ribosome Requires a Transition from an Open to a Closed Form.* Cell, 2002. **111**: p. 721-732.

24. Brian T. Wimberly, D.E.B., V. Ramakrishnan, *Structure of the 30S ribosomal subunit.* Nature, 2000. **407**: p. 327-339.

25. Andrew P. Carter, W.M.C., V. Ramakrishnan, *Functional Insights from the structure of the 30S ribosomal subunit and its interactions with antibiotcs.* Nature, 2000. **407**: p. 340-348.

26. Shajani, Z., M.T. Sykes, and J.R. Williamson, *Assembly of bacterial ribosomes.*, in *Annu. Rev. Biochem.*2011. p. 501-526.

27. Poul Nissen, T.A.S., *The structural basis of ribosome activity in peptide bond synthesis.* Science, 2000. **289**: p. 920-929.

28. Hans-Jorg Rheinberger, K.H.N., *Three tRNA binding sites on Escherichia coli ribosomes.* PNAS, 1981. **78**: p. 5310-5314.

29. Youngman, E.M., et al., *The active site of the ribosome is composed of two layers of conserved nucleotides with distinct roles in peptide bond formation and peptide release.*, in *Cell*2004. p. 589-599.

30. Brunelle, J.L., et al., *Peptide release on the ribosome depends critically on the 2' OH of the peptidyl-tRNA substrate.*, in *RNA*2008. p. 1526-1531.

31. Green, R. and H. Noller, *RIBOSOMES AND TRANSLATION*, 1997. p. 1-38.

32. Ogle, J.M., A.P. Carter, and V. Ramakrishnan, *Insights into the decoding mechanism from recent ribosome structures.*, in *Trends Biochem. Sci.*2003. p. 259-266.

33. Zaher, H.S. and R. Green, *Fidelity at the molecular level: lessons from protein synthesis.*, in *Cell*2009. p. 746-762.

34. Hopfield, J.J., *Kinetic proofreading: A New Mechanism for Reducing Errors in Biosynthetic Processes Requiring High Specificity.* PNAS, 1974. **71**(10): p. 4135-4139.

35. Stone, R.C.T.a.P.J., *Proofreading of the codon-anticodon interaction on ribosomes.* PNAS, 1977. **74**: p. 198-202.

36. Cochella, L. and R. Green, *An active role for tRNA in decoding beyond codon:anticodon pairing.* Science, 2005. **308**(5725): p. 1178-80.

37. Nierhaus, K.H., *The Allosteric three site model for the ribosomal elongation cycle: Features and Future.* Perspectives in Biochemistry, 1990. **29**: p. 4997-5007.

38. Yuri P. Semenkov, M.V.R., and Wolfgang Wintermeyer, *The " allosteric three-site model" of elongation cannot be confirmed in a well defined ribosome system from E. coli.* PNAS, 1996. **93**: p. 12183-12188.

39. Petropoulos, A.D. and R. Green, *Further in vitro exploration fails to support the allosteric three-site model.* J Biol Chem, 2012. **287**(15): p. 11642-8.

40. Nomura, P.T.a.M., *Structure and Function of E. coli ribosomes* PNAS, 1968: p. 778-784.

41. Erdmann, M.N.a.V.A., *Reconstitution of 50S ribosomal subunits from dissociated molecular components.* Nature, 1970. **228**: p. 744-748.

42. Karbstein, K., *Inside the 40S ribosome assembly machinery.* Curr Opin Chem Biol, 2011. **15**(5): p. 657-63.

43. Adilakshmi, T., D.L. Bellur, and S.A. Woodson, *Concurrent nucleation of 16S folding and induced fit in 30S ribosome assembly.* Nature, 2008. **455**(7217): p. 1268-72.

44. Clatterbuck Soper, S.F., et al., *In vivo X-ray footprinting of pre-30S ribosomes reveals chaperone-dependent remodeling of late assembly intermediates.* Mol Cell, 2013. **52**(4): p. 506-16.

45. Lewicki, B.T., et al., *Coupling of rRNA transcription and ribosomal assembly in vivo. Formation of active ribosomal subunits in Escherichia coli requires transcription of rRNA genes by host RNA polymerase which cannot be replaced by bacteriophage T7 RNA polymerase.*, in *J. Mol. Biol.*1993. p. 581-593.

46. Talkington, M.W., G. Siuzdak, and J.R. Williamson, *An assembly landscape for the 30S ribosomal subunit.* Nature, 2005. **438**(7068): p. 628-32.

47. Shoji, S., et al., *Systematic Chromosomal Deletion of Bacterial Ribosomal Protein Genes*, in *J. Mol. Biol.*2011. p. 751-761.

48. Brodersen, D.E. and P. Nissen, *The social life of ribosomal proteins*, in *FEBS Journal*2005. p. 2098-2108.

49. Wilson, D.N. and K.H. Nierhaus, *Ribosomal proteins in the spotlight.*, in *Crit. Rev. Biochem. Mol. Biol.*2005. p. 243-267.

50. Lecompte, O., et al., *Comparative analysis of ribosomal proteins in complete genomes: an example of reductive evolution at the domain scale.*, in *Nucleic Acids Research*2002. p. 5382-5390.

51. Kitakawa, K.I.a.M., *Cluster of ribosomal proteins in E. coli containing genes for proteins S6, S18, and L9.* PNAS, 1978. **75**(12): p. 6163-6167.

52. Nierhaus, R.R.a.K.H., *Assembly map of the large subunit (50S) of Escherichia coli ribosomes.* PNAS, 1981. **79**: p. 729-733.

53. Berk, V., et al., *Structural basis for mRNA and tRNA positioning on the ribosome.* Proc Natl Acad Sci U S A, 2006. **103**(43): p. 15830-4.

54. David W. Hoffman, C.D., Sue Ellen Gerchman, J.H. Kycia, Stephanie J. Porter, Stephen W. White and V.Ramakrishnan, *Crystal structure of prokayotic ribosomal protein L9: a bi-lobed RNA-binding protein.* The EMBO journal, 1994. **13**: p. 205-212.

55. David W. Hoffman, C.S.C., Christopher Davies, Stephen W. White and V. Ramakrishnan, *Ribosomal protein L9: A structure determination by the combined use of X-ray crystallography and NMR spectroscopy.* 1996, 1996. **264**: p. 1058-1071.

56. Huang WM, A.S., Casjens S, Orlandi R, Zeikus, Weiss R, Winge D, Fang M., *A persistent untranslated sequence within bacteriophage T4 DNA topoisomerase gene 60.* Science, 1988. **239**: p. 1005-1012.

57. Robert B. Weiss, W.M.H.a.D.M.D., *A nascent peptide is required for ribosomal bypass of the coding gap in bacteriophage T4 gene 60.* Cell, 1990. **62**: p. 117-126.

58. Herbst, K.L., et al., *A mutation in ribosomal protein L9 affects ribosomal hopping during translation of gene 60 from bacteriophage T4.*, in *Proc. Natl. Acad. Sci. U.S.A.*1994. p. 12525-12529.

59. Adamski, F.M., J.F. Atkins, and R.F. Gesteland, *Ribosomal Protein L9 Interactions with 23 S rRNA: The Use of a Translational Bypass Assay to Study the Effect of Amino Acid Substitutions*, in *J. Mol. Biol.*1996. p. 357-371.

60. Naganathan, A. and S.D. Moore, *Crippling the Essential GTPase Der Causes Dependence on Ribosomal Protein L9.*, in *J. Bacteriol.*2013. p. 3682-3691.

61. Seidman, J.S., B.D. Janssen, and C.S. Hayes, *Alternative fates of paused ribosomes during translation termination.* J Biol Chem, 2011. **286**(36): p. 31105-12.

62. Atkins, J.F. and G.R. Bjork, *A gripping tale of ribosomal frameshifting: extragenic suppressors of frameshift mutations spotlight P-site realignment.* Microbiol Mol Biol Rev, 2009. **73**(1): p. 178-210.

63. Bernhardt, T.G. and P.A.J. de Boer, *Screening for synthetic lethal mutants in Escherichia coli and identification of EnvC (YibP) as a periplasmic septal ring factor with murein hydrolase activity.*, in *Mol. Microbiol.*2004. p. 1255-1269.

64. Egon Amann, B.O., and Karl-Josef Abel, *Tightly regulated tac promoter vectors useful for the expression of unfused and fused proteins in Escherichia coli.* Gene, 1988. **69**: p. 301-315.

65. Caldon, C.E., P. Yoong, and P.E. March, *Evolution of a molecular switch: universal bacterial GTPases regulate ribosome function.*, in *Mol. Microbiol.*2001. p. 289-297.

66. Britton, R.A., *Role of GTPases in Bacterial Ribosome Assembly*, in *Annu. Rev. Microbiol.*2009. p. 155-176.

67. Robinson, V.L., et al., *Domain arrangement of Der, a switch protein containing two GTPase domains.*, in *Structure*2002. p. 1649-1658.

68. Young Jeon, H.-S.P., *Der containing two consecutive GTP-binding domains plays an essential role in chloroplast ribosomal RNA processing and ribosome biogenesis in higher plants.* Jounal of Experimental Botany, 2014. **65**(1): p. 117-130.

69. Hwang, J. and M. Inouye, *The tandem GTPase, Der, is essential for the biogenesis of 50S ribosomal subunits in Escherichia coli.*, in *Mol. Microbiol.*2006. p. 1660-1672.

70. Muench, S.P., et al., *The essential GTPase YphC displays a major domain rearrangement associated with nucleotide binding.*, in *Proc. Natl. Acad. Sci. U.S.A.*2006. p. 12359-12364.

71. Bharat, A., et al., *Cooperative and Critical Roles for Both G Domains in the GTPase Activity and Cellular Function of Ribosome-Associated Escherichia coli EngA*, in *J. Bacteriol.*2006. p. 7992-7996.

72. Blaha, G., R.E. Stanley, and T.A. Steitz, *Formation of the First Peptide Bond: The Structure of EF-P Bound to the 70S Ribosome*, in *Science*2009. p. 966-970.

73. Glick, B.R. and M.C. Ganoza, *Identification of a soluble protein that stimulates peptide bond synthesis.*, in *Proc. Natl. Acad. Sci. U.S.A.*1975. p. 4257-4260.

74. Glick, B.R. and M.C. Ganoza, *Characterization and site of action of a soluble protein that stimulates peptide-bond synthesis.*, in *Eur. J. Biochem.*1976. p. 483-491.

75. Ganoza, B.R.G.a.M.C., *Characterization and site of action of a soluble protein that stimulates peptide-bond synthesis.* Eur J Biochem, 1976. **71**: p. 483-491.

76. Aoki, H., et al., *Molecular characterization of the prokaryotic efp gene product involved in a peptidyltransferase reaction.*, in *Biochimie*1997. p. 7-11.

77. Ude, S., et al., *Translation elongation factor EF-P alleviates ribosome stalling at polyproline stretches.*, in *Science*2013. p. 82-85.

78. Doerfel, L.K., et al., *EF-P is essential for rapid synthesis of proteins containing consecutive proline residues.*, in *Science*2013. p. 85-88.

79. Peil, L., et al., *Lys34 of translation elongation factor EF-P is hydroxylated by YfcM*, in *Nat. Chem. Biol.*2012. p. 695-697.

80. Bullwinkle, T.J., et al., *(R)-β-lysine-modified elongation factor P functions in translation elongation.*, in *Journal of Biological Chemistry*2013. p. 4416-4423.

81. Navarre, W.W., et al., *PoxA, yjeK, and elongation factor P coordinately modulate virulence and drug resistance in Salmonella enterica.* Mol Cell, 2010. **39**(2): p. 209-21.

82. Gutierrez, E., et al., *eIF5A promotes translation of polyproline motifs.* Mol Cell, 2013. **51**(1): p. 35-45.

83. Akanuma, G., et al., *Inactivation of ribosomal protein genes in Bacillus subtilis reveals importance of each ribosomal protein for cell proliferation and cell differentiation.* J Bacteriol, 2012. **194**(22): p. 6282-91.

84. Hauser, R., et al., *RsfA (YbeB) proteins are conserved ribosomal silencing factors.* PLoS Genet, 2012. **8**(7): p. e1002815.

85. Huber, D., et al., *SecA interacts with ribosomes in order to facilitate posttranslational translocation in bacteria.* Mol Cell, 2011. **41**(3): p. 343-53.

86. McGary K, E.N., *RNA polymerase and the ribosome: the close relationship.* 2013.

87. Bubunenko, M., T. Baker, and D.L. Court, *Essentiality of ribosomal and transcription antitermination proteins analyzed by systematic gene replacement in Escherichia coli.* J Bacteriol, 2007. **189**(7): p. 2844-53.

88. Atkins, J.F. and G.R. Bjork, *A Gripping Tale of Ribosomal Frameshifting: Extragenic Suppressors of Frameshift Mutations Spotlight P-Site Realignment*, in *Microbiology and Molecular Biology Reviews*2009. p. 178-210.

89. Selmer, M., et al., *Ribosome engineering to promote new crystal forms*, in *Acta Cryst (2012). D68, 578-583 [doi:10.1107/S0907444912006348]*2012, International Union of Crystallography. p. 1-6.

90. Nierhaus, V.N.a.K.H., *Initiator proteins for the assembly of the 50S subunit from Escherichia coli ribosomes.* PNAS, 1982. **79**: p. 7238-7242.

91. Herr, A.J., J.F. Atkins, and R.F. Gesteland, *Coupling of open reading frames by translational bypassing.*, in *Annu. Rev. Biochem.*2000. p. 343-372.

92. Herr, A.J., et al., *Analysis of the roles of tRNA structure, ribosomal protein L9, and the bacteriophage T4 gene 60 bypassing signals during ribosome slippage on mRNA*, in *J. Mol. Biol.*2001. p. 1029-1048.

93. Leipuviene, R. and G.R. Bjork, *Alterations in the Two Globular Domains or in the Connecting -Helix of Bacterial Ribosomal Protein L9 Induces +1 Frameshifts*, in *J. Bacteriol.*2007. p. 7024-7031.

94. Dunkle, J.A., et al., *Structures of the bacterial ribosome in classical and hybrid states of tRNA binding.* Science, 2011. **332**(6032): p. 981-4.

95. Voorhees, R.M., et al., *The mechanism for activation of GTP hydrolysis on the ribosome.* Science, 2010. **330**(6005): p. 835-8.

96. Lieberman, K.R., et al., *The 23 S rRNA environment of ribosomal protein L9 in the 50 S ribosomal subunit.*, in *J. Mol. Biol.*2000. p. 1129-1143.

97. Jin, H., A.C. Kelley, and V. Ramakrishnan, *Crystal structure of the hybrid state of ribosome in complex with the guanosine triphosphatase release factor 3.* Proc Natl Acad Sci U S A, 2011. **108**(38): p. 15798-803.

98. Hwang, J. and M. Inouye, *An essential GTPase, der, containing double GTP-binding domains from Escherichia coli and Thermotoga maritima.*, in *J. Biol. Chem.*2001. p. 31415-31421.

99. Hwang, J. and M. Inouye, *Interaction of an essential Escherichia coli GTPase, Der, with the 50S ribosome via the KH-like domain.*, in *J. Bacteriol.*2010. p. 2277-2283.

100. Datta, S., N. Costantino, and D.L. Court, *A set of recombineering plasmids for gram-negative bacteria.*, in *Gene*2006. p. 109-115.

101. Carr, A.C., et al., *Rapid depletion of target proteins allows identification of coincident physiological responses.* J Bacteriol, 2012. **194**(21): p. 5932-40.

102. Moore, S.D., *Assembling new Escherichia coli strains by transduction using phage P1.*, in *Methods Mol. Biol.*2011. p. 155-169.

103. Fix, D. *N-Ethyl-N-nitrosourea-induced mutagenesis in Escherichia coli: Multiple roles for UmuC protein*. 1993. **294**, 127-138.

104. Koji, H., *Highly accurate genome sequences of Escherichia coli K-12 strains MG1655 and W3110*. Vol. 2. 2006, Molecular Systems Biology: EMBO and Nature.

105. Pace, C.N., *How to measure and predict the molar absorption coefficient of a protein.* Protein Science, 1995. **4**: p. 2411-2423.

106. Foucher, A.E., et al., *Potassium acts as a GTPase-activating element on each nucleotide-binding domain of the essential Bacillus subtilis EngA.* PLoS One, 2012. **7**(10): p. e46795.

107. *Ingerman Nunnari regenerative GTPase assay* 2012. p. 1-6.

108. Niedhardt, F.C., *Culture Medium for Enterobacteria.* Journal of Bacteriology, 1974. **119**(3): p. 736-747.

109. Hwang, J. and M. Inouye, *A bacterial GAP-like protein, YihI, regulating the GTPase of Der, an essential GTP-binding protein in Escherichia coli.*, in *J. Mol. Biol.*2010. p. 759-772.

110. Britton, R.A., *Role of GTPases in bacterial ribosome assembly.*, in *Annu. Rev. Microbiol.*2009. p. 155-176.

111. Gasper, R., et al., *The role of the conserved switch II glutamate in guanine nucleotide exchange factor-mediated nucleotide exchange of GTP-binding proteins.* J Mol Biol, 2008. **379**(1): p. 51-63.

112. Vetter, I.R. and A. Wittinghofer, *The guanine nucleotide-binding switch in three dimensions.* Science, 2001. **294**(5545): p. 1299-304.

113. Cherfils, J. and M. Zeghouf, *Regulation of small GTPases by GEFs, GAPs, and GDIs.* Physiol Rev, 2013. **93**(1): p. 269-309.

114. DW, T., *Influence of growth condition on the concentration of potassium in Bacillus subtilis var. niger and its possible relationship to cellular ribonucleic acid, teichoic acid and teichuronic acid.* Biochem. J., 1968. **106**: p. 237-243.

115. J, M., *The regulation of potassium fluxes for the adjustment and maintenance of potassium levels in Escherichia coli.* Eur. J. Biochem, 1981. **119**: p. 165-170.

116. MJ, T.d.M., *Bioenergetic consequences of microbial adaptation to low-nutrient environments.* J. Biotechnol., 1997. **59**: p. 117-126.

117. Schaefer, L., et al., *Multiple GTPases participate in the assembly of the large ribosomal subunit in Bacillus subtilis.* J Bacteriol, 2006. **188**(23): p. 8252-8.

118. Tu, C., et al., *The Era GTPase recognizes the GAUCACCUCC sequence and binds helix 45 near the 3' end of 16S rRNA.* Proc Natl Acad Sci U S A, 2011. **108**(25): p. 10156-61.

119. Hwang, J. and M. Inouye, *RelA functionally suppresses the growth defect caused by a mutation in the G domain of the essential Der protein.*, in *J. Bacteriol.*2008. p. 3236-3243.

120. Zaher, H.S. and R. Green, *A primary role for release factor 3 in quality control during translation elongation in Escherichia coli.*, in *Cell*2011. p. 396-408.

121. Nakatogawa, H., A. Murakami, and K. Ito, *Control of SecA and SecM translation by protein secretion.*, in *Curr. Opin. Microbiol.*2004. p. 145-150.

122. Ling, J., N. Reynolds, and M. Ibba, *Aminoacyl-tRNA synthesis and translational quality control.*, in *Annu. Rev. Microbiol.*2009. p. 61-78.

123. Herold, M. and K.H. Nierhaus, *Incorporation of six additional proteins to complete the assembly map of the 50 S subunit from Escherichia coli ribosomes.*, in *J. Biol. Chem.*1987. p. 8826-8833.

124. Herr, A.J., et al., *Analysis of the roles of tRNA structure, ribosomal protein L9, and the bacteriophage T4 gene 60 bypassing signals during ribosome slippage on mRNA.* J Mol Biol, 2001. **309**(5): p. 1029-48.

125. Frances M. Adamski, J.F.A.a.R.F.G., *Ribosomal protein L9 interactions with 23S rRNA: The use of a translational bypass assay to study the effect of amino acid substitutions.* J. Mol. Biol, 1996. **261**: p. 357-371.

126. Schmeing, T.M., et al., *The crystal structure of the ribosome bound to EF-Tu and aminoacyl-tRNA.* Science, 2009. **326**(5953): p. 688-94.

127. Gao, Y.-G., et al., *The structure of the ribosome with elongation factor G trapped in the posttranslocational state.*, in *Science*2009. p. 694-699.

128. Selmer, M., et al., *Ribosome engineering to promote new crystal forms.* Acta Crystallogr D Biol Crystallogr, 2012. **68**(Pt 5): p. 578-83.

129. Lieberman, K.R., et al., *The 23 S rRNA environment of ribosomal protein L9 in the 50 S ribosomal subunit.* J Mol Biol, 2000. **297**(5): p. 1129-43.

130. Ude, S., et al., *Translation elongation factor EF-P alleviates ribosome stalling at polyproline stretches.* Science, 2013. **339**(6115): p. 82-5.

131. Peil, L., et al., *Lys34 of translation elongation factor EF-P is hydroxylated by YfcM.* Nat Chem Biol, 2012. **8**(8): p. 695-7.

132. Doerfel, L.K., et al., *EF-P is essential for rapid synthesis of proteins containing consecutive proline residues.* Science, 2013. **339**(6115): p. 85-8.

133. Bullwinkle, T.J., et al., *(R)-beta-lysine-modified elongation factor P functions in translation elongation.* J Biol Chem, 2013. **288**(6): p. 4416-23.

134. Bailly, M. and V. de Crécy-Lagard, *Predicting the pathway involved in post-translational modification of elongation factor P in a subset of bacterial species.*, in *Biol. Direct*2010. p. 3.

135. Zaher, H.S. and R. Green, *Quality control by the ribosome following peptide bond formation.* Nature, 2009. **457**(7226): p. 161-6.

136. Yanagisawa, T., et al., *A paralog of lysyl-tRNA synthetase aminoacylates a conserved lysine residue in translation elongation factor P.* Nat Struct Mol Biol, 2010. **17**(9): p. 1136-43.

137. Roy, H., et al., *The tRNA synthetase paralog PoxA modifies elongation factor-P with (R)-β-lysine*, in *Nat. Chem. Biol.*2011. p. 667-669.

138. Peil, L., et al., *Distinct XPPX sequence motifs induce ribosome stalling, which is rescued by the translation elongation factor EF-P.*, in *Proc. Natl. Acad. Sci. U.S.A.*2013. p. 15265-15270.

139. Korepanov, A.P., et al., *Protein L5 is crucial for in vivo assembly of the bacterial 50S ribosomal subunit central protuberance.* Nucleic Acids Res, 2012. **40**(18): p. 9153-9.

140. Biswajoy Roy-Chaudhuri, N.K., and Gloria Culver, *Appropriate maturation and folding of 16S rRNA during 30S subunit biogenesis are critical for translational fidelity.* PNAS, 2010. **107**: p. 4567-4572.

141. Demirci, H., et al., *A structural basis for streptomycin-induced misreading of the genetic code.*, in *Nat Commun*2013. p. 1355.

142. Roy-Chaudhuri, B., et al., *Suppression of a cold-sensitive mutation in ribosomal protein S5 reveals a role for RimJ in ribosome biogenesis.* Mol Microbiol, 2008. **68**(6): p. 1547-59.

143. Jomaa, A., et al., *Functional domains of the 50S subunit mature late in the assembly process.* Nucleic Acids Res, 2014. **42**(5): p. 3419-35.

144. Frazier, A.D. and W.S. Champney, *Impairment of ribosomal subunit synthesis in aminoglycoside-treated ribonuclease mutants of Escherichia coli.*, in *Arch. Microbiol.*2012. p. 1033-1041.

145. Simon Lebaron, C.S., Robert W van Nues, Agata Swiatkowska, Dietrich Walsh, Bettina Bottcher, Sander Granneman, Nicholas J Watkins, and David Tollervey, *Proofreading of pre-40S ribosome maturation by a translation initiation factor and 60S subunits.* Nature Structural and Molecular Biology, 2012. **19**: p. 744-753.

146. Jarosloav M. Belotserkovsky, E.R.D.a.L.A.I., *Mutations in 16S rRNA that suppress cold-sensitive initiation factor 1 affect ribosomal subunit association.* FEBS, 2011. **278**: p. 3508-3517.

147. Connolly, K. and G. Culver, *Overexpression of RbfA in the absence of the KsgA checkpoint results in impaired translation initiation.* Mol Microbiol, 2013. **87**(5): p. 968-81.

148. Baba, T., et al., *Construction of Escherichia coli K-12 in-frame, single-gene knockout mutants: the Keio collection.* Mol Syst Biol, 2006. **2**: p. 2006 0008.

149. Masanari Kitagawa, T.A., Mohammad Arifuzzaman, TOmoko Ioka-Nakamichi, Eiji Inamoto, Hiromi Toyonaga, and Hirotada Mori, *Complete set of ORF clones of E. coli ASKA library* DNA res, 2005. **12**: p. 291-299.

150. Sacchi, P.C.a.N., *The single-step method of RNA isolation by acid guanidinium thiocyanate phenol chloroform extraction: twenty something years on.* Nature Protocol, 2006. **2**: p. 581-585.

151. Moore, S.D. and R.T. Sauer, *Ribosome rescue: tmRNA tagging activity and capacity in Escherichia coli.* Mol Microbiol, 2005. **58**(2): p. 456-66.

152. Shajani, Z., M.T. Sykes, and J.R. Williamson, *Assembly of bacterial ribosomes.* Annu Rev Biochem, 2011. **80**: p. 501-26.

153. Leong, V., et al., *Escherichia coli rimM and yjeQ null strains accumulate immature 30S subunits of similar structure and protein complement.* RNA, 2013. **19**(6): p. 789-802.

154. Laursen, B.S., et al., *Initiation of Protein Synthesis in Bacteria*, in *Microbiology and Molecular Biology Reviews*2005. p. 101-123.

155. Lebaron, S., et al., *Proofreading of pre-40S ribosome maturation by a translation initiation factor and 60S subunits.* Nat Struct Mol Biol, 2012. **19**(8): p. 744-53.

156. LaRiviere, F.J., et al., *A late-acting quality control process for mature eukaryotic rRNAs.* Mol Cell, 2006. **24**(4): p. 619-26.

157. Jacob, A.I., et al., *Conserved bacterial RNase YbeY plays key roles in 70S ribosome quality control and 16S rRNA maturation.* Mol Cell, 2013. **49**(3): p. 427-38.

158. Sykes, M.T. and J.R. Williamson, *A complex assembly landscape for the 30S ribosomal subunit.* Annu Rev Biophys, 2009. **38**: p. 197-215.

159. Gupta, N. and G.M. Culver, *Multiple in vivo pathways for Escherichia coli small ribosomal subunit assembly occur on one pre-rRNA.* Nat Struct Mol Biol, 2014. **21**(10): p. 937-43.

160. Zhang, X., et al., *Structural insights into the function of a unique tandem GTPase EngA in bacterial ribosome assembly.* Nucleic Acids Res, 2014.

161. Strunk, B.S., et al., *A translation-like cycle is a quality control checkpoint for maturing 40S ribosome subunits.* Cell, 2012. **150**(1): p. 111-21.

162. Strunk, B.S., et al., *Ribosome assembly factors prevent premature translation initiation by 40S assembly intermediates.* Science, 2011. **333**(6048): p. 1449-53.

163. Fei, J., et al., *Allosteric collaboration between elongation factor G and the ribosomal L1 stalk directs tRNA movements during translation.*, in *Proc. Natl. Acad. Sci. U.S.A.*2009. p. 15702-15707.

164. Cornish, P.V., et al., *Following movement of the L1 stalk between three functional states in single ribosomes.*, in *Proc. Natl. Acad. Sci. U.S.A.*2009. p. 2571-2576.

165. Bock, L.V., et al., *Energy barriers and driving forces in tRNA translocation through the ribosome.* Nat Struct Mol Biol, 2013. **20**(12): p. 1390-6.

166. Brandt, F., et al., *The Native 3D Organization of Bacterial Polysomes*, in *Cell*2009, Elsevier Inc. p. 261-271.

167. Zhou, J., et al., *Crystal structures of EF-G-ribosome complexes trapped in intermediate states of translocation.* Science, 2013. **340**(6140): p. 1236086.

168. Tourigny, D.S., et al., *Elongation Factor G Bound to the Ribosome in an Intermediate State of Translocation*, in *Science*2013. p. 1235490-1235490.

169. Pulk, A. and J.H. Cate, *Control of ribosomal subunit rotation by elongation factor G.* Science, 2013. **340**(6140): p. 1235970.

170. T.T., W., *A model for three-point analysis of random general transduction.* Genetics 1966. **54**(405-410).

171. Das, S.C. and A.K. Pattnaik, *Role of the hypervariable hinge region of phosphoprotein P of vesicular stomatitis virus in viral RNA synthesis and assembly of infectious virus particles.*, in *J. Virol.*2005. p. 8101-8112.

172. Wills, N.M., et al., *Translational bypassing without peptidyl-tRNA anticodon scanning of coding gap mRNA*, in *EMBO J*2008. p. 2533-2544.